



UNIVERSITÀ DEGLI STUDI DI PADOVA
FACOLTÀ DI INGEGNERIA

TESI DI LAUREA MAGISTRALE IN INGEGNERIA CIVILE
CURRICULUM EDILE

**SEISMIC ANALYSIS AND SIMULATION OF
COLLAPSE MECHANISM
OF A MASONRY CHURCH**

Relatore: Chiar.mo Prof. CLAUDIO MODENA

Correlatore: Chiar.mo Prof. PERE ROCA

Dott. Ing. LUCA PELÀ

Laureanda: ALICE DE CONTI

ANNO ACCADEMICO 2012 – 2013

ABSTRACT

Author: Alice De Conti

Tutor: Claudio Modena, Pere Roca Fabregat, Luca Pelà

Keywords: San Marco church, Abruzzo earthquake, masonry structure, kinematic analysis, non-linear static analysis, non-linear dynamic analysis

The main aim of thesis is to understand the structural causes that led to the collapse of the church of San Marco, located in the historical center of L'Aquila, Italy. The building was damaged during the earthquake in April 2009, rated 5,8 on the Richter scale. After the first emergency phases of building protection it was necessary to perform the analysis of the historical building, in order to estimate the structural response and mechanical parameters.

The paper presents the conclusions withdrawn from different analyses which were carried out to determine the structural behavior of the church subjected to a seismic event.

In particular, the study was focused on the possible reason that underlies the partial collapse of the upper part of the left façade. In fact, since it's not possible to directly determine which kind of mechanism led to the collapse of this part of the building, it was necessary to compare the results obtained through the kinematics analysis with those deriving from the FE analyses. Moreover the different calculation techniques are compared to prove the reliability of the methods themselves.

General objective of these analyses, where the structure is already damaged because of the earthquake, is to confirm the mechanisms that led to the present condition of the church and so explain the surveyed crack pattern. In many occasions, the historical performance of the building, for example the response shown during past earthquakes, can be used to obtain conclusions on the structural performance and strength.

ASTRATTO

Laureanda: Alice De Conti

Relatore: Claudio Modena, Pere Roca Fabregat, Luca Pelà

Parole chiave: Chiesa di San Marco, terremoto Abruzzo, struttura in muratura esistente, analisi cinematica, analisi statica non lineare, analisi dinamica non lineare

L'obiettivo principale della tesi è quello di comprendere le cause strutturali che hanno portato al collasso della chiesa di San Marco, ubicata nel centro storico dell'Aquila, Italia. L'edificio è stato danneggiato durante il terremoto del 6 aprile del 2009, classificato 5,8 nella scala Richter. Dopo le prime fasi di protezione d'emergenza della costruzione è stato necessario realizzare un'analisi storica dell'edificio, per stimare la risposta strutturale e i parametri meccanici.

Il documento presenta le conclusioni tratte da differenti analisi che sono state realizzate per determinare il comportamento strutturale della chiesa sottoposta all'azione sismica.

In particolare, lo studio è stato focalizzato sulla possibile ragione che ha portato al collasso parziale della parte superiore della facciata sinistra. In realtà, poiché risulta complicato determinare direttamente che tipo di meccanismo ha portato al crollo di questa parte dell'edificio, è stato necessario confrontare i risultati ottenuti attraverso l'analisi cinematica con quelli derivanti dalla analisi FE. Inoltre le tecniche di calcolo differenti sono state confrontate per provare l'affidabilità dei metodi stessi.

L'obiettivo generale di queste analisi, in cui la struttura è già danneggiata a causa del terremoto, è di confermare i meccanismi che hanno portato alla condizione attuale della chiesa e quindi spiegare il quadro fessurativo. In molte occasioni, la performance storica del palazzo, ad esempio, la risposta evidenziata durante terremoti passati, può essere utilizzato per ottenere conclusioni sulle prestazioni strutturali e sulla resistenza.

INDEX

1. INTRODUCTION.....	11
1.1 GENERAL	11
1.2 GENERAL OBJECTIVES	11
1.3 SPECIFIC OBJECTIVES	12
2. STATE OF THE ART	14
2.1 EXISTING MASONRY BUILDINGS	14
2.2 METHODS OF ANALYSIS	15
2.2.1 ELASTIC ANALYSIS	15
2.2.2 LIMIT ANALYSIS.....	16
2.2.3 STATIC AND DYNAMIC ANALYSIS	17
2.3 STRUCTURE MODELING	19
2.3.1 EXTENSIONS OF MATRIX CALCULATION FOR LINEAR MEMBERS	19
2.3.2 USE OF RIGID AND DEFORMABLE MACRO-ELEMENTS	19
2.3.3 FEM BASED APPROACHES:.....	20
2.3.4 HOMOGENIZATION.....	22
2.3.5 DISCRETE ELEMENT METHOD	22
3. SAN MARCO CHURCH.....	24
3.1 HISTORICAL RESEARCH	24
3.2 DESCRIPTION OF THE BUILDING	26
3.3 INTERVENTIONS.....	31
4. PRESENT STATE	35
5. KINEMATIC ANALYSIS.....	36
5.1 INTRODUCTION	36
5.2 DAMAGE MECHANISMS ACTIVATED.....	42
5.3 EARTHQUAKE X DIRECTION.....	50
5.4 EARTHQUAKE Y DIRECTION.....	63
5.5 SUMMARY:	69



6. NON-LINEAR STATIC ANALYSIS:	71
6.1 INTRODUCTION.....	71
6.2 MODELING STRATEGY	71
6.3 REFERENCE CASE	75
6.3.1 EARTHQUAKE X DIRECTION	75
6.3.2 EARTHQUAKE Y DIRECTION	78
6.4 WEAK BUTTRESSES CASE.....	80
6.4.1 EARTHQUAKE X DIRECTION	81
6.4.2 EARTHQUAKE Y DIRECTION	84
6.5 SUMMARY	86
7. NON-LINEAR DYNAMIC ANALYSIS	87
7.1 INTRODUCTION.....	87
7.2 MODELING STRATEGY	87
7.3 EARTHQUAKE X DIRECTION	92
7.4 EARTHQUAKE Y DIRECTION	96
7.5 SUMMARY	99
8. FINAL CONCLUSIONS	100
8.1 GENERAL CONCLUSIONS	100
8.2 COMPARISON BETWEEN THE METHODS.....	100
8.3 COMPARISON WITH REAL COLLAPSES AND LIMITATIONS OF METHODS	101
8.4 SEISMIC CAPACITY	102
8.5 INTERVENTION NEEDS AND POSSIBLE ACTIONS	103
8.6 FUTURE RESEARCH	105
REFERENCES.....	107

APPENDIX A1: PHOTOGRAPHIC REPORT

APPENDIX A2: CALCULATION RESULTS

LIST OF FIGURES

figure 2.1 - typical behavior of almost-brittle under uniaxial loading: (a) tensile behavior, (b) compression behavior (c) shear behavior [pelà, 2009].....	4
figure 2.2 - a) modular element of a masonry panel, b) detailed micro-modeling, c) simplified micro-modeling, d) macro-modeling [pelà, 2009].....	21
figure 2.3 - basic cell for masonry and homogenization process [lourengo, 2007].	22
figure 3.1 - localization of the san marco church.....	24
figure 3.2 - main façade.	27
figure 3.3 - north elevation – via de neri.....	27
figure 3.4 - south elevation – piazza della prefettura.	28
figure 3.5 - plant.....	28
figure 3.6 - black indicates the masonry of the xiii century.....	20
figure 3.7 - transverse section.	29
figure 3.8 - longitudinal section.....	30
figure 3.9 - covering.....	30
figure 3.10 - covering made by prefabricated beams.....	31
figure 3.11 - rc elements.	32
figure 3.12 - new eaves.	32
figure 3.13 - new bell towers roof.....	33
figure 3.14 - roof section.....	33
figure 4.1 - san marco church, left façade.....	35
figure 5.1 - non-linear analysis with the kinematic approach.	37
figure 5.2 - response spectrum [program spettri NTC 2008].....	40
figure 5.3 - partial confidence factor [linee guida; §4.2].	41
figure 5.4 - out-of-plane movement of the main façade a), b), c), d).....	43
figure 5.5 - in-plane movement of the main façade a), b), c), d).	44
figure 5.6 - lateral façade a), b), c), d).	45
figure 5.7 - out-of-plane movement of the chapel walls a), b), c), d).	47



figure 5.8 - arches collapse mechanisms.	47
figure 5.9 - chapels vaults collapse a), b), c), d), e), f).....	48
figure 5.10 - non-linear analysis of the buttress.	51
figure 5.11 - collapse mechanism of a single arch.	52
figure 5.12 - collapse mechanism of arch and of both buttresses.....	53
figure 5.13 - collapse mechanism of arch and of one buttress.	55
figure 5.14 - collapse mechanism of two consecutive arches case a.....	57
figure 5.15 - collapse mechanism of two consecutive arches with resisting spandrels case b.....	60
figure 5.16 - non-linear analysis of the main façade (partially connected).	62
figure 5.17 - non-linear analysis of the top wall of the lateral façade(vertical deflection) 64	
figure 5.18 - non-linear analysis of the top wall of the lateral façade (overturning).....	65
figure 5.19 - non-linear analysis of the frontal façade (in-plane movement).....	68
figure 6.1 - rankine/drucker-prager model	71
figure 6.2 - tension cut-off in two-dimensional principal stress space.....	72
figure 6.3 - tension softening.....	72
figure 6.4 - fem model.....	72
figure 6.5 - locations of the weak connections and no connections.	73
figure 6.6 - capacity curves at the control point at the top of the tower, top of the nave wall, top of buttress and on the vaults (reference case).....	75
figure 6.7 - initial principal tensile strain, x direction (vaults view) in reference case.	76
figure 6.8 - ultimate principal tensile strain, x direction (internal view) in reference case	76
figure 6.9 - ultimate principal tensile strain, x direction (vaults view) in reference case..	76
figure 6.10 - ultimate deformation, x direction (internal view) in reference case.....	77
figure 6.11 - ultimate principal tensile strain, x direction (external view) in reference case.....	77
figure 6.12 - ultimate deformation, y direction (external view) in reference case.	77

figure 6.13 - capacity curves at the control point at the top of the tower, top of the bottom wall on the left facade, top of the top wall on the left facade, top of buttress and on the vaults (reference case)..... 78

figure 6.14 - ultimate principal tensile strain, y direction (internal view) in reference case.....79

figure 6.15 - ultimate principal tensile strain, y direction (external view) in reference case.....79

figure 6.16 - ultimate deformation, y direction (external view) in reference case.....79

figure 6.17 - capacity curves at the control point at the top of the tower, top of the nave wall, top of buttress and on the vaults (weak buttresses case). 81

figure 6.18 - initial principal tensile strain, x direction (vaults view) in weak buttresses case.82

figure 6.19 - initial principal tensile strain, x direction (buttresses view) in weak buttresses case..... 82

figure 6.20 - ultimate principal tensile strain, x direction (internal view) in weak buttresses case..... 82

figure 6.21 - ultimate principal tensile strain, x direction (external view) in weak buttresses case..... 83

figure 6.22 - ultimate deformation, x direction (arches view) in weak buttresses case. ... 83

figure 6.23 - ultimate deformation, x direction (external view) in weak buttresses case.. 83

figure 6.24 - capacity curves at the control point at the top of the tower, top of the bottom wall on the left facade, top of the top wall on the left facade, top of buttress and on the vaults (weak buttresses case). 84

figure 6.25 - ultimate principal tensile strain, y direction (internal view) in weak buttresses case..... 85

figure 6.26 - ultimate principal tensile strain, y direction (external view) in weak buttresses case..... 85

figure 6.27 - ultimate deformation, y direction (external view) in weak buttresses case.. 85

figure 7.1 - accelerogram of l'aquila earthquake (2009) in the ew direction..... 87

figure 7.2 - accelerogram of l'aquila earthquake (2009) in the ns direction..... 87

figure 7.3 - rayleigh damping model..... 88

figure 7.4 - comparison between response spectra.....	90
figure 7.5 - time displacement curve at the top of the tower, top of the nave wall, top of buttress and on the vaults.	92
figure 7.6 - principal tensile strain to the period $t=2,56$ sec, x direction (vaults view)....	93
figure 7.7 - principal tensile strain to the period $t=2,56$ sec, x direction (internal view) ..	93
figure 7.8 - deformation to the period $t=2,56$ sec, x direction (internal view).	93
figure 7.9 - principal tensile strain to the period $t=2,56$ sec, x direction (external view)..	94
figure 7.10 - deformation to the period $t=2,56$ sec, x direction (external view).	94
figure 7.11 - displacement request at the top of the buttress obtained from the n2 method.....	95
figure 7.12 - displacement request at the top of the main facade obtained from the n2 method.....	95
figure 7.13 - time-displacement curve at the top of the tower, top of the bottom wall on the left facade, top of the top wall on the left facade, top of buttress and on the vaults. ..	96
figure 7.14 - principal tensile strain to the period $t = 1,86$ sec, y direction (internal view).....	96
figure 7.15 - principal tensile strain to the period $t = 1,86$ sec, y direction (external view).....	97
figure 7.16 - deformation to the period $t = 1,86$ sec, y direction (external view).	97
figure 7.17 - displacement request at the top of the buttress obtained from the n2 method.....	98
figure 7.18 - displacement request at the top of the top wall of the nave obtained from the n2 method.....	98
figure A1.1 - covering made by prefabricated beams a), b).....	A1-5
figure A1.2 - location of the rc elements.....	A1-5
figure A1.3 - eaves before the intervention a), b)	A1-6
figure A1.4 - new eaves a), b).....	A1-6
figure A1.5 - old bell towers roof a), b)	A1-7
figure A1.6 - new bell towers roof a), b), c).....	A1-7

figure A1.7 - building phases a), b), c), d).....	A1-8
figure A1.8 - roof section.....	A1-8
figure A1.9 - maintenance work on the church façades a), b), c), d).....	A1-9
figure A1.10 - phases of frp installation a), b), c), d), e), f).....	A1-10
figure A1.11 - apse collapse a), b), c), d).....	A1-11
figure A1.12 - dome collapse a), b)	A1-12
figure A1.13 - barrel vault collapse a), b).....	A1-12
figure A1.14 - rc tympanum collapse a), b), c).....	A1-13
figure A1.15 - left façade collapse a), b), c), d), e).....	A1-14
figure A1.16 - out-of-plane movement of the main façade a), b), c), d).....	A1-15
figure A1.17 - in-plane movement of the main façade a), b), c), d), e), f).....	A1-16
figure A1.18 - out-of-plane movement of the chapel walls a), b), c), d), e), f).....	A1-17
figure A1.19 - right façade a), b)	A1-18
figure A1.20 - bell towers a), b).....	A1-18
figure A1.21 - chapels vaults collapse a), b), c), d), e), f), g), h), i), l), m), n).	A1-20
figure A2.1 - non-linear analysis of the buttress 1	A2-2
figure A2.2 - non-linear analysis of the buttress 2.....	A2-4
figure A2.3 - collapse mechanism of a single arch.	A2-6
figure A2.4 - collapse mechanism of arch and of both buttresses.	A2-6
figure A2.5 - collapse mechanism of arch and of one buttress.	A2-8
figure A2.6 - collapse mechanism of two consecutive arches case a.....	A2-10
figure A2.7 - collapse mechanism of two consecutive arches case b.	A2-12
figure A2.8 - collapse mechanism of two consecutive arches at the same height.	A2-14
figure A2.9 - collapse mechanism of two consecutive arches with resisting spandrels case a.....	A2-17
figure A2.10 - collapse mechanism of two consecutive arches with resisting spandrels case b.....	A2-19
figure A2.11 - non-linear analysis of the main façade (simply supported).....	A2-21



figure A2.12 - non-linear analysis of the main façade (partially connected). A2-23

figure A2.13 - non-linear analysis of the lower wall of the lateral façade (simply supported)..... A2-25

figure A2.14 - non-linear analysis of the lower wall of the lateral façade (horizontal deflection) A2-27

figure A2.15 - non-linear analysis of the top wall of the lateral façade (vertical deflection). A2-29

figure A2.16 - non-linear analysis of the top wall of the lateral façade (overturning).A2-30

figure A2.17 - non-linear analysis of the top wall of the lateral façade (horizontal deflection) A2-33

figure A2.18 - non-linear analysis of the masonry strip in the lateral facade..... A2-35

figure A2.19 - non-linear analysis of the frontal façade (in -plain movement)..... A2-38

LIST OF TABLES

table 5.1 - seismic action (kinematic analysis)..... 40

table 5.2 - analysis loads. 49

table 6.1 - mechanical properties – reference case..... 74

table 6.2 - mechanical properties – weak buttresses case..... 80

table 7.1 - mechanical properties – dynamic analysis. 89

table 7.2 - seismic action (pushover analysis) 89

1. INTRODUCTION

1.1 GENERAL

In recent years many models have been proposed for the calculation of the seismic response of masonry buildings; they have different levels of detail and different theoretical assumptions. The diversity between theoretical assumptions is often a consequence of the wide variety of objects studied: the masonry walls may differ considerably in material, texture and construction details. Therefore, a single model of absolute applicability and general validity can't be defined. However, it's necessary to identify some basic common elements among all models, in order to avoid significant errors in the prediction of the response. In so doing, these models can be used in a large enough range for practical applications.

1.2 GENERAL OBJECTIVES

This main objective of the present work has consisted of the characterization of the seismic performance of San Marco church, a building located in the historical center of l'Aquila and severely damaged by Abruzzo earthquake of year 2009. The conclusions are drawn from different analyses methods utilized to simulate partial collapse mechanisms that led to the present condition of the church and so explain the surveyed damage condition and crack pattern.

The knowledge gained through the comparison between different calculation techniques, both numerical and analytical methods, may permit the definition of more efficient intervention strategies, which reveal to be extremely important for the preservation of this type of buildings in the case of future seismic events. In fact, an accurate modeling, may contribute to an efficient and optimal strengthening and, in some cases, may allow us to limit intervention to specific elements or parts of the structure that are most vulnerable.

The application of sufficiently reliable models for the analysis of historical masonry buildings is a topic of great practical interest, especially when applied to structures of high historical and artistic value like churches.

This application acquires even more significance if we consider that the Italian legislation, for the evaluation of the seismic risk for existing buildings, requires a global seismic, and the study of local mechanisms.

1.3 SPECIFIC OBJECTIVES

The study of San Marco church is carried out in a rigorous manner, by following the procedures recommended for constructions of the architectural heritage [Linee Guida, 2008; Circolare 617 02/02/2009 and ICOMOS-ISCARSAH recommendations, 2005].

First of all, it is necessary to carry out the following tasks:

- a historical research in order to identify the different construction phases of the building, the geometry, the materials, the quality of the connections between the different structural elements and the possible vulnerabilities;
- a study of the damage and of the collapses experienced during the earthquake. Through the evaluation of the damage and of the cracks it is possible to make assumptions about the structural behavior of the church, the active mechanisms and their activation level.

Secondly, the results obtained through the different calculation techniques for seismic analysis (kinematic analysis, pushover analysis, dynamic in time domain) are compared to

- evaluate their capability to predict the real collapsing mechanisms;
- make consideration of different hypotheses on the collapse of the building;
- prove the reliability of the methods themselves. They are used to check to which extent different hypothesis, typical of each method, may influence the final result;
- calibrate the models by comparing with real collapsing mechanisms;
- draw conclusions on the seismic capacity of the building and needs for strengthening.

Due to their architectural complexity and intrinsic seismic vulnerability, the structures of churches show in many cases a high level of seismic risk. From the study of different case studies it has emerged that, even when the masonry shows good characteristics, the development of mechanisms of collapse is likely due to the loss of equilibrium of different parts behaving as rigid blocks. Consequently, the damages takes place at local level and the structure can be divided into

macroelements which are characterized by a mostly independent structural behaviour from the rest of the building. On the basis of these considerations, the kinematic approach, founded on equilibrium limit analysis, is adopted as a possible criterion to verify the safety of these local mechanisms. For the non-linear static analysis and transient dynamic analysis, the finite element program TNO-DIANA is applied. The aim of using this type of structural analysis software has been to help identify and simulate the mechanisms that led to the current condition of the damaged church.

The three aforementioned calculation methods have been chosen against other available methods for many reasons. Firstly, the experience has shown their accuracy in many cases. Secondly, they are very different from each other, since they are based on different assumptions, and their comparison may provide a more meaningful and deep understanding of the response of the building. Finally, the selected methods provide a realistic simulation of the behavior of the masonry, taking into account the material and geometric non-linearity and the limits of compression and tension.

2. STATE OF THE ART

2.1 EXISTING MASONRY BUILDINGS

Historical or traditional materials such as earth, brick or stone masonry and wood are characterized by very complex mechanical and strength phenomena still challenging our modeling abilities. In particular, masonry is characterized by its composite character (it includes stone or brick in combination with mortar or day joints), a brittle response in tension (with almost null tensile strength), a frictional response in shear (once the limited bond between units and mortar is lost) and anisotropy (for the response is highly sensitive to the orientation of loads).

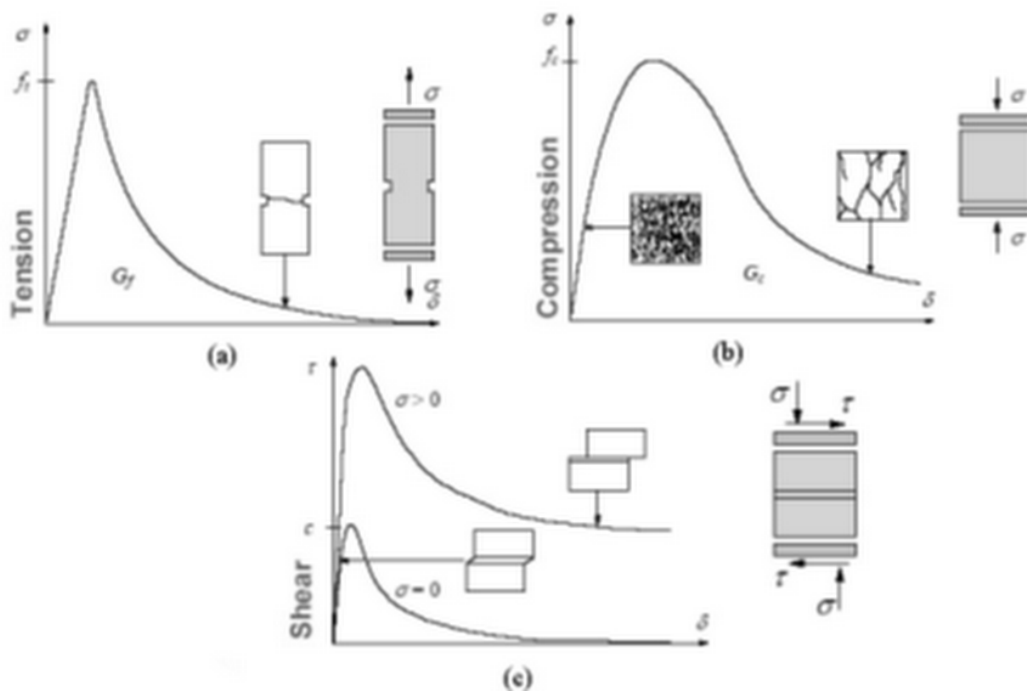


Figure 2.1 - typical behavior of almost-brittle under uniaxial loading: (a) tensile behavior, (b) compression behavior, (C) shear behavior [Pelà, 2009].

Brick and stone masonry are normally very heterogeneous even in a single building or construction member.

Moreover, historical structures often show many additions, repairs done with different materials and show complex internal structures including several layers, filling, material, cavities, metal insertions and other possible singularities. Connections are singular regions featuring specific geometric and morphological

treats. The transference of forces may activate specific resisting phenomena (contact problems, friction, eccentric loading). Modeling morphology and connections in detail may be extremely demanding from a computational point of view. Nevertheless, the main difficulty is found in physically characterizing them by means of minor- or non-destructive procedures. In practice, only limited and partial information can be collected. Additional assumptions on morphology and material properties may be needed in order to elaborate a model.

Historical structures are often characterized by a very complex geometry. . They often include straight or curved members and they combine slender members with massive ones. However, today numerical methods (such as FEM) do afford a realistic and accurate description of geometry.

Moreover this structures may have experienced (and keep on experiencing) actions of very different nature, including the effects of gravity forces in the long term (such as those related to long-term creep), earthquake, environmental effects (thermal effects, chemical or physical attack), and anthropogenic actions such as architectural alterations, intentional destruction, inadequate restorations.

The actions may have caused damage, deformation and they may have had influence on the structural response. These alterations may affect significantly the response of the structure and so they are to be modeled to grant adequate realism and accuracy in the prediction of the actual performance and capacity.

The interaction of the structure with the soil is also to be taken into account except for cases it is judged to be irrelevant. Certain types of analyses, as in particular dynamic one, may require the inclusion of neighboring buildings into the model with an adequate description of existing connections. This is so because of their possible effect on the modal shapes and overall dynamic response. Modeling accurately the dynamic response will often require to construct a global model incorporating all the distinct parts of a complex structure.

2.2 METHODS OF ANALYSIS

2.2.1 Elastic Analysis

Linear elastic analysis is commonly used in the calculation of steel and reinforced concrete structures. However, its application to masonry structures is, in principle,

inadequate because it does not take into account the non-tension response and other essential features of masonry behavior. It must be noted that, due to its very limited capacity in tension, masonry shows a complex non-linear response even at low or moderate stress levels. Moreover, simple linear elastic analysis cannot be used to simulate masonry strength responses, typically observed in arches and vaults, characterized by the development of partialized subsystems working in compression. Attempts to use linear elastic analysis to dimension arches may result in very conservative or inaccurate approaches. Linear elastic analysis is not useful, in particular, to estimate the ultimate response of masonry structures and should not be used to conclude on their strength and structural safety. The linear analysis is often performed, prior to the application of more sophisticated approaches, to allow a quick and first assessment of the adequacy of the structural models regarding the definition of meshes, the values and distribution of loads and reactions, and the likelihood of the overall results.

2.2.2 Limit Analysis

The limit theorems of plasticity can be applied to masonry structures provided the following conditions are verified: (1) the compression strength of the material is infinite; (2) Sliding between parts is impossible; (3) The tensile strength of masonry is null. These conditions enable the application of the well-known limit theorems of plasticity.

In spite of its ancient origin, limit analysis is regarded today as a powerful tool realistically describing the safety and collapse of structures composed by blocks (including not only arches and structures composed of arches, but also towers, façades and entire buildings). It must be remarked,

however, that it can hardly be used to describe the response and predict damage for moderate or service load levels not leading to a limit condition. Strictly speaking, limit analysis can only be used to assess the stability or safety of structures.

Limit analysis is a very realistic method and should be always considered as a complementary tool, or at least as a guiding intuition, when performing alternative computer analyses. Experience shows that, no matter the level of sophistication of

any computer method, it will produce, at ultimate condition, results foreseeable by means of limit analysis.

Based on the observation of real seismic failure modes of historical and traditional buildings in Italy, Giuffré [Giuffrè, 1991 and Giuffrè, 1995] proposed an approach for the study of the seismic vulnerability of masonry buildings based on their decomposition into rigid blocks. The collapse mechanisms are then analyzed by applying kinematic limit analysis. This approach is particularly interesting as a tool for seismic analysis of buildings which do not conform to box behavior because of lack of stiff floor slabs or because of weaker partial collapses affecting the façade or inner walls.

More recently, Giuffré's proposal has experienced renewed interest thanks to the possibility of combining block analysis with the capacity spectrum method [Fajfar, 1999; Lagomarsino et al. 2003 and Lagomarsino, 2006] for the seismic assessment of masonry structures. The method is applied to buildings, churches and towers. The resulting verification methodology has been adopted by the seismic Italian code [Circolare 617 02/02/2009; §C8.7.1.6].

2.2.3 Static and Dynamic Analysis

Static analysis is used to determine the displacements, stresses, strains, and forces in structures or components caused by loads that do not induce significant inertia and damping effects. Steady loading and response conditions are assumed; that is, the loads and the structure's response are assumed to vary slowly with respect to time.

The linear static analysis provides reliable results only for regular buildings in height and with short fundamental period, structures without significant torsional modes and for which the first vibration mode dominates the seismic response (the mass involved in the first vibration mode must be 90% of the total mass). It involves the application of a system of horizontal static forces applied in the masses barycenter on the various floors of the structure. It allows the calculation of the stresses and deformations induced by the earthquake. In addition to the eccentricity effect, an accidental eccentricity and an amplification

factors, which takes account of accidental torsion phenomena, are also taken into account [DM 14/01/2008; §7.3.3.2].

The linear dynamic analysis allows for decoupling the dynamic response of a structure in the response of each individual mode so that contributes to the overall response (mode with participating mass of more than 5% or the total mass of which participant is greater than 85%). The response is calculated for each individual vibration mode through the spectrum of design. The total stresses and total deformations can be obtained through methods that allows to summate the individual responses [DM 14/01/2008; §7.3.3.1].

Non-linear static analysis allows the incrementally application, to a model under to gravity loads and with non-linear behavior of the material, of two different distributions of horizontal static forces. These forces have the task of pushing the structure in the non-linear condition until it collapses. The result of the analysis is the capacity curve (base shear - displacement of a control point considered significant for the global behavior). The pushover is based on the assumption that it is possible to compare the seismic response of the real structure with that of a simple oscillator with one degree of freedom. The traditional pushover method does not take into account that the applied forces create damage in the structure which in turn changes the period and the structure vibrate mode. The more sophisticated methods change, while the analysis progresses, the distribution of the applied forces, in order to take account of the effect of stiffness degradation with the entry in the elastic range [DM 14/01/2008; §7.3.4.1].

Non-linear dynamic analysis (sometimes called time-history analysis) is a technique used to determine the dynamic response of a structure under the action of any general time-dependent loads. You can use this type of analysis to determine the time-varying displacements, strains, stresses, and forces in a structure as it responds to any combination of static, transient, and harmonic loads. The time scale of the loading is such that the inertia or damping effects are considered to be important [DM 14/01/2008; §7.3.4.2].

2.3 STRUCTURE MODELING

2.3.1 Extensions of Matrix Calculation for Linear Members

The limitations of linear elastic analysis, on the one hand, and limit analysis, on the other hand, can be partly overcome by means of simple generalizations of matrix calculation of frame structures, extended with (1) Improved techniques for the description of complex geometries (curved members with variable sections) and (2) Improved description of the material (for instance, including simple constitutive equations yet affording the consideration of cracking in tension and yielding / crushing in compression, yielding in shear).

These tools are, in principle, only applicable to 2D or 3D systems composed of linear members (namely, skeletal structures). However, there are some proposals to treat 2D members (vaults, walls) as equivalent systems composed of beams.

In fact, the application of conventional frame discretization yields inaccurate results when dealing with shear wall systems [Karantoni and Fardis, 1992]. However, these results can be improved through the definition of a set of special devices to represent more realistically the shear deformation of the walls.

2.3.2 Use of Rigid and Deformable Macro-elements

Important research efforts have been devoted to the development of computational approaches based on rigid and deformable macro-elements. Each macro-element models an entire wall or masonry panel, reducing drastically the number of degrees of freedom of the structure. Brencich, Gambarotta and Lagomarsino (1998) use two nodes macro-elements taking into account the overturning, damage and frictional shear mechanisms experimentally observed in masonry panels. The overall response of buildings to horizontal forces superimposed to the vertical loads is obtained by assembling shear walls and flexible floor diaphragms.

2.3.3 FEM Based Approaches:

Macro-Modeling, Micro-Modeling and Discontinuous Models

The finite element method offers a widespread variety of possibilities concerning the description of the masonry structures within the frame of detailed non-linear analysis.

Most of modern possibilities based on FEM fall within two main approaches referred to as macro-modeling and micro-modeling. Macro-modeling is probably the most popular and common approach due to its lesser calculation demands. In practice-oriented analyses on large structural members or full structures, a detailed description of the interaction between units and mortar may not be necessary. In these cases, macro-modeling, which does not make any distinction between units and joints, may offer an adequate approach to the characterization of the structural response. The macro-modeling strategy regards the material as a fictitious homogeneous orthotropic continuum. A complete macro-model must account for different tensile and compressive strengths along the material axes as well as different inelastic properties along each material axis. This type of modeling is most valuable when a compromise between accuracy and efficiency is needed.

The macro-models, also termed Continuum Mechanics finite element models, can be related to plasticity or damage constitutive laws. A drawback of the macro-modeling approach lays in its description of damage as a smeared property spreading over a large volume of the structure. In real unreinforced masonry structures, damage appears normally localized in isolate large cracks or similar concentrated lesions. A smeared modeling of damage provides a rather unrealistic description of damage and may result in predictions either inaccurate or difficult to associate with real observations.

The so-called detailed micro-models describe the units and the mortar at joints using continuum finite elements, whereas the unit-mortar interface is represented by discontinuous elements accounting for potential crack or slip planes. Detailed micro-modeling is probably the more accurate tool available to simulate the real behavior of masonry. It is particularly adequate to describe the local response of the material. Elastic and inelastic properties of both unit and mortar can be realistically taken into account.

The micro-modeling approaches are suitable for small structural elements with particular interest in strongly heterogeneous states of stress and strain. The primary aim is to closely represent masonry based on the knowledge of the properties of each constituent and the interface. The necessary experimental data must be obtained from laboratory tests on the constituents and small masonry samples. Nevertheless, the high level of refinement required means an intensive computational effort (i.e. great number of degrees of freedom of the numerical model), which limits micro-models applicability to the analysis of small elements (as laboratory specimens) or small structural details.

Macro-models encounter a significant limitation in their inability to simulate strong discontinuities between different blocks or parts of the masonry construction. Such discontinuities, corresponding either to physical joints or individual cracks formed later in the structure, may experience phenomena such as block separation, rotation or frictional sliding which are not easily describable by means of a FEM approach strictly based on continuum mechanics. A possible way of overcoming these limitations consists of the inclusion within the FEM mesh of joint interface-elements to model the response of discontinuities.

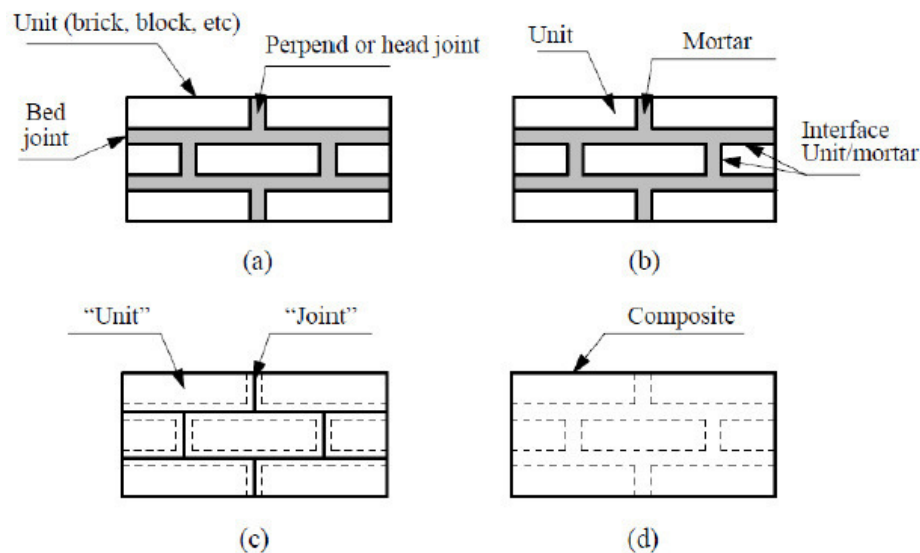


Figure 2.2 - a) modular element of a masonry panel, b) detailed micro-modeling, c) simplified micro-modeling, d) macro-modeling [Pelà, 2009].

2.3.4 Homogenization

Midway between micro-modeling and macro-modeling stands the so-called homogenized modeling. If the structure is composed by a finite repetition of an elementary cell, masonry is seen as a continuum whose constitutive relations are derived from the characteristics of its individual components, namely blocks and mortar, and from the geometry of the elementary cell. Most of the methods of homogenization simplify the geometry of the basic unit with a 2 step introduction of vertical and horizontal joints and thus without taking into account the regular offset of vertical mortar joints. However, this kind of approach results in significant errors when applied to non-linear analysis.

The main advantages of this method, compared with classical micro-modeling, are the following: (1) the finite element mesh does not have to reproduce the exact pattern of the masonry units nor it has to be so fine. The structure can be meshed automatically.

(2) Once the homogeneous properties have been calculated from the micro-mechanical model, standard finite element method can be used to perform the analysis avoiding the complications introduced by elements interfaces.

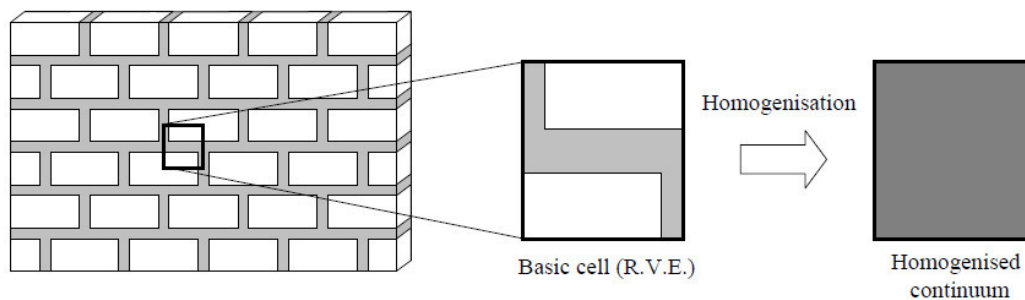


Figure 2.3 - Basic cell for masonry and homogenization process [Lourenço, 2007].

2.3.5 Discrete Element Method

The Discrete element method (DEM) is characterized by the modeling of the material as an assemblage of distinct blocks interacting along the boundaries. The name “discrete element” applies to a computer approach only if (1) it allows finite displacements and rotations of discrete bodies, including the complete detachment

and (2) it can recognize new contacts between blocks automatically as the calculation progresses.

The common idea in the different applications of the discrete element method to masonry is the idealization of the material as a discontinuous material where joints are modeled as contact surfaces between different blocks. This approach affords the modeling of various sources of non-linear behavior, including large displacements, and suits the study of failures in both the quasi static and dynamic ranges [Roca et al. (2010)].

The typical characteristics of discrete element methods are: (a) the consideration of rigid or deformable blocks (in combination with FEM); (b) connection between vertices and sides /faces; (c) interpenetration is usually possible; (d) integration of the equations of motion for the blocks (explicit solution) using the real damping coefficient (dynamic solution) or artificially large (static solution). The main advantages are an adequate formulation for large displacements, including contact update, and an independent mesh for each block, in case of deformable blocks. The main disadvantages are the need of a large number of contact points required for accurate representation of interface stresses and a rather time consuming analysis, especially for 3D problems [Lourenço, 2007].

3. SAN MARCO CHURCH

3.1 HISTORICAL RESEARCH

The San Marco's church is located in the city of L'Aquila, Abruzzo, precisely between Via de Neri and Piazza della Prefettura. It was one of the first churches to be built in the capital of Abruzzo in the second half of the XIII century, thanks to the initiative of the inhabitants of Pianola. This particular aspect highlights how strongly this church is regarded by the citizens as a symbolic element which makes it extremely important to secure “la memoria del luogo”.



Figure 3.1 - Localization of the San Marco church.

The present building is the result of three historical moments and three architectural phases: the medieval age, the XVI century and the Baroque of the XVIII century.

The building stands in a narrow rectangular area and lays on a stone foundation that is typical of the XIII century, when the temple was built.

Medieval traces can mainly be found on the outer walls and in the side portal of the XIV century; on the contrary, the portal opening onto the main facade appears to be more recent. The main facade and the right side of the building, which consist of the typical “apparecchio aquilano”, date back approximately to the XV century. On the left side there were some buildings that were demolished after the earthquake of 1703. At that time the wall of this side was rebuilt.

The church is set on a simple plan with a single nave, marked by chapels on its sides and ends in a semicircular apse. The side compartments are presumably the repetition of a sixteenth-century scheme, characterized by the construction of masonry vaults and the opening of chapels.

After the earthquake of 1703 it was necessary to rebuild the building. Exactly in this period the top of the facade was raised, together with the construction of the two towers and the re-arrangement of the presbytery. In the twenties, the Piazza della Prefettura, was finally re-organized as it appears today. During this working phase, two main changes occurred on the left side of the church: the ogival portal was added and two windows were replaced with single trefoil ogives.

3.2 DESCRIPTION OF THE BUILDING

It was not possible to perform a direct geometric survey and therefore it was taken from the report entitled “Chiesa Di San Marco – L’Aquila” and made by the Politecnico di Milano (2009).

The church of San Marco follows a regular plant, it is about 16 meters long and 48.8 meters wide. It consists of a single nave with three chapels on each side, which leads to a semicircular apse. The vaults of the side chapels are made up of mixed masonry stone and brick. The “frenelli” was made up of heterogeneous material (fragments of tiles and stones) juxtaposed without mortar.

In the front of the apse a core cross is created by the presence of two large lateral niches, covered with a dome very depressed at their center. The rest of the nave is covered by a barrel vault made of “cannucciato” (reed) with wooden beams on the extrados and embedded in the walls.

The longitudinal vault of the nave is divided into six transverse arches of brick that connect the wall from north to south and leaning on the side buttresses create small side chapels along the nave.

The light enters through eight large windows located at the bottom of the barrel vault and through six small windows at the top of the chapels.

The main building material is, definitely, the stone, it seen in the facades of churches, and it is covered with plaster inside. Inside consists, mostly, of small square stones while the dome and arches are made of bricks. Outside are observed both regular stones that not regular and stone of different forms except that in the main facade which it consists entirely of white ashlar.

The surveys carried out before the earthquake of April 2009 are reported below.

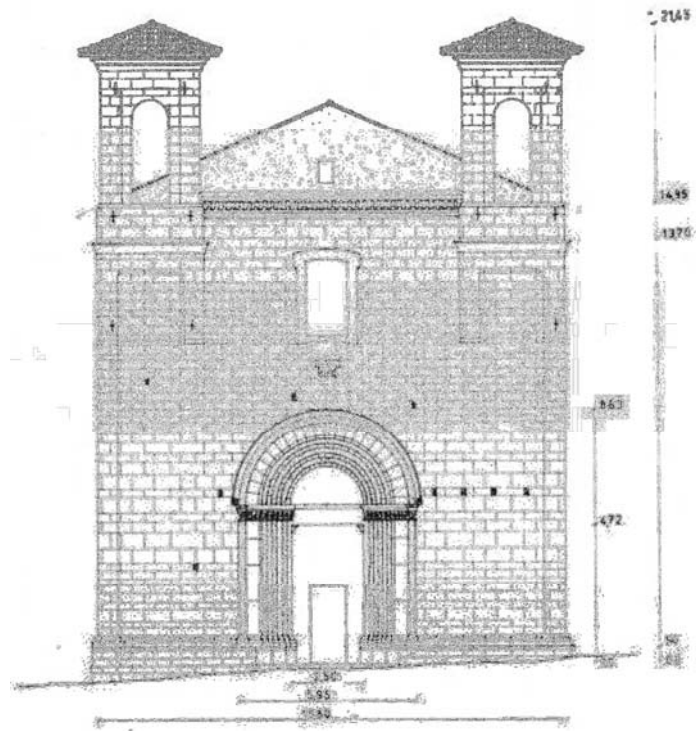


Figure 3.2 - Main façade.

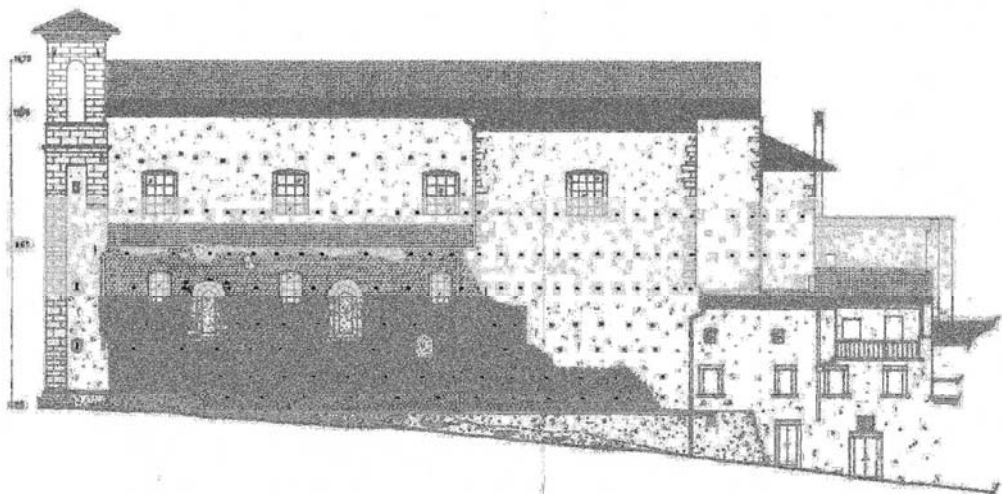


Figure 3.3 - North elevation – Via de Neri.



Figure 3.4 - South elevation – Piazza della Prefettura.

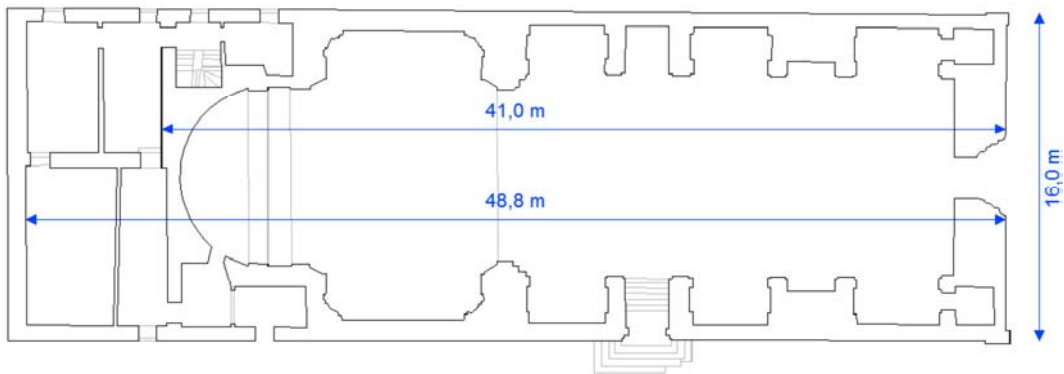


Figure 3.5 – Plant.



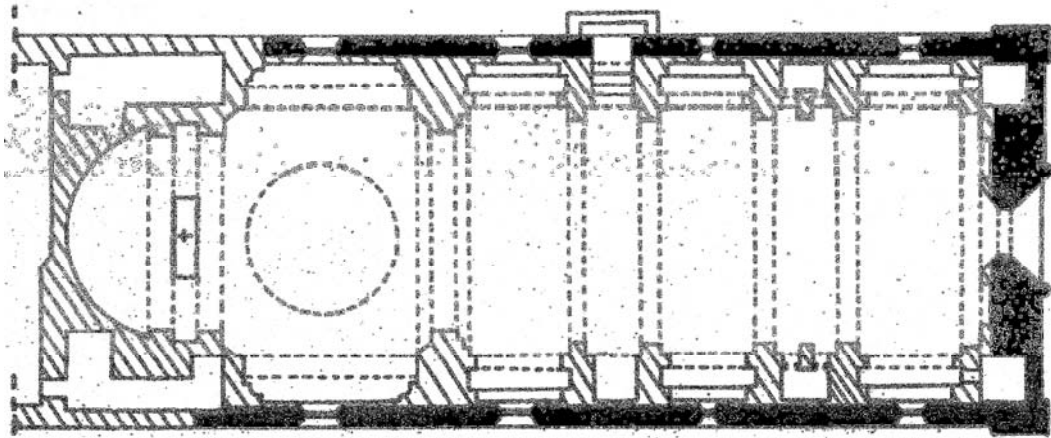


Figure 3.6 - Black indicates the masonry of the XIII century.

SEZIONE B-B

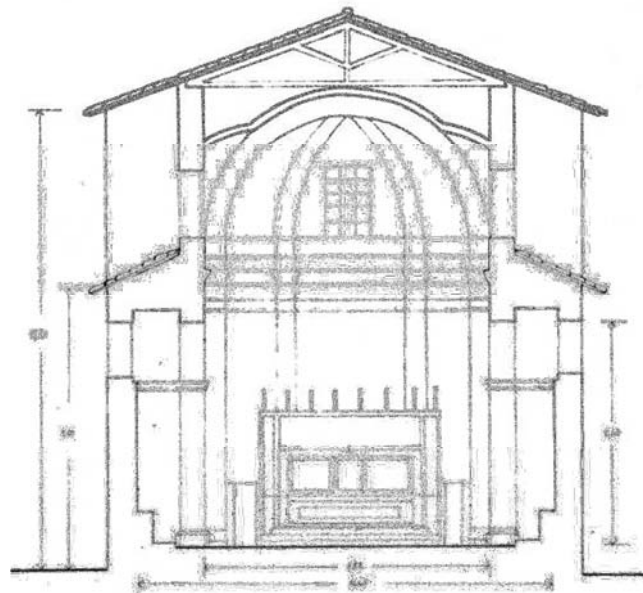


Figure 3.7 – Transverse section.

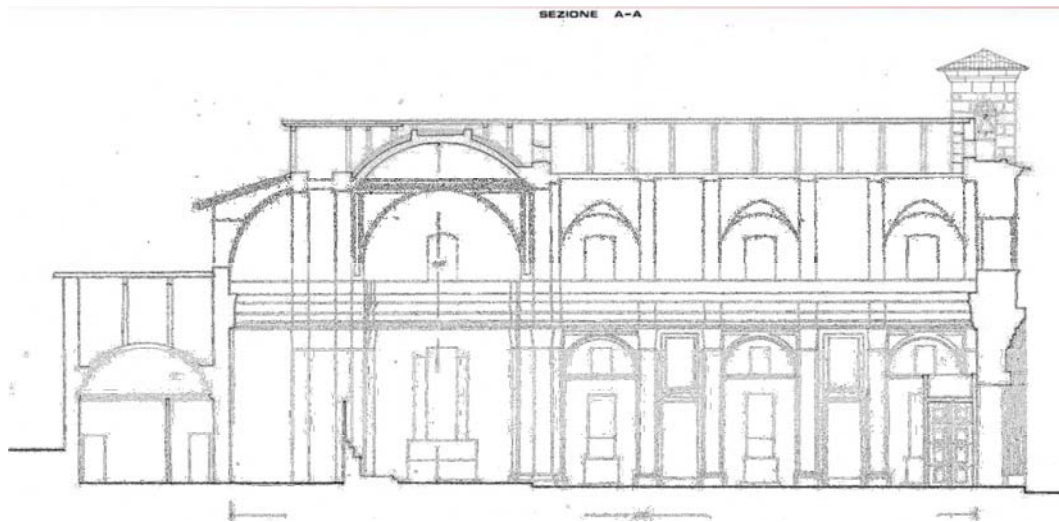


Figure 3.8 - Longitudinal section.

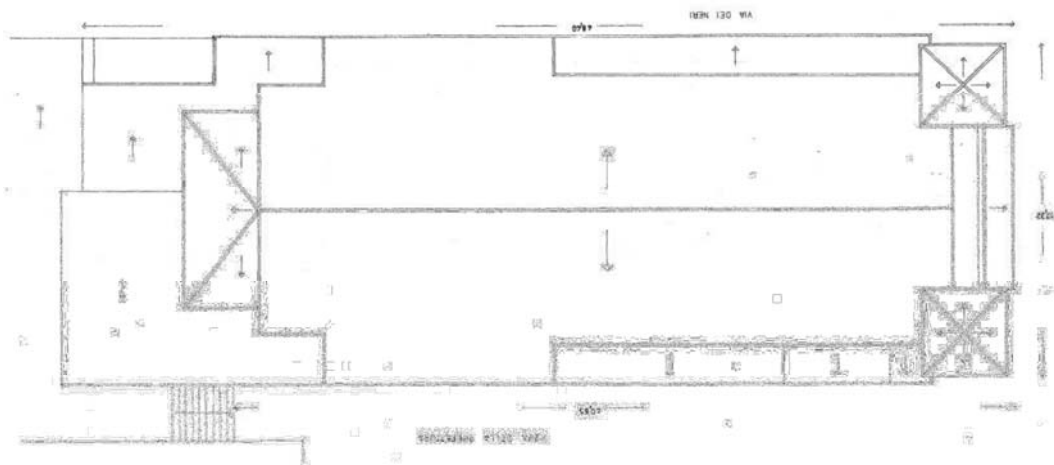


Figure 3.9 - Covering.

3.3 INTERVENTIONS

The main interventions that underwent the San Marco church were performed in 1970, 2005 and 2007.

Interventions in 1970:

- Remove the old wooden roof and replacing it with one made in prefabricated beams and hollow flat blocks bricks. In order to make this type of self-supporting coverage of the steel tie rods were positioned parallel to the warping in correspondence of each joist. The ridge beam, on which the joists are joined, however, was built in situ.

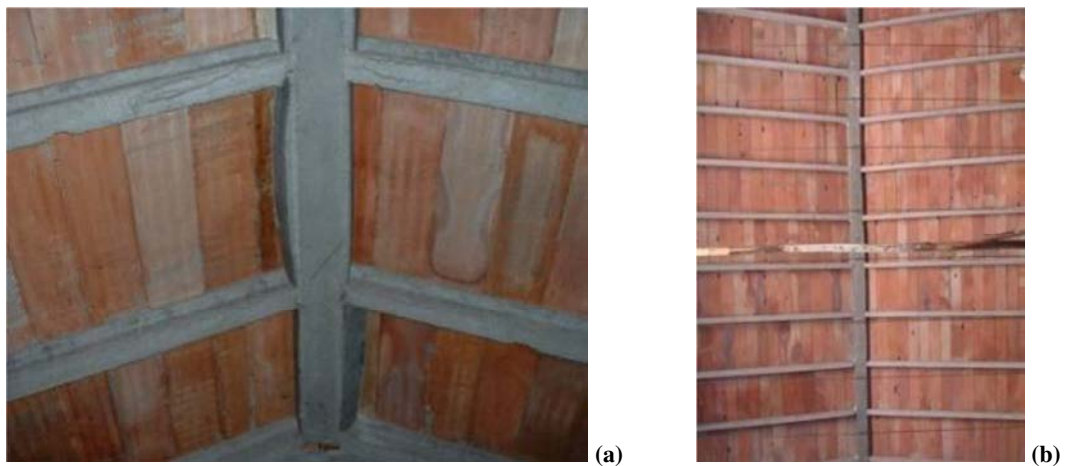


Figure 3.10 - Covering made by prefabricated beams.

- It was also made a box in R.C. placed over the presbytery, specifically in the central part of the transept. This structure is formed by two R.C. beams, parallel to the main aisle and two R.C. tympanums places in the transverse direction, one that separates the transept from the aisle and the other which delimits the transept from the apse. The box in R.C. has been designed to make sure that the weight of the cover does burdensome to dome but on the two tympanums; although this system, while

downloading mainly on the perimeter walls, exerts a distributed load on the arches.

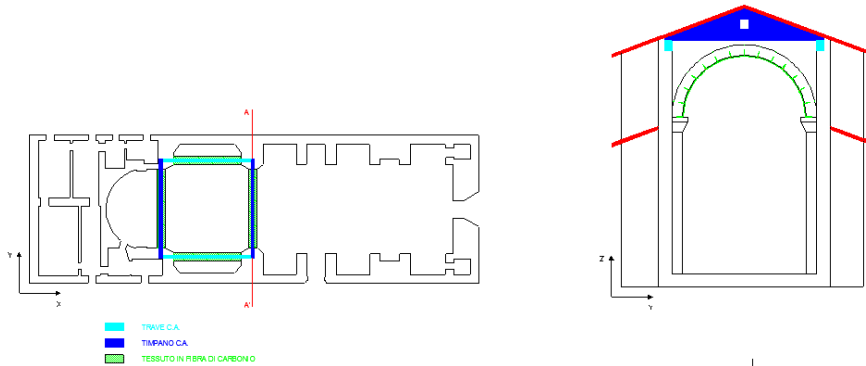


Figure 3.11 - RC elements.

Interventions in 2005:

- Replacing the old eaves which were affected by diffused vegetation and a high state of degradation.

Its supporting structure was performed with wooden elements of rectangular cross-section fixed on the outer walls. The anchored part of these joists was then covered with a layer of cement mortar on which was applied a layer of insulation. Above this plan were laid planks of wood, which were lying on the tiles.



Figure 3.12 - New eaves.

- Installation of a wooden roof on the bell towers and replacement of old containment ties. The old wooden roof of the two belfries has been replaced with a more wood but with metal reinforcements applied to connections. Above this structure has been applied a state insulation which also performs the function of support for the tiles.



Figure 3.13 - New bell towers roof.

- Waterproofing of the roof of the church and the installation of thermal insulation over the entire church.

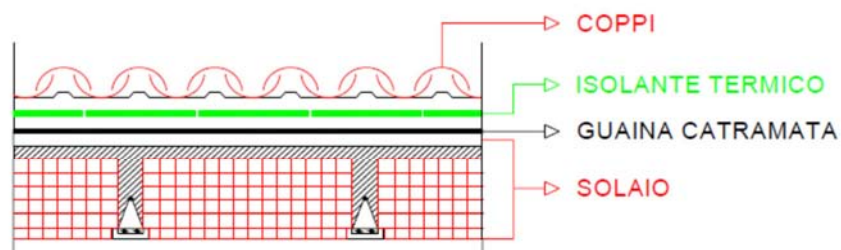


Figure 3.14 - Roof section.

- Maintenance of the lateral facades and main façade and consolidation of the front facade divided into:
 - Clean the lateral and frontal façades with a water jet;
 - Closing the joints with compatible mortar;
 - Injection of localized areas on the frontal façade, with the objective of improving the connection between the external stones of regular masonry and the internal ones composed by irregular masonry.

Interventions in 2007:

- Application of Carbon Fibre on the intrados of the arches of the dome in the transept.

At the center of the transept is the dome, which rests on four perimeter arches. The application process consists mainly of:

- Injection of the central part of the arch;
- Regularization of the surface with mortar;
- Application of the glue over the regularized surface;
- Application of the carbon fiber layers;
- Fixation of the C.F. layers to the arches using C.F strings;
- Final regularization layer applied over the C.F. layers

4. PRESENT STATE

The inspection after the earthquake has revealed severe damage to the church immediately after the earthquake. In particular, the total collapses were detected in the apse, the collapse of two arches on which set the dome of the transept, a portion of the wall of the lateral façade in the left side, a considerable portion of the chapels in the left side, the separation of right facade from its orthogonal walls, and the almost total collapse of the barrel vault of the nave. Instead the tie beams, in the bell towers, ensured a good response abutment towers during the seismic shock.

It is presented below the crack found:



Figure 4.1 – San Marco church, left façade.

5. KINEMATIC ANALYSIS

5.1 INTRODUCTION

Often, the existing masonry buildings don't have connection elements between the walls, at the level of the horizontal structures; this involves a vulnerability to local mechanisms. These vulnerabilities can cause loss of balance not only of individual walls, but also of wider portions of the building. Local mechanisms occur in masonry walls mainly for actions that are orthogonal to their plane, while in the case of arc systems also for actions in the plan.

The checks may be carried out through the limit equilibrium analysis, according to the kinematic approach, whose basic hypotheses are:

- non-tensile strength of masonry,
- unlimited compressive strength,
- monolithic masonry that can be represented as rigid block.

The kinematic analysis is used to evaluate the entity of the horizontal acceleration that starts the mechanism and for the estimation of the displacement ultimate capacity.

The objective of this analysis is to identify, for each mechanism, the collapse coefficient $c = \frac{a}{g}$ and to define the first mechanism that will be activated.

Applying the principle of virtual work for each chosen mechanism, it's possible to estimate the overall seismic capacity in terms of resistance (linear kinematic analysis) and of displacement by evaluating finite shifts (non-linear kinematic analysis) [Circolare 617 02/02/2009; §C8A.4].

The seismic coefficient c , that induces the loss of equilibrium, is obtained evaluating the rotations between the blocks due to the kinematic mechanism, only considering their geometry.

The seismic performance of the structure is analyzed till to the collapse ($c=0$) by increasing the displacement d_k of a properly chosen control point and applying the principle of virtual works to the corresponding configurations.

The curve obtained through the incremental kinematic analysis can be transformed into the equivalent SDOF system capacity curve. A comparison between the displacement ultimate capacity and the displacement request can be done.

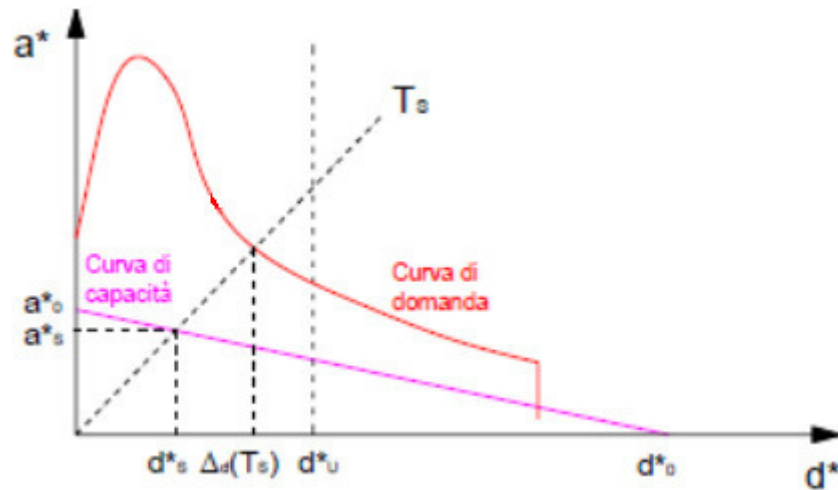


Figure 5.1 - Non-linear analysis with the kinematic approach.

The parameters used in the analysis are the following:

Mass involved:

$$M^* = \frac{\left(\sum_{i=1}^{n+m} P_i \delta_{x,i} \right)^2}{g \sum_{i=1}^{n+m} P_i \delta_{x,i}^2} = \quad (5.1)$$

Fraction of mass involved:

$$e^* = \frac{g \cdot M^*}{\sum_{i=1}^{n+m} P_i} \quad (5.2)$$

Spectral acceleration which activates the mechanism:

$$a_0^* = \frac{\alpha_0 \cdot \sum_{i=1}^{n+m} P_i}{M^* \cdot F_C} \quad (5.3)$$

Checking SLU with **LINEAR ANALYSIS** [DM 14/01/2008; §7.8.2.2] :

$$a_0^* \geq \max \left(\frac{a_g(0.10) \cdot S}{q}; \frac{S_e(T_1) \cdot \frac{Z}{H} \cdot \frac{3N}{2N+1}}{q} \right) \quad (5.4)$$

Where:

Z: height between the bottom of the blocks involved in the mechanism and the foundation of the building

H: structure height

N: number of floors of the building

$$q = 2$$

Checking SLU with **NON-LINEAR ANALYSIS** [DM 14/01/2008; §7.3.4.1] :

$$d_u^* \geq \max \left(S_{De}(T_s); S_{De}(T_1) \cdot \frac{Z}{H} \cdot \frac{3N}{2N+1} \cdot \frac{\left(\frac{T_s}{T_1}\right)^2}{\sqrt{\left(1 - \frac{T_s}{T_1}\right)^2 + 0.02 \frac{T_s}{T_1}}} \right) \quad (5.5)$$

Where:

Spectral displacement of the equivalent oscillator with 1 degree of freedom:

$$d_0^* = d_{k0} \cdot \frac{\sum_{i=1}^{n+m} P_i \delta_{x,i}^2}{\delta_{x,k} \sum_{i=1}^{n+m} P_i \delta_{x,i}} \quad (5.6)$$

Control point displacement (barycentre of the seismic masses):

$$d_{k0} = h_{bar} \cdot \sin \theta_{k0} \quad (5.7)$$

Final spectral displacement: $d_u^* = 0,4 \cdot d_0^*$ (5.8)

Secant period: $T_s = 2\pi \sqrt{\frac{d_s^*}{a_s^*}}$ (5.9)

Where: $d_s^* = 0.40 \cdot d_u^*$ (5.10) $a^* = a_0^* \cdot \left(1 - \frac{d_s^*}{d_0^*}\right)$ (5.11)

In order to perform this analysis it is necessary to define some parameters like the seismic action and the confidence factor. Since it wasn't possible to obtain accurate values to the soil resistant capacity, it was assumed in this analysis a type B foundation soil and topographic amplification coefficient equal to 1.

The seismic action has been calculated using the program "Spettri NTC 2008" and values obtained are as follows:

Peak ground acceleration	a_g	0.300g
Maximum spectral amplification factor	F_0	2.384
Period corresponding to the beginning of the section with constant speed of the horizontal acceleration spectrum	T_c^*	0.356 s
Nominal lifetime of the building	V_N	50
Importance factor	C_u	1.15
Probability of exceedance	P_{VR}	10%
Structure factor	q	2.25
Type soil	B	
Amplification stratigraphic coefficient	S_S	1.114
	C_C	1.352
Amplification topographic coefficient	S_T	1.000
Period corresponding to the beginning of the spectrum section with constant acceleration	T_B	0.161 s
Period corresponding to the beginning of the spectrum section with constant speed	T_C	0.482 s
Period corresponding to the beginning of the spectrum section with constant displacement	T_D	2.799 s

Table 5.1 – Seismic action (kinematic analysis).

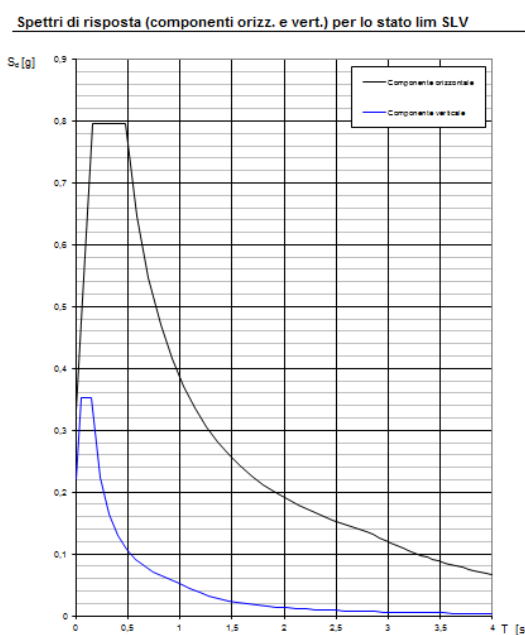


Figure 5.2 – Elastic response spectrum [Program Spettri NTC 2008].

San Marco church is a building of significant historical and cultural interest, it is locating in an old town, so for the calculation of the confidence factor were added the various factors confidence partial, as specified by Italian Guidelines [Linee Guida; §4.2] assuming:

Geometric survey complete with graphic rendering $FC1 = 0$

Limited relief material and construction details $FC2 = 0.12$

Limited investigation of mechanical properties of materials $FC3 = 0.06$

Limited investigations on the ground and in the absence geological data $FC4 = 0.06$.

For an FC result of 1.24.

Rilievo geometrico	Rilievo materico e dei dettagli costruttivi	Proprietà meccaniche dei materiali	Terreno e fondazioni
Rilievo geometrico completo $F_{C1} = 0.05$	Limitato rilievo materico e dei dettagli costruttivi $F_{C2} = 0.12$	Parametri meccanici desunti da dati già disponibili $F_{C3} = 0.12$	Limitate indagini sul terreno e le fondazioni, in assenza di dati geologici e disponibilità d'informazioni sulle fondazioni $F_{C4} = 0.06$
Rilievo geometrico completo, con restituzione grafica dei quadri fessurativi e deformativi	Esteso rilievo materico e degli elementi costruttivi $F_{C2} = 0.06$	Limitate indagini sui parametri meccanici dei materiali $F_{C3} = 0.06$	Disponibilità di dati geologici e sulle strutture fondazionali; limitate indagini sul terreno e le fondazioni $F_{C4} = 0.03$
$F_{C1} = 0.0$	Esaustivo rilievo materico e degli elementi costruttivi $F_{C2} = 0.0$	Estese indagini sui parametri meccanici dei materiali $F_{C3} = 0.0$	Estese o esaustive indagini sul terreno e le fondazioni $F_{C4} = 0.$

Figure 5.3 – Partial confidence factor [Linee Guida; §4.2].

5.2 DAMAGE MECHANISMS ACTIVATED

For the kinematic analysis the failure mechanisms that appeared to be more significant and that may have influenced the structural behavior of the upper wall of the side facade were selected [Modello A-DC, 2006].

- **MAIN FAÇADE:**

In the subsequent analysis of the front facade two different types of collapse mechanism were considered: the-out-of plane movement of a monolithic wall which was not connected but simply supported to the orthogonal walls, and the movement in the plane of a limited portion of the wall. Initially, for the calculation of the first mechanism, the facade was hypothesized as totally disconnected from the orthogonal walls. Subsequently it was imagined as effectively connected at least up to the highest part of the lower wall on the left façade.

Out-of-plane movement

Vertical cracks on the connection between frontal and lateral facades indicate the activation of the façade overturning and the formation of a cylindrical hinge, to horizontal axis, by the strong foundations. The main structural causes of this mechanism are the weak connection with the orthogonal walls and the absence of links on the top.

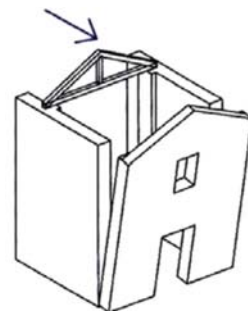




Figure 5.4 - Out-of-plane movement of the main façade.

In-plane mechanism

Inclined shear cracks in the facade show its response in its plane. These cracks cross all the wall section and their direction is influenced by the presence of the opening in the center of the facade.

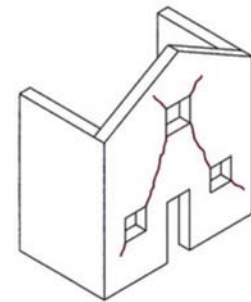




Figure 5.5 - In-plane movement of the main façade.

- **LEFT FAÇADES:**

For the analysis of the left side facade different types of mechanisms were considered.

As regards the lower wall, the out of plane movement of a solely supported wall and the horizontal deflection of a monolithic wall not effectively confined were verified.

For the top wall, instead, the coefficient of collapse in the case of vertical deflection of a monolithic wall, the overturning and the horizontal deflection were calculated.

The horizontal deflection occurs in the case in which the walls are effectively connected to the orthogonal walls but not confined in respect of movements in the plane or in the absence of constraint in the top. It is studied in the case where this flexion occurs for horizontal instability due to removal of the orthogonal walls and not for the crushing of the material.

The vertical deflection occurs in the case in which the walls are effectively connected on the top and, consequently, to the roofing beams, but present a lack of connection with the orthogonal walls. This connection prevents from the overturning of the whole section. Nevertheless, in the point where the resultant of the forces touches the outer edge of the section, a cylindrical hinge dividing the wall into two blocks will appear.

Moreover, we studied the possible horizontal deflection of the masonry strip between the two covers, different in height, on the left side facade. This strip is assumed to be well connected to the wall of the transept and to the buttress which is located in the point where the height of the cover changes. The flexion in this section is therefore due to the instability of the buttresses.



Figure 5.6 - Lateral façade.

- **CHAPELS:**

Out-of-plane movement of the buttresses

In the area of the lateral chapels it's possible to notice both the separation of the buttresses from the lateral facade and their out of plane movement. Also, the visible horizontal cracks near the base of the pillars show the transversal behavior of the church and the loss of pillar material caused by a tension / compression phenomenon which is the result of the cyclic transversal movement of the church during the earthquake.

It's important to stress that the church was originally designed with a single nave and that the lateral chapels were built later. This aspect might imply a weak connection between the side facades and the buttresses of the chapels. The overturning of the buttresses was therefore calculated regarding them as totally disconnected from the bottom wall of the side facade. In order to consider the horizontal and vertical loads deriving from both vaults connected to the buttress, the wall was divided into three parts, each of which ended in a loads application point.



(a)



(b)



Figure 5.7 – Out-of-plane movement of the chapel walls.

Chapels vaults

The vaults of the chapels in the left nave are almost fully collapsed.

The test of this collapse was divided into four parts. Firstly, we calculated the activation coefficients of the mechanism related only to the arch, without taking into account the buttresses. Secondly, we hypothesized the possible overturning of one and then of both buttresses at the base of the arch. Finally, the last estimated case of loss of balance concerned the union of the 2-3 vaults.

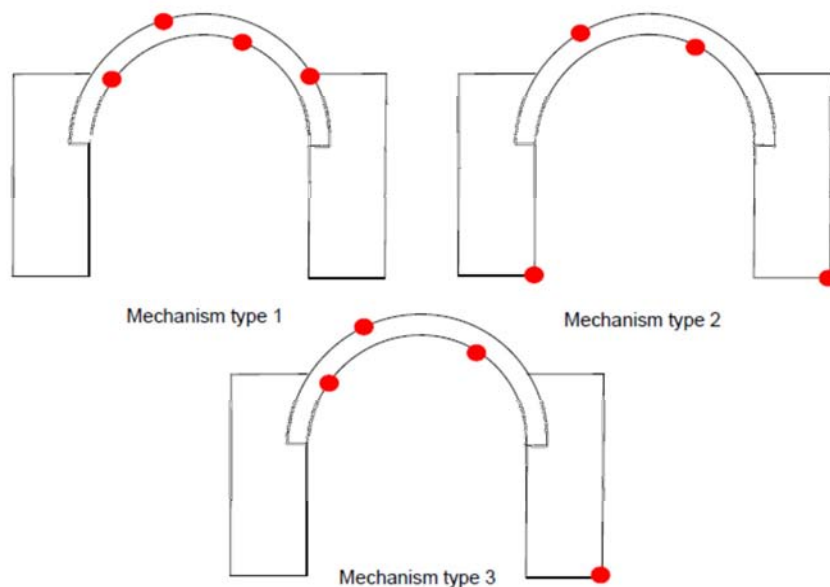


Figure 5.8 - Arches collapse mechanisms.



Figure 5.9 – Chapels vaults collapse.

In order to perform this analysis, besides the previously defined seismic action it is necessary to set the geometrical properties, the material properties and the applied loads.

The geometrical properties and the material properties of the different elements of the church were obtained from previous studies carried out on the church of San Marco [Zografou, 2010 and Niker Project , 2012].

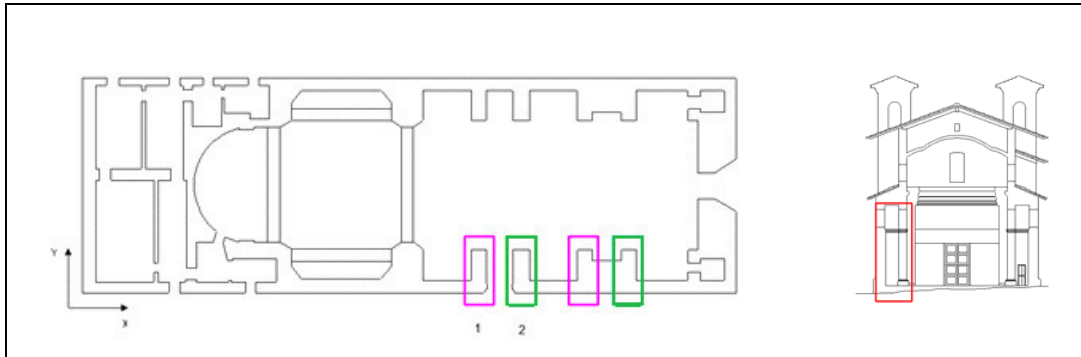
The loads are reported in the following table:

Analysis loads			
Upper wall (left facade)	120	KN/m	
Lower wall (left facade)	152	KN/m	
Roof	39.24	KN/m	
Chapels roof	12.26	KN/m	
Big vaults	$N_v = 15.9$	KN/m	$N_o = 5.8$ KN/m
Small vaults	$N_v = 10.7$	KN/m	$N_o = 3.9$ KN/m
Wall on small vaults	1.6	KN/m	
Bell tower	440	KN	

Table 5.2 – Analysis loads.

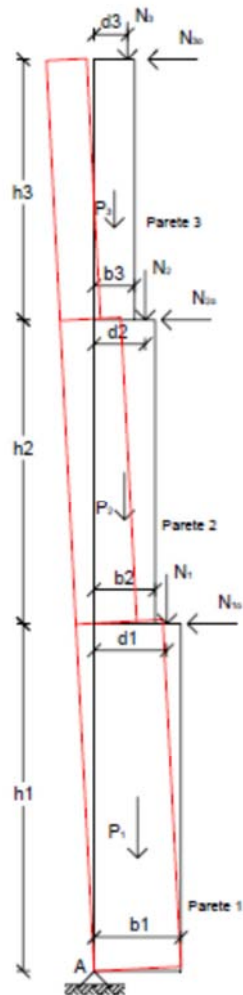
The most significant results of the kinematic analysis for the identification of the main and real collapse mechanism are reported below. The other analysis can be found in ANNEX 2 – CALCULATION.

5.3 EARTHQUAKE X DIRECTION



Out of plane movement of a monolithic wall simply supported

Buttress 1:



Geometrical properties

H1	3.5	m
B1	0.85	m
H2	2.5	m
B2	0.85	m
H3	2	m
B3	0.85	m
H _{tot}	8	m

Loads

P1	59.5	KN
N1	12.8	KN
N1o	-3.9	KN
D1	0.14	m
P2	42.5	KN
N2	15.9	KN
N2o	5.8	KN
D2	0.70	m
P3	34	KN
N3	275.35	KN
D3	0.45	m

Material properties

f _c	4	MPa
f _t (5% f _c)	0.2	MPa
γ	20	KN/m ³

$$c = \frac{a}{g} = 0.060$$

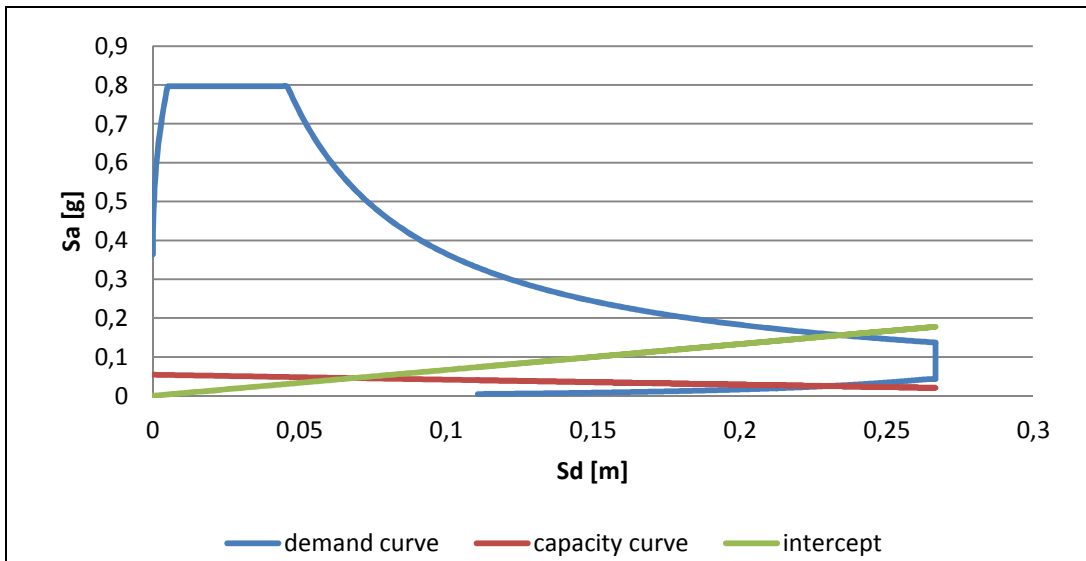


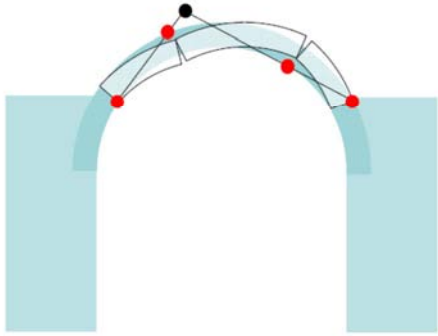
Figure 5.10 - Non-linear analysis of the buttress.

Mass involved	M^*	99.34	Kg	
Fraction of mass involved	e^*	0.92		
Spectral acceleration which activates the mechanism	a_0^*	0.053g		
Final spectral displacement	d_u^*	0.171	m	
SLU WITH LINEAR ANALYSIS	a^*	0.167g		NOT CHECKED
SLU WITH NON LINEAR ANALYSIS	Δd	0.235	m	NOT CHECKED

By performing the non-linear analysis, the value obtained was $d_u^* = 0.171$ m, while the value required by the Italian code was $\Delta d = 0.235$ m. The calculated value is very far from the required one. The buttress has been divided into three part and to the upper end of each part were applied loads due to:

- the geometry and the self-weight of the smallest vault, the dead load of the wall resting on the smaller vault,
- the geometry and the self-weight of the biggest vault,
- the dead load of the upper wall of the lateral façade and of the roof.

The horizontal force of the vault, that is associated to its geometry, contributes to the calculation of stabilizing-overturning moment. However, this force isn't linked to a mass and therefore mustn't be counted in the calculation of the inertia force and in the calculation of the mass involved in the mechanism.

Loss of balance of a single arch			
Arch:			
 <p>Mechanism type 1</p>	Geometrical properties		
	Re	2.28	m
	Ri	2	m
	s	0.85	m
	L	4	m
	θ_1	29	°
	θ_2	80	°
	θ_3	120	°
	θ_4	153	°
	Loads		
	PV	28.80	KN
	N	636.96	KN
D	2.00	m	
Material properties			
f_c	4	MPa	
f_t (5% f_c)	0.2	MPa	
γ	20	KN/m ³	
$c = \frac{a}{g} = 0.911$			

The value of the collapse coefficient is very high as a consequence it is difficult that this is the mechanism that has led to the collapse.

The vertical loads considered in this analysis are: the vault self-weight and the dead load of the wall and of the roof resting on the vault.

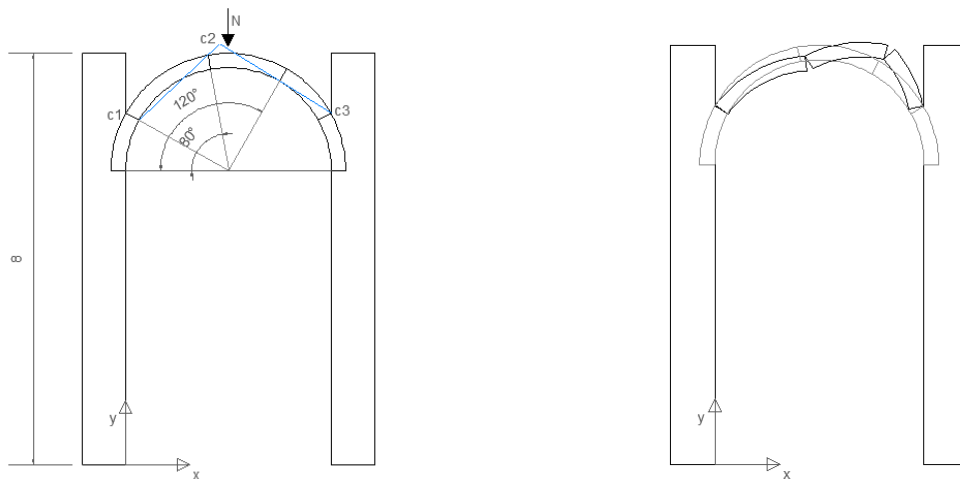


Figure 5.11 – collapse mechanism of a single arch.

Loss balance of the arch and of both buttresses

Arch:

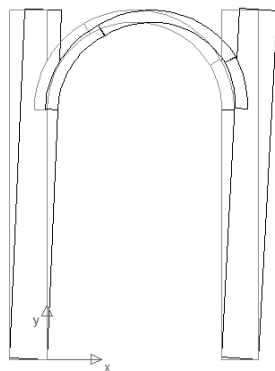
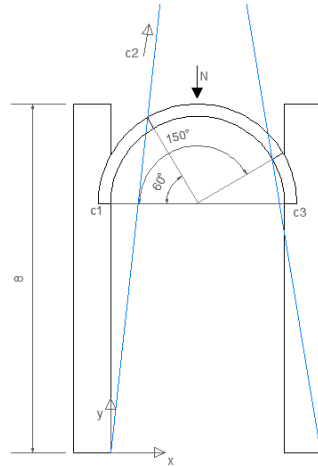
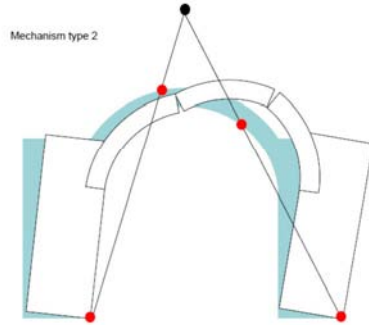


Figure 5.12 –collapse mechanism of arch and of both buttresses.

Geometrical properties

B	0.85	m
H	8	m
Re	2.28	m
Ri	2	m
s	2.4	m
L	0.85	m
θ1	- 91	°
θ2	60	°
θ3	150	°
θ4	244	°

Loads

PP	326.4	KN
N1	115.6	KN
D1	- 0.425	m
PV	28.8	KN
N2	636.96	KN
D2	2.00	m
PP	115.6	KN
N3	342.37	KN
D3	4.425	m

Material properties

fc	4	MPa
ft (5% fc)	0.2	MPa
γ	20	KN/m ³

$$c = \frac{a}{g} = 0.031$$

The value of the collapse coefficient is too low but it does not seem to be what caused the collapse.

This is probably due to the fact that, considering a unitary depth, the buttresses are slender in comparison to the vault. The vertical loads considered in this analysis are:

- the vault self-weight and the dead load of the wall and of the roof resting on the vault.
- the buttresses self-weight and the dead load of the wall and of the roof resting on the buttresses.

Loss balance of the arch and of one buttress			
Arch:			
	Geometrical properties		
	B	0.85	m
	H	8	m
	Re	2.28	m
	Ri	2	m
	s	0.85	m
	L	4	m
	θ_1	29	°
	θ_2	90	°
	θ_3	180	°
	θ_4	244	°
	Loads		
	PV	28.80	KN
	N1	636.96	KN
	D1	2.00	m
PP	115.6	KN	
N2	342.37	KN	
D2	4.425	m	
Material properties			
f_c	4	MPa	
f_t (5% f_c)	0.2	MPa	
γ	20	KN/m ³	
<p>Figure 5.13 – collapse mechanism of arch and of one buttress.</p> $c = \frac{a}{g} = 0.912$			

The value of the collapse coefficient is very high as a consequence it is difficult that this is the mechanism that has led to the collapse.

The vertical loads considered in this analysis are:

- the vault self-weight and the dead load of the wall and of the roof resting on the vault.
- the right buttress self-weight and the dead load of the wall and of the roof resting on the buttress.

Loss balance of two consecutive arches

Arches:

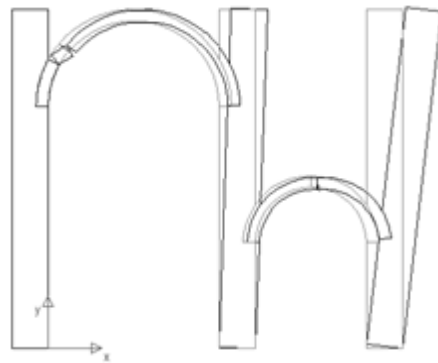
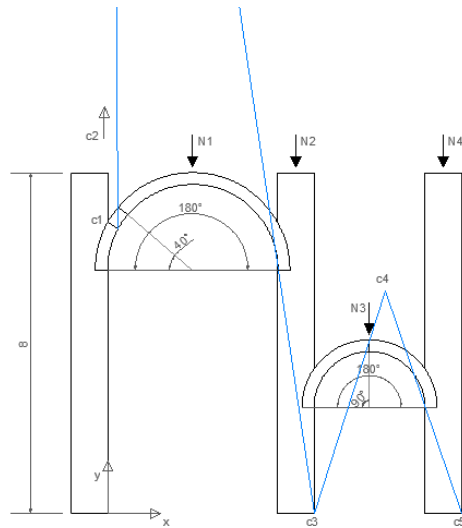
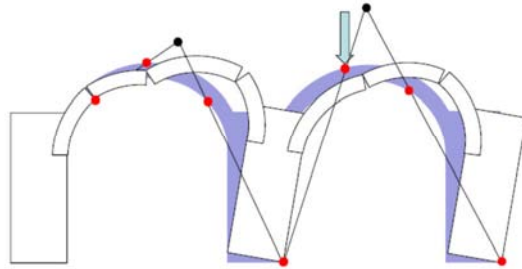


Figure 5.14 – collapse mechanism of two consecutive arches case a.

Geometrical properties

B	0.85	m
H	8	m
s	0.85	m
Re1	2.28	m
Ri1	2	m
L1	4	m
θ1	29	°
θ2	40	°
θ3	180	°
θ4	244	°
Re2	1.58	m
Ri2	1.3	m
L2	2.6	m
β1	90	°
β2	180	°
β3	230	°

Loads

PVg	28.8	KN
N1	636.96	KN
D1	2.00	m
PP	115.6	KN
N2	342.37	KN
D2	4.425	m
PVp	19.38	KN
N3	4.16	KN
D3	6.15	m
PP	115.6	KN
N4	342.37	KN
D4	7.875	m

Material properties

fc	4	MPa
ft (5% fc)	0.2	MPa
γ	20	KN/m ³

$$c = \frac{a}{g} = 0.095$$

The value of the collapse coefficient has a value credible but the position of the hinges in the biggest vault does not seem to be that which is verified in the real case.

The vertical loads considered in this analysis are:

- the vaults self-weight and the dead load of the wall and of the roof resting on the vaults,
- the buttresses self-weight and the dead load of the wall and of the roof resting on the buttresses.

Loss balance of two consecutive arches with resisting spandrels			
Arches:			
	Geometrical properties		
	B	0.85	m
H	8	m	
s	0.85	m	
Re1	2.28	m	
Ri1	2	m	
L1	4	m	
θ1	29	°	
θ2	50	°	
θ3	110	°	
θ4	244	°	
Re2	1.58	m	
Ri2	1.3	m	
L2	2.6	m	
β1	35	°	
β2	180	°	
β3	230	°	
	Loads		
	PVg	28.8	KN
N1	636.96	KN	
D1	2.00	m	
PP	115.6	KN	
N2	342.37	KN	
D2	4.425	m	
PVp	19.38	KN	
N3	342.37	KN	
D3	7.875	m	
PP	115.6	KN	
Material properties			
fc	4	MPa	
ft (5% fc)	0.2	MPa	
γ	20	KN/m ³	
$c = \frac{a}{g} = 0.099$			

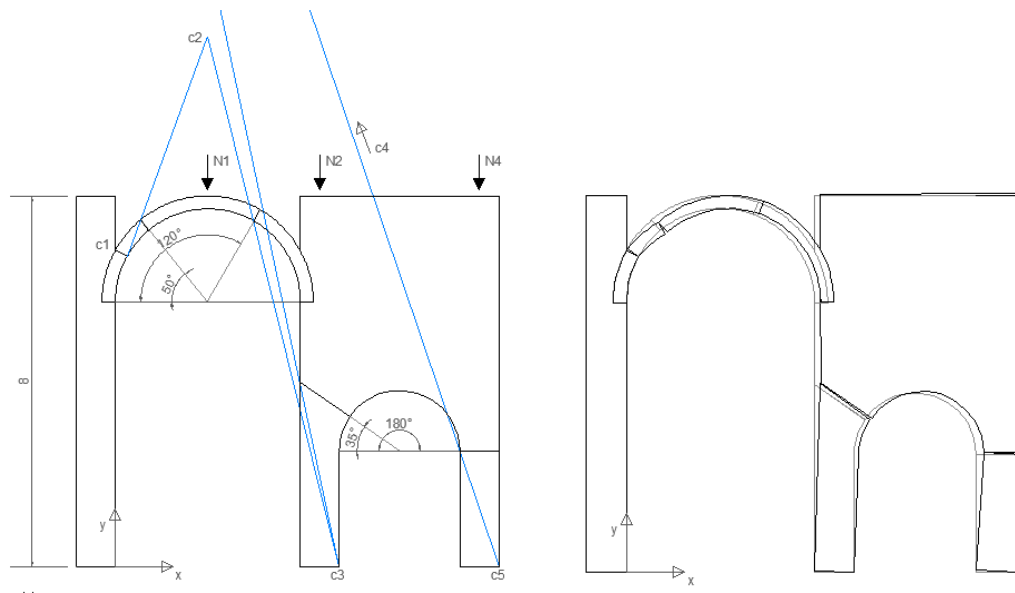
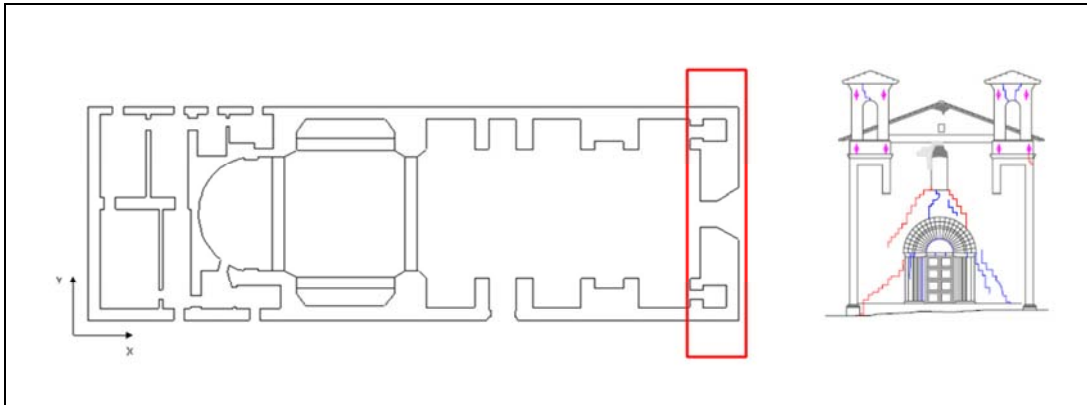


Figure 5.15 – collapse mechanism of two consecutive arches with resisting spandrels case b.

In this case the arches were supposed with resisting spandrels but assuming the break in the foothills. The collapse coefficient assumes a plausible value and also the position of the hinges is very similar to the real case. Therefore, it can be the mechanism that was triggered during the earthquake.

The vertical loads considered in this analysis are:

- the vaults self-weight and the dead load of the wall and of the roof resting on the vaults,
- the buttresses self-weight and the dead load of the wall and of the roof resting on the buttresses.



Out of plane movement of a monolithic wall simply supported and partially connected with the orthogonal walls

Main facade:

Geometrical properties		
H1	4	m
B1	2.50	m
H2	11	m
B2	2.50	m
Loads		
P1	200	KN
N1o	- 19	KN
P2	550	KN
N2	55.00	KN
D2	0.74	m
Material properties		
fc	4	MPa
ft (0.5% fc)	0.02	MPa
γ	20	KN/m ³

* N1o= (ft*8*0.95*10³)/8

$$c = \frac{a}{g} = 0.163$$

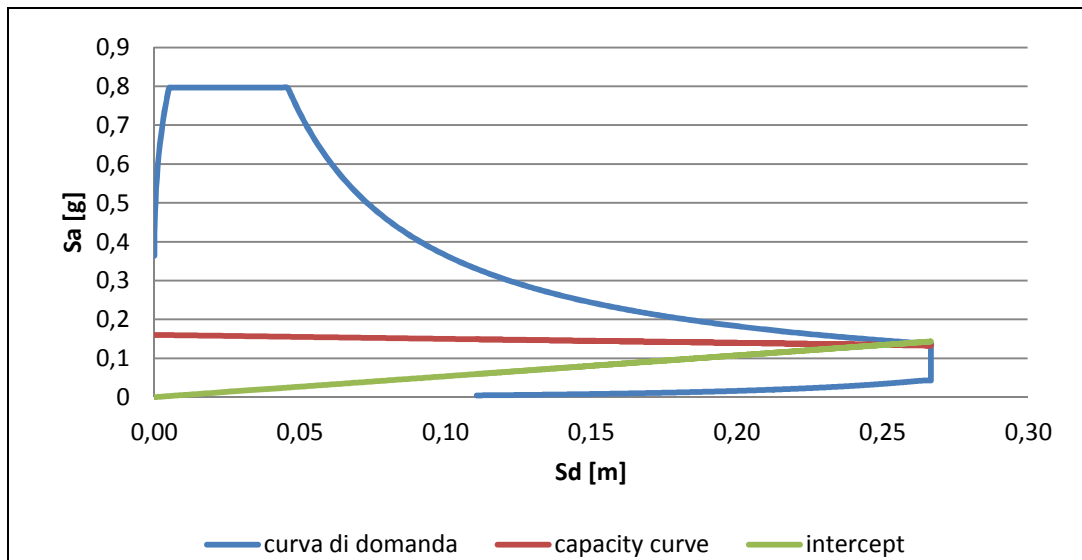


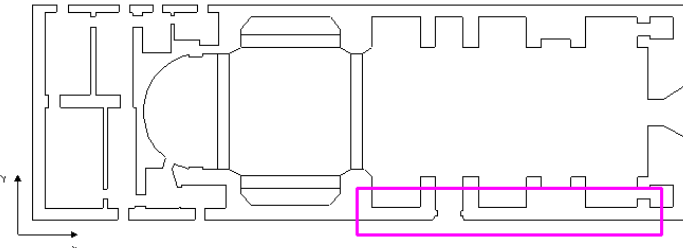
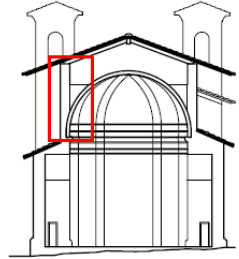
Figure 5.16 - Non-linear analysis of the main façade (partially connected).

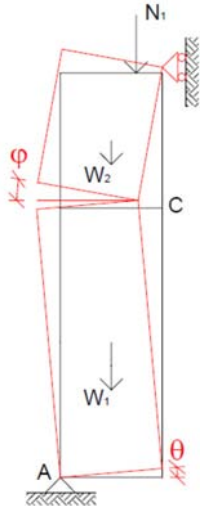
Mass involved	M^*	1243.59	Kg	
Fraction of mass involved	e^*	0.95		
Spectral acceleration which activates the mechanism	a_0^*	0.139g		
Final spectral displacement	d_u^*	0.628	m	
SLU WITH LINEAR ANALYSIS	a^*	0.162g		NO CHECKED
SLU WITH NON LINEAR ANALYSIS	Δd	0.260	m	CHECKED

By performing the non-linear analysis, the value obtained was $d_u^* = 0.628$ m, while the value required by the Italian code was $\Delta d = 0.260$ m. The calculated value is much higher than the required one.

The barrel vault of the nave doesn't transmit practically any orthogonal force on to the analysed façade, as so the only external forces applied in this structural element are the vertical loads coming from the bell towers. The load applied over the frontal wall, is equal to half weight of the tower. This consideration is related with the fact that only half part of the bell tower is directly acting over the façade. The lateral façade wall was supposed connected to the main facade, at least up to the highest part of the lower wall on the left facade. For this reason, in order to calculate the activation of the out of plane movement on the main facade, the wall has been divided into two parts and a horizontal force of retention was taken into consideration.

5.4 EARTHQUAKE Y DIRECTION

Vertical deflection																																
Lateral facade - top wall																																
	<table border="1" style="width: 100%; border-collapse: collapse;"> <thead> <tr style="background-color: #d9e1f2;"> <th colspan="3">Geometrical properties</th> </tr> </thead> <tbody> <tr> <td style="width: 20%;">H1</td> <td style="width: 20%;">7.5</td> <td style="width: 60%;">m</td> </tr> <tr> <td>B1</td> <td>0.80</td> <td>m</td> </tr> <tr style="background-color: #d9e1f2;"> <th colspan="3">Loads</th> </tr> <tr> <td>P1</td> <td>120.00</td> <td>KN</td> </tr> <tr> <td>N1</td> <td>39.24</td> <td>KN</td> </tr> <tr style="background-color: #d9e1f2;"> <th colspan="3">Material properties</th> </tr> <tr> <td>fc</td> <td>4</td> <td>MPa</td> </tr> <tr> <td>ft (5% fc)</td> <td>0.2</td> <td>MPa</td> </tr> <tr> <td>γ</td> <td>20</td> <td>KN/m³</td> </tr> </tbody> </table>		Geometrical properties			H1	7.5	m	B1	0.80	m	Loads			P1	120.00	KN	N1	39.24	KN	Material properties			fc	4	MPa	ft (5% fc)	0.2	MPa	γ	20	KN/m ³
Geometrical properties																																
H1	7.5	m																														
B1	0.80	m																														
Loads																																
P1	120.00	KN																														
N1	39.24	KN																														
Material properties																																
fc	4	MPa																														
ft (5% fc)	0.2	MPa																														
γ	20	KN/m ³																														
$c = \frac{a}{g} = 0.517$																																

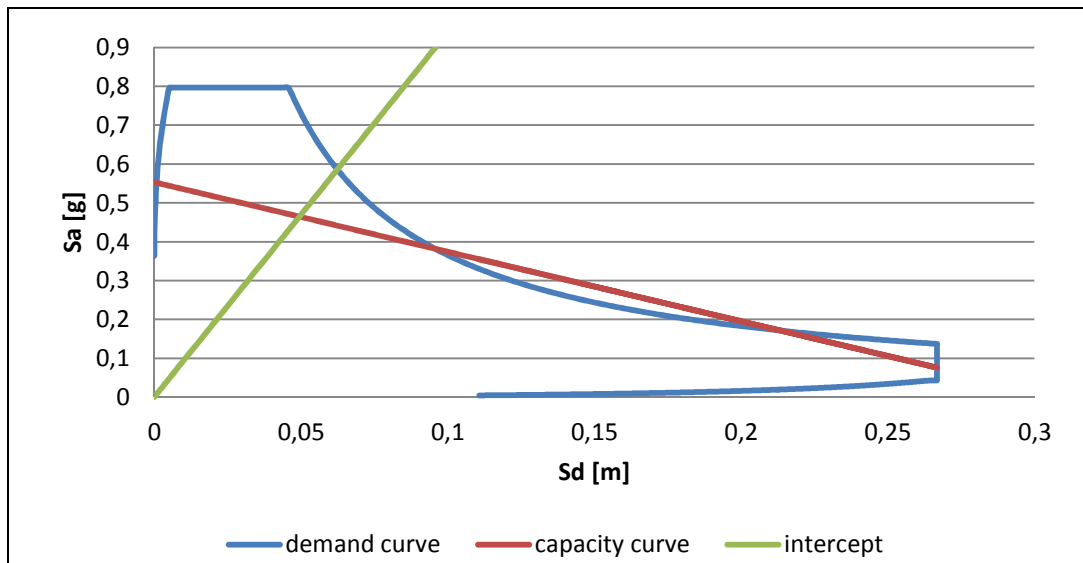


Figure 5.17 - Non-linear analysis of the top wall of the lateral façade (vertical deflection).

Mass involved	M^*	251.98	Kg	
Fraction of mass involved	e^*	0.75		
Spectral acceleration which activates the mechanism	a_0^*	0.556g		
Final spectral displacement	d_u^*	0.124	m	
SLU WITH LINEAR ANALYSIS	a^*	0.216g		CHECKED
SLU WITH NON LINEAR ANALYSIS	Δd	0.062	m	CHECKED

This mechanism has been studied considering just the upper part of the lateral wall, in order to verify the presence of a relation between it and the partial collapse of the lateral façade occurred during the earthquake.

However, applying the kinematic method to the mechanism of vertical deflection of the top wall even linear analysis is checked.

The vertical loads considered in this analysis are related with the roof self-weight. The horizontal forces coming from the roof are balanced by the presence of steel ties.

Out of plane movement of a monolithic wall simply supported			
Lateral facade - top wall			
	Geometrical properties		
	H1	7.5	m
	B1	0.80	m
	Loads		
	P1	120.00	KN
	N1	39.24	KN
	N1o	-	KN
D1	0.65	m	
Material properties			
fc	4	MPa	
ft (5% fc)	0.2	MPa	
γ	20	KN/m ³	
$c = \frac{a}{g} = 0.099$			

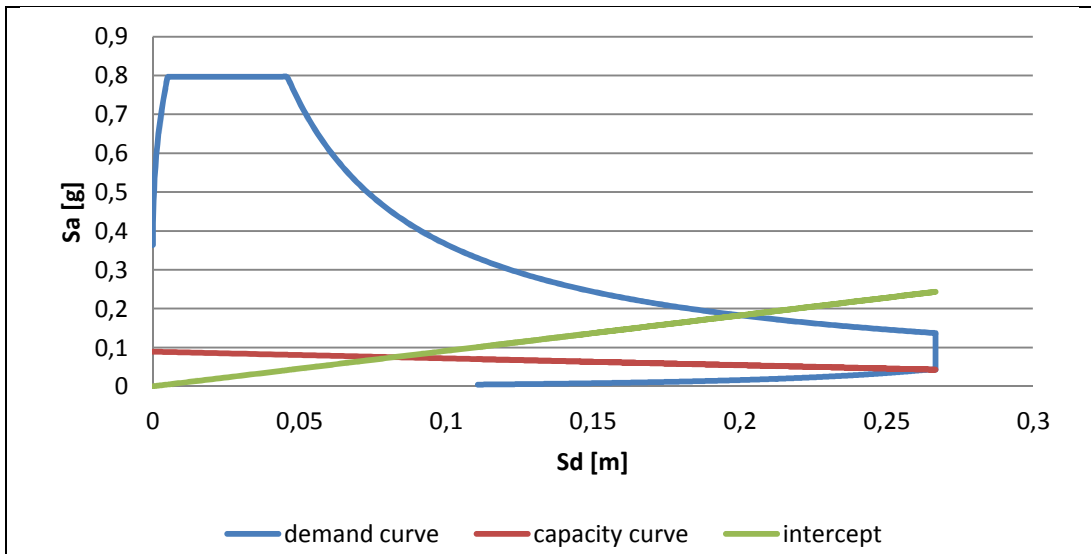
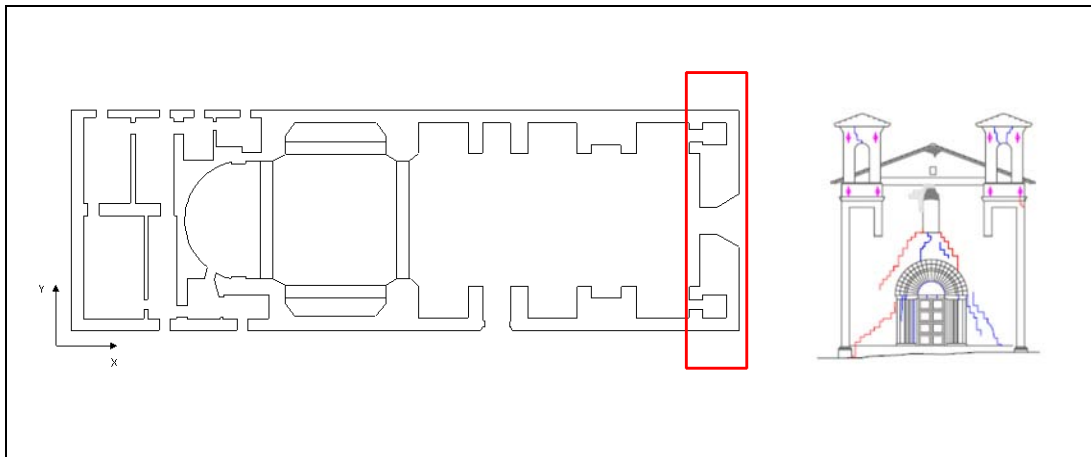


Figure 5.18 - Non-linear analysis of the top wall of the lateral facade (overturning).

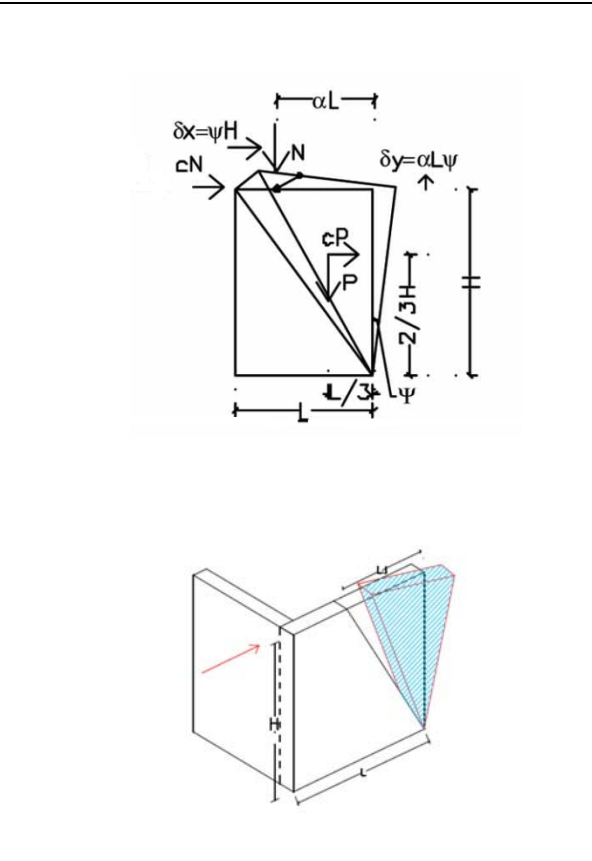
Mass involved	M*	298.68	Kg	
Fraction of mass involved	e*	0.89		
Spectral acceleration which activates the mechanism	a ₀ *	0.089g		
Final spectral displacement	d _u *	0.205	m	
SLU WITH LINEAR ANALYSIS	a*	0.216g		NOT CHECKED
SLU WITH NON LINEAR ANALYSIS	Δd	0.200	m	CHECKED

This mechanism has been studied considering just the upper part of the lateral wall, in order to verify if the roof, in measure, opposed this collapse mechanism. By performing the non-linear analysis, the value obtained was $d_u^* = 0.205$ m, while the value required by the Italian code was $\Delta d = 0.200$ m. The calculated value is quite close to that required but it is sufficient to check the analysis. The load applied is the same as in the previous case: the self-weight roof.



Plane movement of a limited portion of the wall

Main facade:



Geometrical properties		
H	15	m
B	2.5	m
L	16.0	m
L1	8.00	m
Loads		
P	3000	KN
N	440	KN
$\alpha L1$	1.75	
Material properties		
f_c	4	MPa
f_t (5% f_c)	0.2	MPa
γ	20	KN/m ³

$$c = \frac{a}{g} = \frac{P \frac{L1}{3} + N \alpha L1}{P \frac{2}{3} H + N H} = 0.349$$

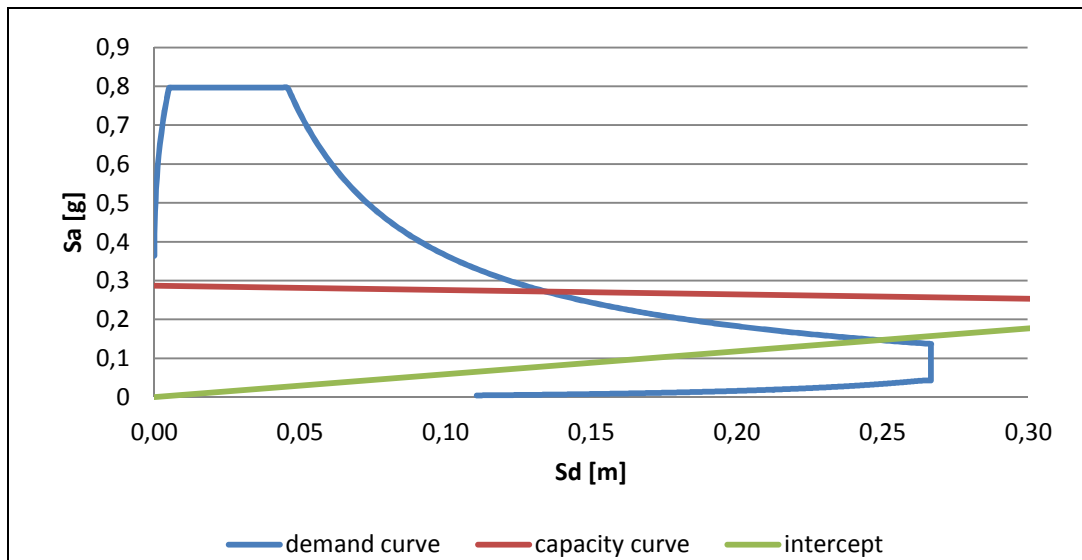


Figure 5.19 - Non-linear analysis of the frontal façade (in-plane movement).

Mass involved	M^*	342.46	Kg	
Fraction of mass involved	e^*	0.98		
Spectral acceleration which activates the mechanism	a_0^*	0.287g		
Final spectral displacement	d_u^*	1.027	m	
SLU WITH LINEAR ANALYSIS	a^*	0.167g		CHECKED
SLU WITH NON LINEAR ANALYSIS	Δd	0.256	m	CHECKED

By performing the non-linear analysis, the value obtained was $d_u^* = 1.027$ m, while the value required by the Italian code was $\Delta d = 0.256$ m. The calculated value is much greater than the required one.

This collapse mechanism has a seismic coefficient very high because it is in plane movement.

So before reaching the collapse, the wall must crack and the rotation mechanism must be activated. The façade, to rotate in its plane, must lift the self-weight and it must raise the tower weight which opposes the rotation.

The vertical loads considered in this analysis are related with the bell tower self-weight. This dead load is applied to half width of the tower.

5.5 SUMMARY:

As a result of the kinematic analysis of the considered mechanisms, it was attained that the first mechanism that is activated on the church is the out of plane movement of the buttresses supporting the chapel vaults, which corresponds to the lowest value of the collapse coefficient ($c=0.060$). Subsequently this mechanism evolves up to a value of c equal to 0.099, causing a loss of balance of the overstanding vaults. The collapse of this vaults leads to the destruction of the overstanding wall.

The closest mechanism to the real case consists in the union of the two vaults, a larger and a smaller one. Of the three buttresses underlying the two vaults, the first is assumed to be fixed and the other two are free to rotate. The inversion of the seismic action will cause the formation of hinges, symmetrical to the axis of symmetry of the smaller vault, in the arch resting on the wall that divides the nave from the transept, which is assumed to be fixed.

This type of mechanism is displayed in the pictures, which show significant collapses and cracks in these points. Furthermore, this approach is confirmed by the presence of the central hinge in the smallest arch. In fact, the latter is connected to the alternation of the loads, which deform the arches in both directions and cause a significant concentration of forces in this point, that is the point of symmetry.

The study of the out of plane movement of the front left side bottom wall, that is not properly connected to the main facade and the transept, shows that the activation coefficient is very low. Since this collapse mechanism didn't occur, it is possible to state that the wall is connected to the wall of the transept and to that of the main facade, at least up to the highest part of the lower wall on the left facade. This conclusion is confirmed both by the crack and the results of the finite element analysis performed by TNO DIANA. For this reason, in order to calculate the activation of the out of plane movement on the main facade, a horizontal force of retention was taken into consideration.

The new roof and its additional load can't be considered among the principal causes of the San Marco seismic response. On the contrary, the iron ties presence certainly limited the horizontal thrust coming from the roof. As a consequence there weren't any mechanisms outside plane in the upper part of the left

facade. The only aim of calculating the activation coefficient related to this mechanism was to allow the comparison with the one proposed by the analysis of TNO DIANA and, as a consequence, to verify the possibility of collapse caused by the plasticization of the material..

Moreover, the cyclic movement of the earthquake caused a shift of the application point of the roof load that together with the deformation of the wall cause the collapse of a wall portion. This is possible because the new roof induces a much greater load than the original roof and, being even more rigid, it absorbs a greater amount of seismic force.

This mechanism, activated by the cover, is visible in both sides of the nave facades through horizontal cracks located near the church roof and the side chapels. These cracks occur at a nearly constant height for the entire structure, which implies a good connection between the joists and the masonry on the one hand and an inappropriate distribution of tensions along the height of the wall on the other hand.

Consequently, the geometric nonlinearity might have influenced on the collapse of this wall. Nevertheless, this type of collapse is difficult to calculate and to verify through both the kinematic analysis and the FE analysis.

6. NON-LINEAR STATIC ANALYSIS:

6.1 INTRODUCTION

We chose to run a non-linear static analysis as it is the closest to the real behaviour of the historical masonry structures and it provides more reliable results. The analysis is carried out with the FEM program TNO DIANA on a global model of San Marco's church. Seismic pushover analysis is done in X directions (longitudinal direction) and Y direction (transversal direction) which apply the mass-distributed seismic force.

6.2 MODELING STRATEGY

The original global shell-element model was prepared by the University of Padova [Zografou, 2010]. The model modified and used for this analysis is derived from NIKER Project–Deliverable 8.4 (2012). The model is composed of 16006 quadrilateral four-node shell elements, 1333 triangular three-node elements, 205 straight two-node 3D beam elements and 115 one-node translation mass elements which apply the dead load over the roof trusses. The total number of nodes is 17659.

The material model used for the behaviour of masonry combines a smeared cracking model for tension (Rankine failure criterion), with a plasticity model for compression (Drucker-Prager failure criterion).

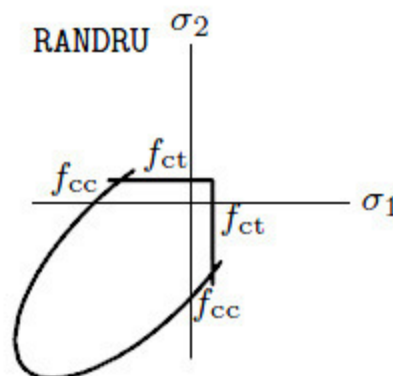


Figure 6.1 – Rankine/Drucker-Prager model

Smearred cracking is specified as a combination of tension cut-off, tension softening and shear retention. Constant stress cut-off was chosen. Linear tension softening based on fracture energy was selected. In this case Diana calculates the ultimate crack strain as $\varepsilon = \frac{2Gf}{f_t h}$ with h is the crack bandwidth. By default Diana assumes a value of h related to the area or the volume of the element. Finally, constant shear retention was chosen because due to the cracking of the material the shear stiffness is usually reduced.

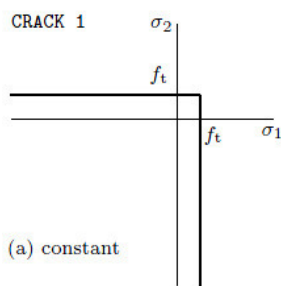


Figure 6.2 - Tension cut-off in two-dimensional principal stress space.

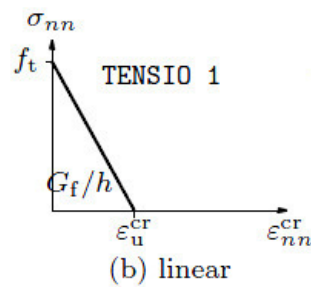


Figure 6.3 - Tension softening.

The Drucker-Prager plasticity is used to model the failure surface in plane stress and so the friction angle Φ is 10° otherwise the biaxial strength is overestimated. The cohesion then follows from $c = \frac{f_c(1 - \sin\Phi)}{2\cos\Phi}$. The strain hardening is the only one available for the Drucker-Prager model.

Considering the symmetry, half of the model is utilised for the analysis of the longitudinal direction with the appropriate boundary conditions introduced.

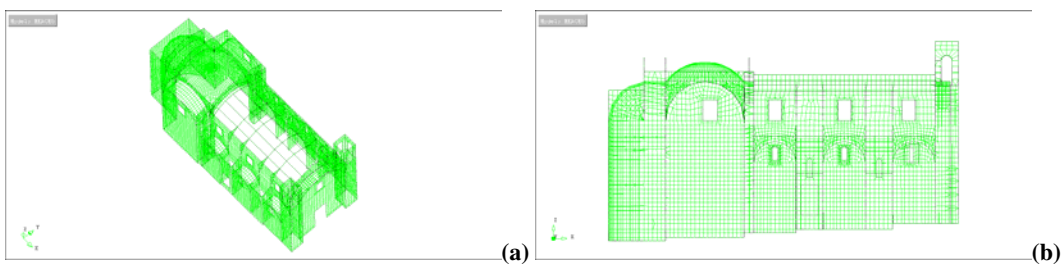


Figure 6.1- FEM model

By means of a pushover analysis we examined the behavior of the structure after the intervention of 1970, but with the removal of the roof. The elimination of the link between trusses and walls was carried out to avoid an overestimation of the stiffening effect given by the flexible roof. In other words, only the mass-weight of the new roof was taken into consideration.

In addition to that, lower values of the mechanical properties were applied to the connections. These values are used in connections between facade and upper wall of the nave, transept and nave, transept and apse.

The buttresses supporting the chapel vaults are assumed totally disconnected from the bottom wall of the nave.

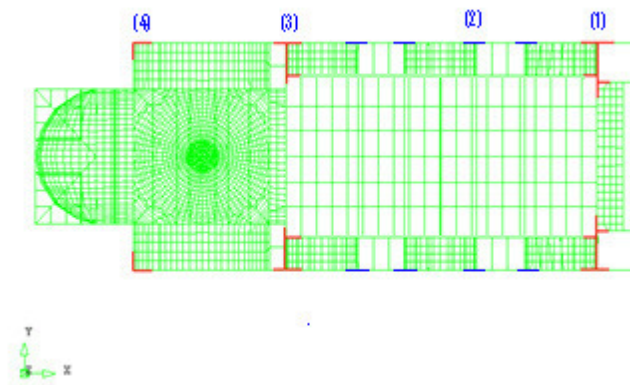


Figure 6.5 - Locations of the weak connections and no connections.

St. Marco's church has three basic materials: Stone masonry, brick masonry and concrete. The material properties of the different elements church are identified through the in-situ visual inspection carried out by Silva et al. (2010). To perform non-linear analysis, the mechanical properties have been derived from "Deliverable 8.4 - Reliably quantification of building performance and response parameters for use in seismic assessment and design – NIKER Project".

The reference mechanical properties used are shown in Table 6.1.



Property	stone masonry	brick masonry	connection	concrete
Density (kg/m³)	2000	1800	2000	2400
Compressive strength f_c (MPa)	4	4	2	-
Young's modulus E (MPa)	500×f _c (2000)	500×f _c (2000)	50×f _c (100)	30000
Tensile strength f_t (MPa)	5%f _c (0.2)	5%f _c (0.2)	1%f _c (0.02)	-
Poisson's ratio ν	0.2	0.2	0.2	0,2
Fracture energy G_{ft} (N/m)	50	50	5	

Table 6.1 - Mechanical properties – reference case.

6.3 REFERENCE CASE

6.3.1 EARTHQUAKE X DIRECTION

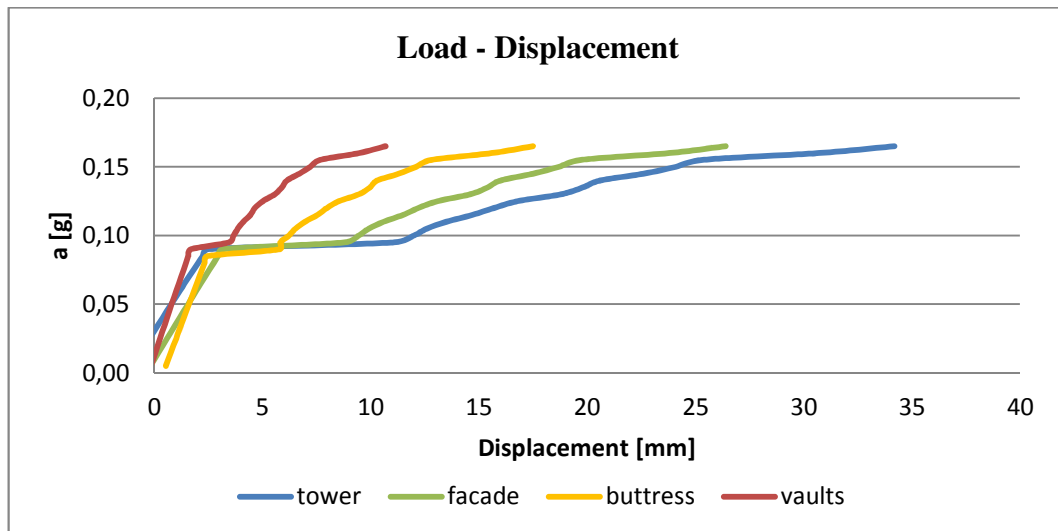


Figure 6.6 – Capacity curves at the control point at the top of the tower, top of the nave wall, top of buttress and on the vaults (reference case).

In the X direction, the collapse mechanisms are the loss of balance of the chapel's vaults and the overturning of the facade. The first mechanism begins with the cracking of chapel vaults, which corresponds to an acceleration of 0.095g. The second mechanism begins at an acceleration of 0.095g, then the capacity increases up to the ultimate value of 0.170g, which corresponds to the overturning of the facade and the parting of the nave wall.

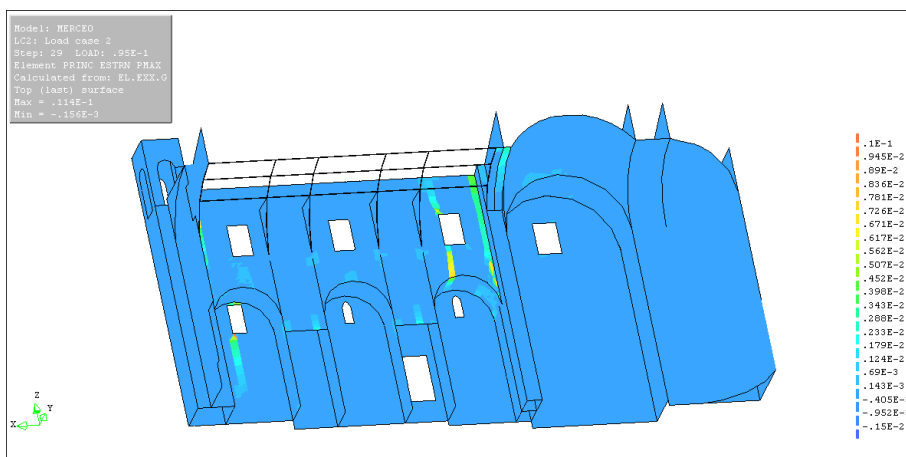


Figure 6.7 – Initial principal tensile strain, X direction (vaults view) in reference case.

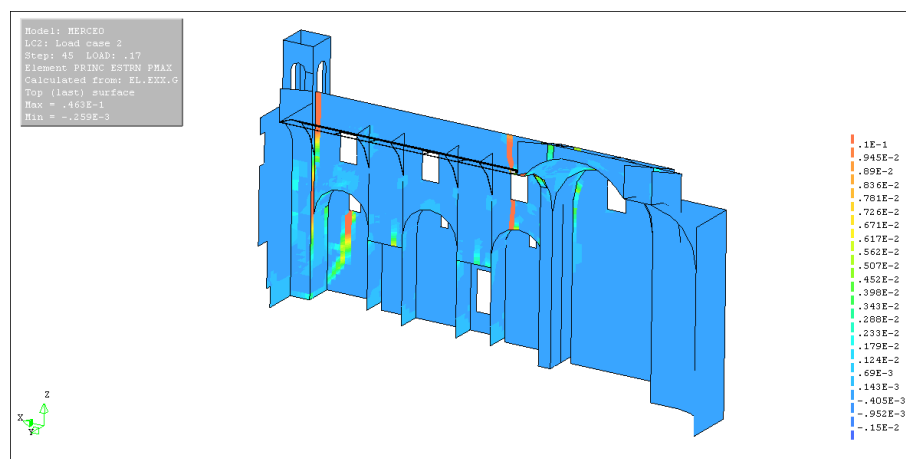


Figure 6.8 – Ultimate principal tensile strain, X direction (internal view) in reference case.

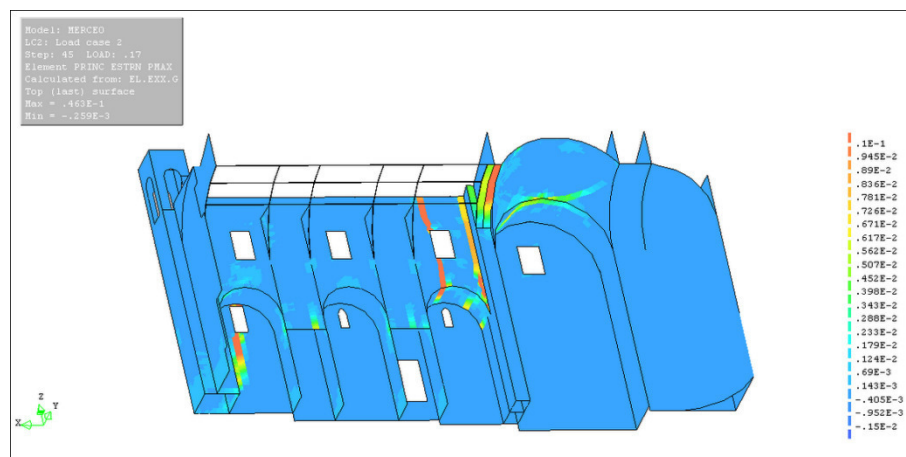


Figure 6.9 – Ultimate principal tensile strain, X direction (vaults view) in reference case.

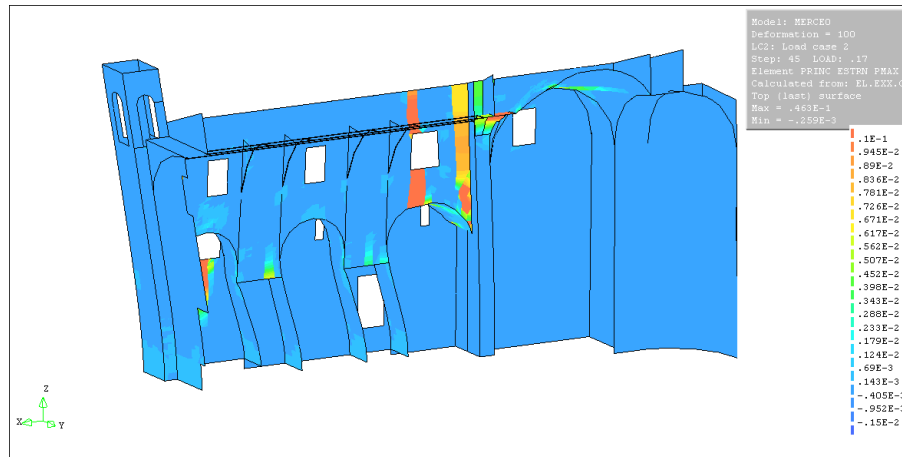


Figure 6.10 – Ultimate deformation, X direction (internal view) in reference case.

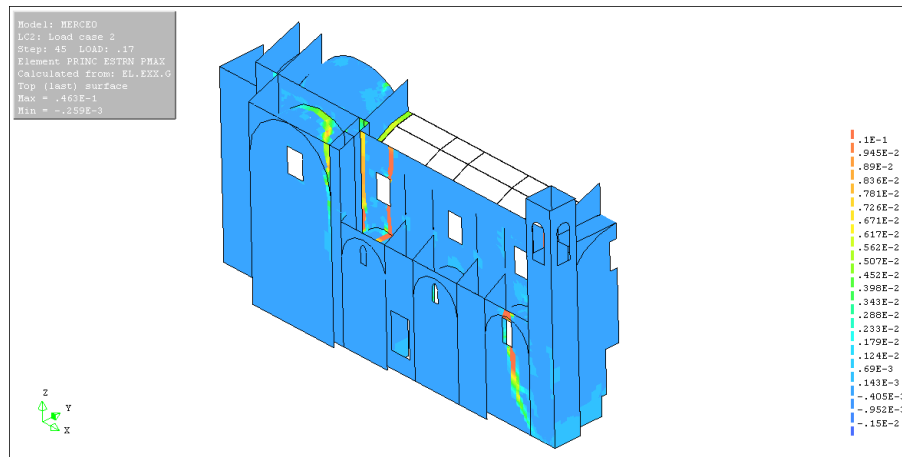


Figure 6.11 – Ultimate principal tensile strain, X direction (external view) in reference case.

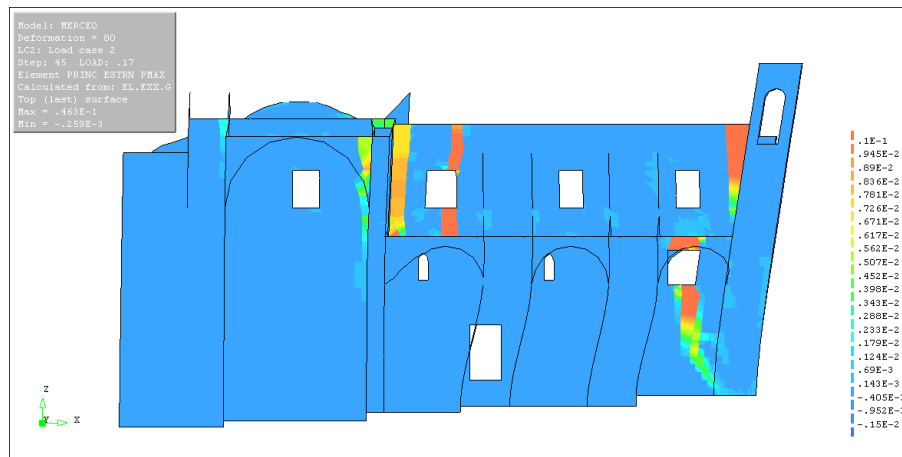


Figure 6.12 – Ultimate deformation, Y direction (external view) in reference case.

6.3.2 EARTHQUAKE Y DIRECTION

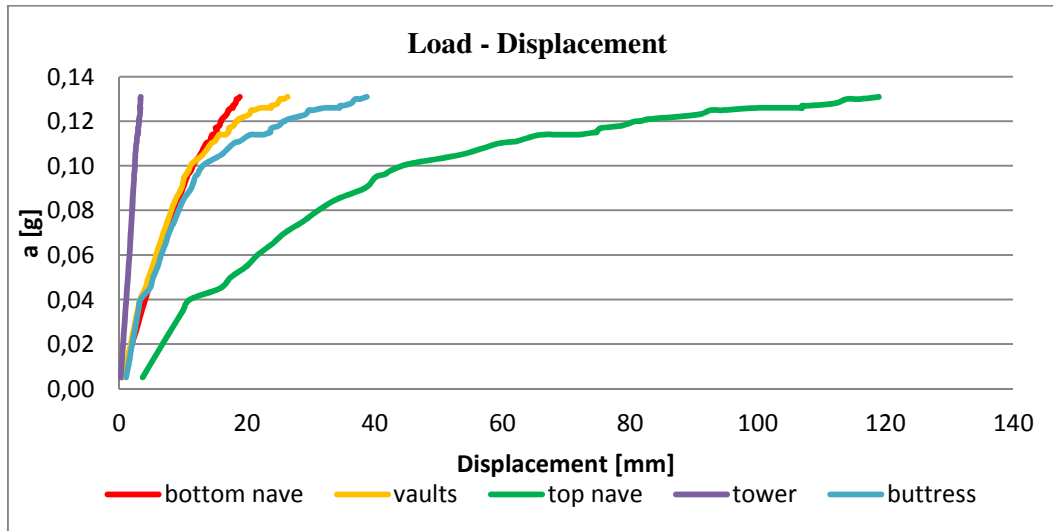


Figure 6.13 – Capacity curves at the control point at the top of the tower, top of the bottom wall on the left facade, top of the top wall on the left facade, top of buttress and on the vaults (reference case).

In the Y direction, the cause of the collapse is the crash of the material of the lateral facade. This mechanism starts at an acceleration of 0.045g that corresponds to the initial local destruction of the connection between the nave walls and the bells towers. Then the capacity increases up to the ultimate value of 0.131g.

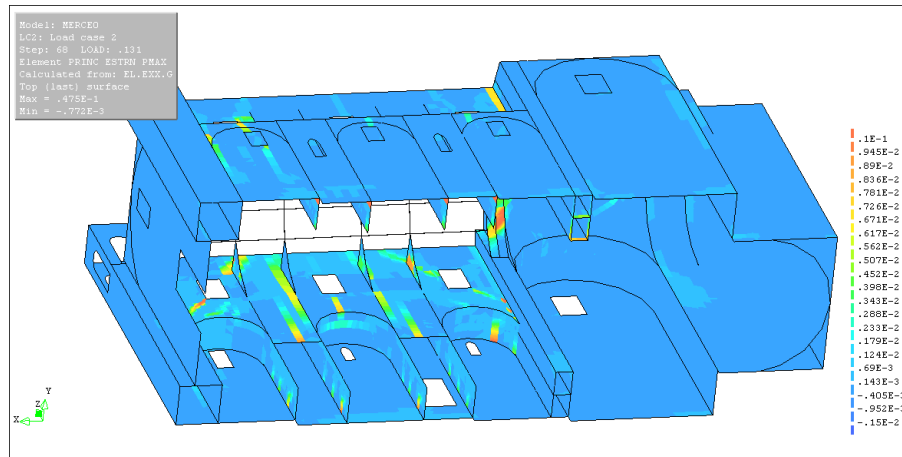


Figure 6.14 - Ultimate principal tensile strain, Y direction (internal view) in reference case.

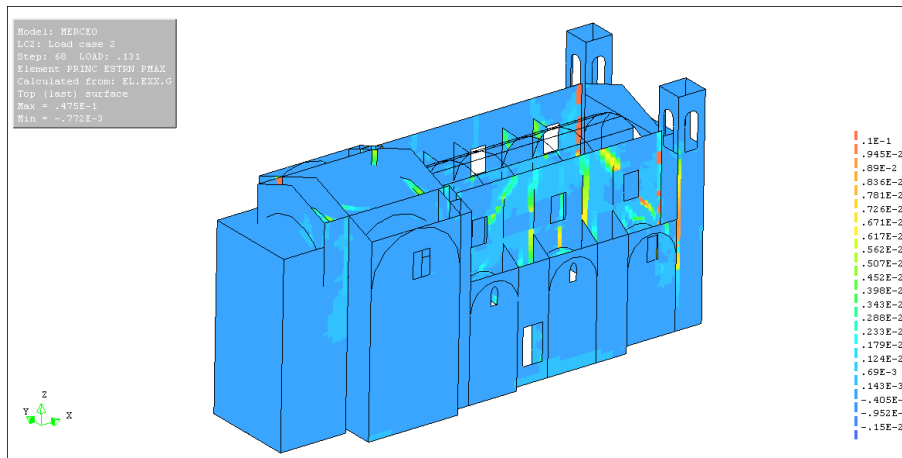


Figure 6.15 - Ultimate principal tensile strain, Y direction (external view) in reference case.

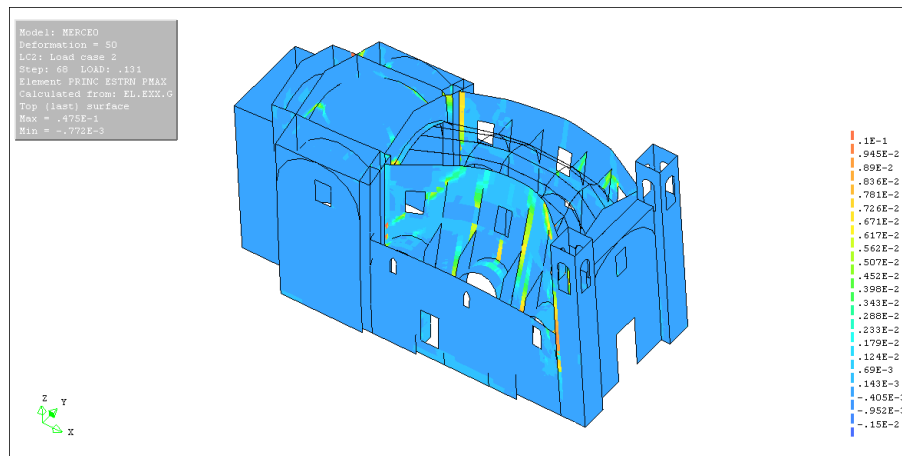


Figure 6.16 - Ultimate deformation, Y direction (external view) in reference case.

6.4 WEAK BUTTRESSES CASE

An additional analysis is carried out with lower values of the buttresses' mechanical properties.

This assumption is made because the results, of the previous analysis, don't show the breakdown of the buttresses' material, as it has occurred in the real case.

The reference mechanical properties used are shown in Table 6.2.

Property	stone masonry	brick masonry	buttresses	connection	concrete
Density (kg/m^3)	2000	1800	2000	2000	2400
Compressive strength f_c (MPa)	4	4	4	2	-
Young's modulus E (MPa)	$500 \times f_c$ (2000)	$500 \times f_c$ (2000)	$500 \times f_c$ (2000)	$50 \times f_c$ (100)	30000
Tensile strength f_t (MPa)	$5\% f_c$ (0.2)	$5\% f_c$ (0.2)	$1\% f_c$ (0.02)	$1\% f_c$ (0.02)	-
Poisson's ratio ν	0.2	0.2	0.2	0.2	0,2
Fracture energy G_{ft} (N/m)	50	50	5	5	

Table 6.2 - Mechanical properties – weak buttresses case.

6.4.1 EARTHQUAKE X DIRECTION

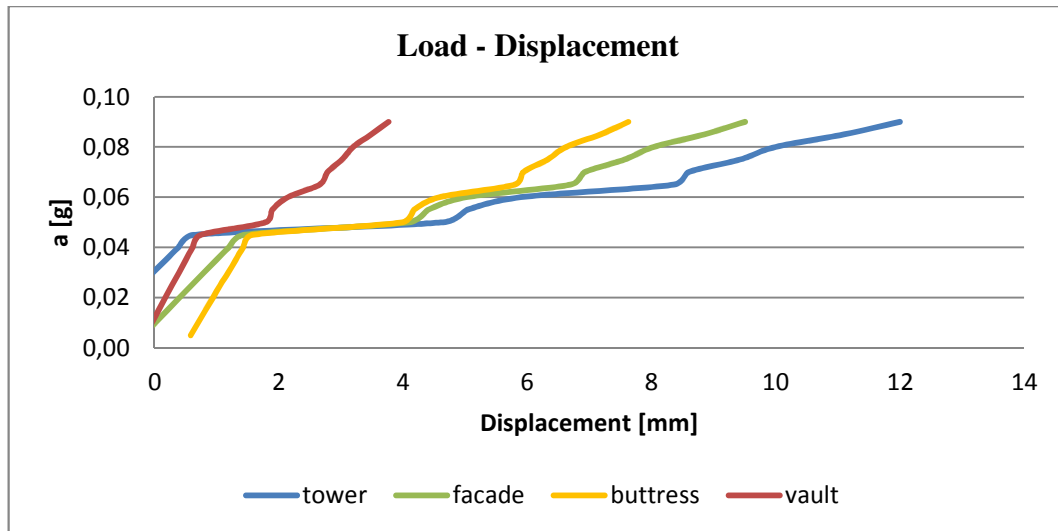


Figure 6.17 - Capacity curves at the control point at the top of the tower, top of the nave wall, top of buttress and on the vaults (weak buttresses case).

The collapse mechanism is the same as previous case (loss of balance of the chapel's vaults and the overturning of the façade). However, the capacity curves shown a very different ultimate load factor. In the previous analysis the ultimate acceleration was equal to 0.170g; in this analysis the ultimate value is of 0.095g. The cracks of vaults and of the upper part of the buttresses start at a value of the acceleration equal to 0.050g. This value can be compared with the value obtained for the overturning of the buttresses in the kinematics analysis ($c=0.060$). This assumption seems quite correct because it is closest to the results obtained with the kinematics analysis ($c=0.099$).

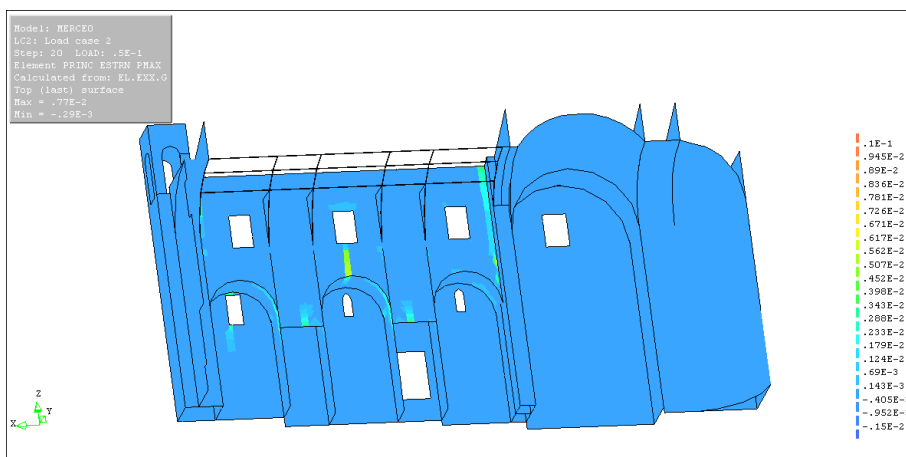


Figure 6.18 - Initial principal tensile strain, X direction (vaults view) in weak buttresses case.

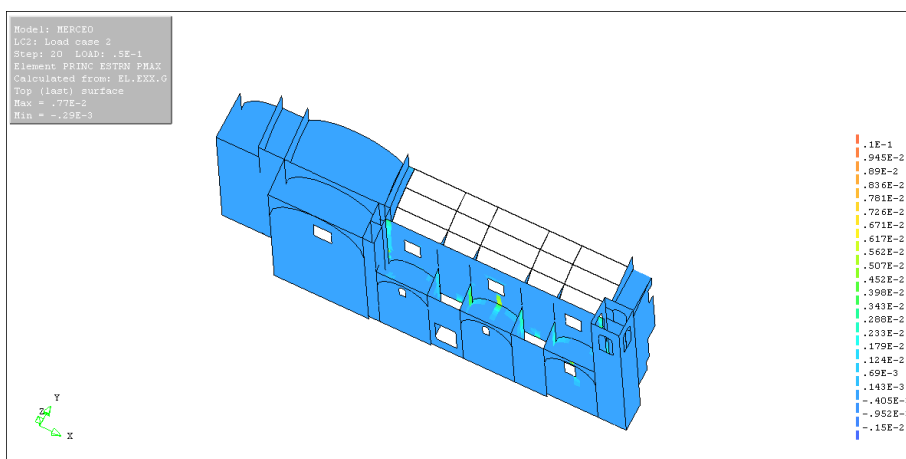


Figure 6.19 - Initial principal tensile strain, X direction (buttresses view) in weak buttresses case.

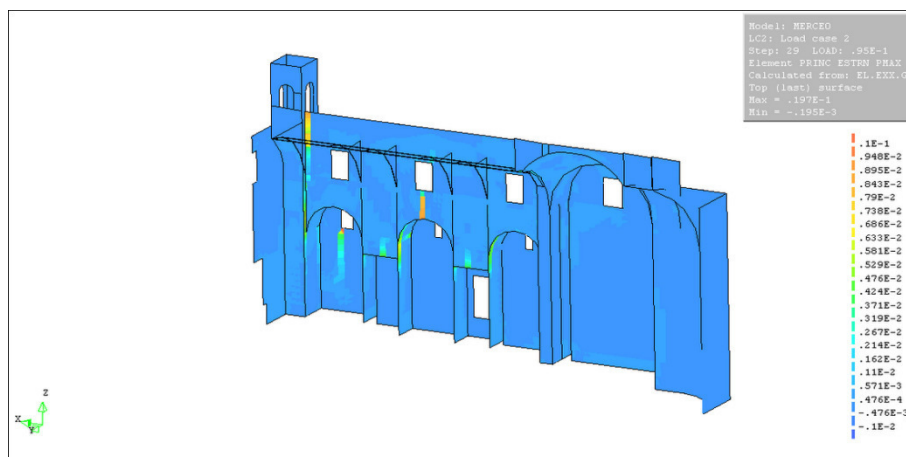


Figure 6.20 - Ultimate principal tensile strain, X direction (internal view) in weak buttresses case.

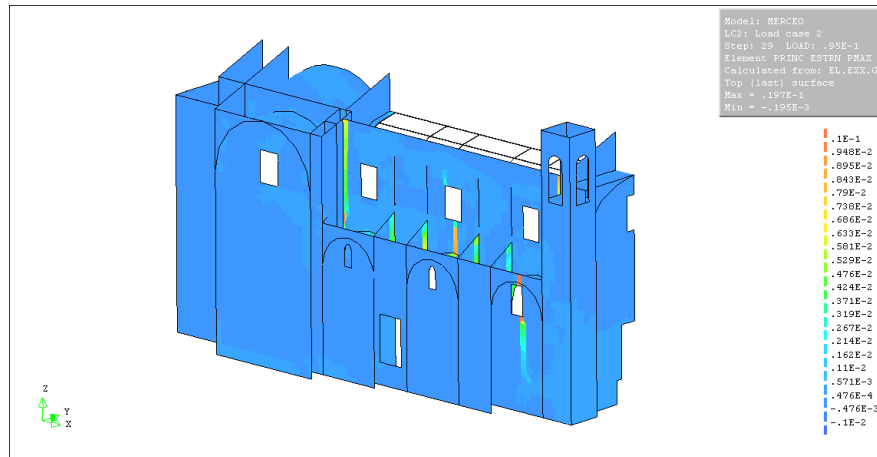


Figure 6.21 - Ultimate principal tensile strain, X direction (external view) in weak buttresses case.

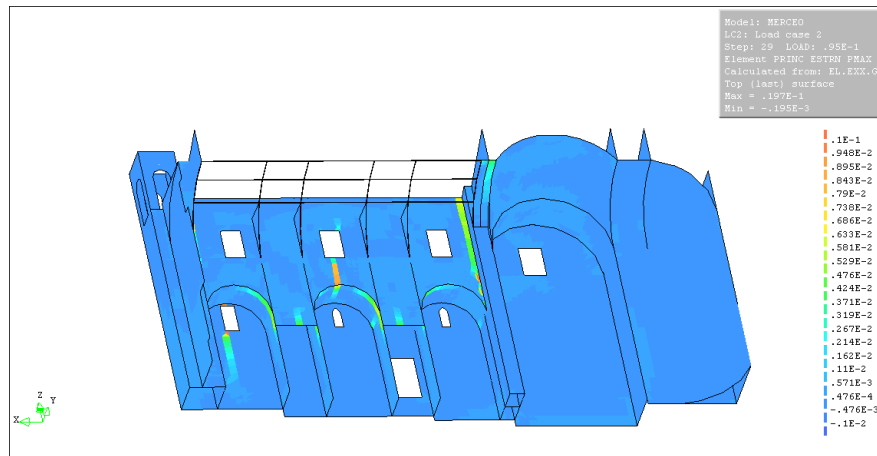


Figure 6.22 - Ultimate deformation, X direction (arches view) in weak buttresses case.

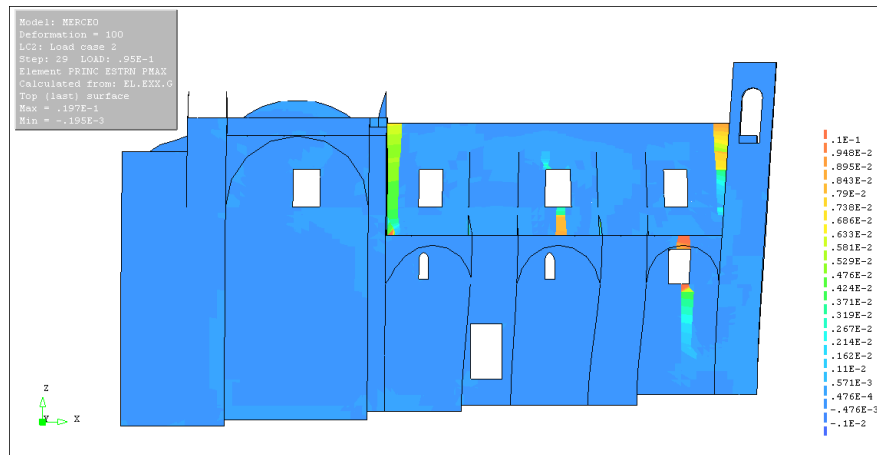


Figure 6.23 - Ultimate deformation, X direction (external view) in weak buttresses case.

6.4.2 EARTHQUAKE Y DIRECTION

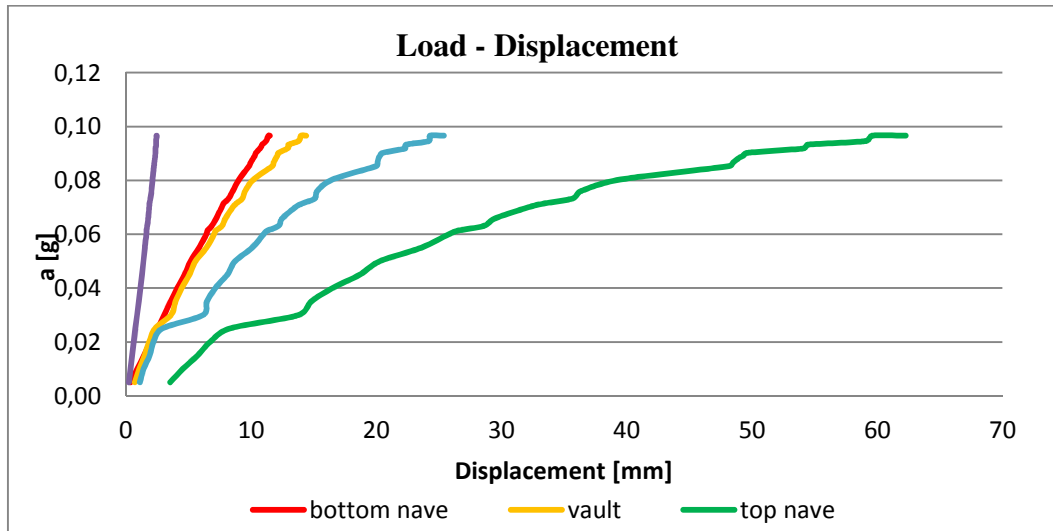


Figure 6.24 – Capacity curves at the control point at the top of the tower, top of the bottom wall on the left facade, top of the top wall on the left facade, top of buttress and on the vaults (weak buttresses case).

In the Y direction, as for the previous case, the cause of the collapse is the crash of the material of the lateral facade. However, the structural capacity of the case with weak buttresses is lower than that of the previous case.

In this case the ultimate value is 0.097g, in the previous analysis was equal to 0.131g. This decrease is due to the poor resistance of the buttresses supporting the top wall on the left facade.

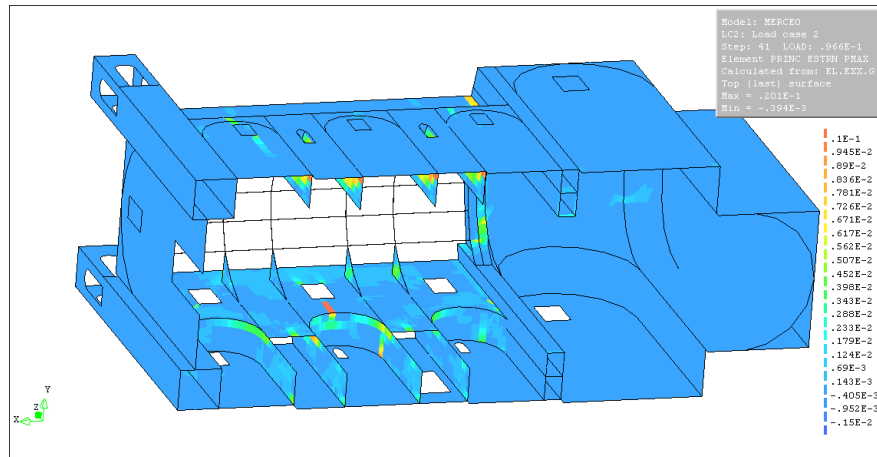


Figure 6.25 - Ultimate principal tensile strain, Y direction (internal view) in weak buttresses case.

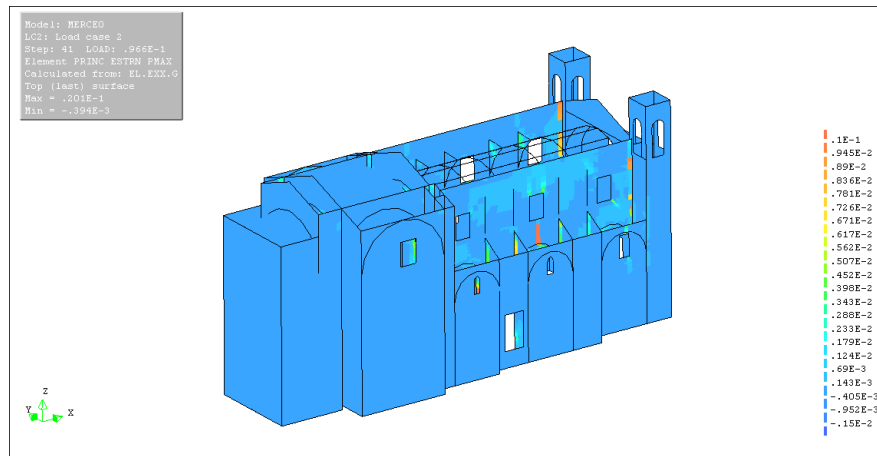


Figure 6.26 - Ultimate principal tensile strain, Y direction (external view) in weak buttresses case.

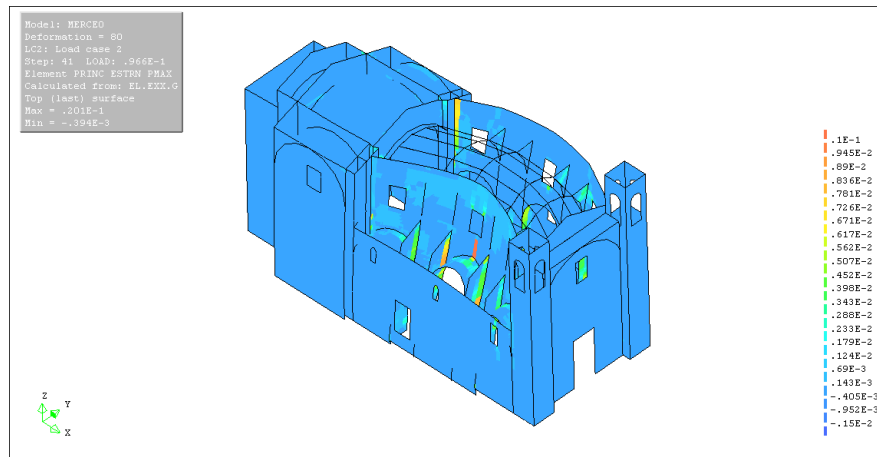


Figure 6.27 - Ultimate deformation, Y direction (external view) in weak buttresses case.

6.5 SUMMARY

In the results obtained through the structural analysis in the X direction it is possible to notice the high deformation of the buttresses supporting the chapel vaults. Although the activation coefficient of the mechanism resulting from the structural analysis is similar to that obtained performing the kinematic analysis, it is impossible to obtain the exact coefficient value corresponding to the loss of balance of the chapel's vaults. For this reason the collapse is due to the overturning of the main facade and its detachment from the nave walls.

It's highly probable that the buttresses' material is of lower quality than the ones used for the other walls. Consequently, the material tensile strength in the buttresses might have been overcome and this led to its breakdown. In fact as is possible to see in the second analysis, lowering the buttresses' mechanical property, the structural capacity decreases greatly ($c = 0.095$).

As concerns the overturning of the buttresses, the activation coefficient of the mechanism obtained through the kinematic analysis is equal to 0.060 and the one corresponding to the loss of balance of the vaults is equal to 0.099. In the structural analysis the cracking of the vaults start at an acceleration of 0.095g.

The overturning of the facade occurs with a load factor value of 0.163, in the case of kinematic analysis performed on the facade well connected to the lower wall of the lateral facade. The acceleration in the structural analysis is equal to 0.170g.

In the Y direction the outcome of the structural analysis can be compared to the result of the simple overturning of the lateral facade's top wall obtained through the kinematic analysis.

The activation coefficient of the mechanism resulting from the kinematic analysis is equal to 0.0989, while the one obtained through the structural analysis is 0.131.

The slight difference between these values might be due to the fact that the kinematic analysis considers the wall as completely detached, while in the structural analysis there is still a connection, even though it is weak, between the lateral facade and the transept and between the lateral facade and the main facade.

7. NON-LINEAR DYNAMIC ANALYSIS

7.1 INTRODUCTION

We chose to run a transient dynamic analysis to compare its results to those of the non-linear static analysis. The analysis is carried out with the FEM program TNODIANA on a global model of San Marco's church. The dynamic analysis is carried out using the accelerogram generated from the main earthquake of L'Aquila (at 3:32 (local time) AM 6th of April, 2009) which was measured at the Spanish fort (station AQU). The information is obtained from website of ITACA. In this study the applied accelerogram lasts 12 seconds.

7.2 MODELING STRATEGY

The model used for the dynamic analysis is the same that was used to perform the pushover analysis. The accelerogram generated by the earthquake has been divided according to the two main directions of the church. In X direction is applied to the structure the accelerogram in Figure 7.1.

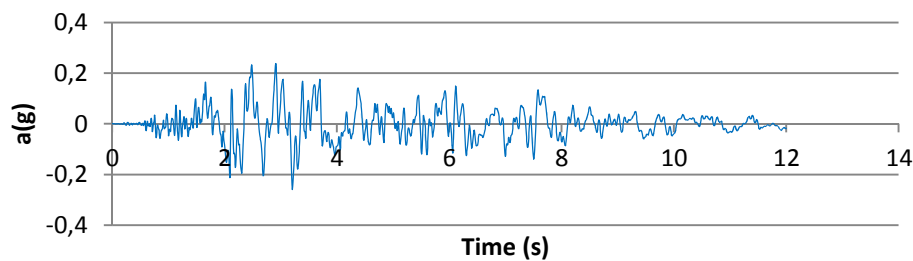


Figure 7.1 - Accelerogram of L'Aquila earthquake (2009) in the EW direction

While in the Y direction is applied accelerogram in Figure 7.2

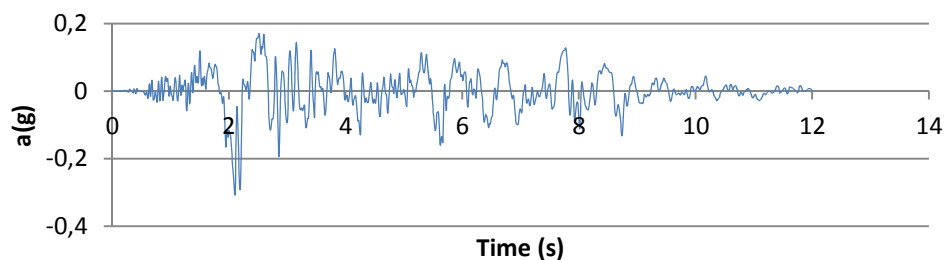


Figure 7.2 - Accelerogram of L'Aquila earthquake (2009) in the NS direction.

In the transient dynamic analysis, it is necessary to specify the damping parameters.

The Rayleigh damping coefficients are specified to simulate viscous damping that is proportional to the velocity.

The mass-proportional and stiffness-proportional damping coefficients are $a = 2\omega_1\omega_2\beta = 0.5808$ and $b = 2\beta = 0.0042$. Where ω_1 and ω_2 are the two lowest frequencies, $\alpha = \frac{\omega_1}{\omega_2}$, $\beta = \frac{(1-\alpha)\zeta}{\omega_2 - \alpha\omega_1}$ and ζ the damping coefficient.

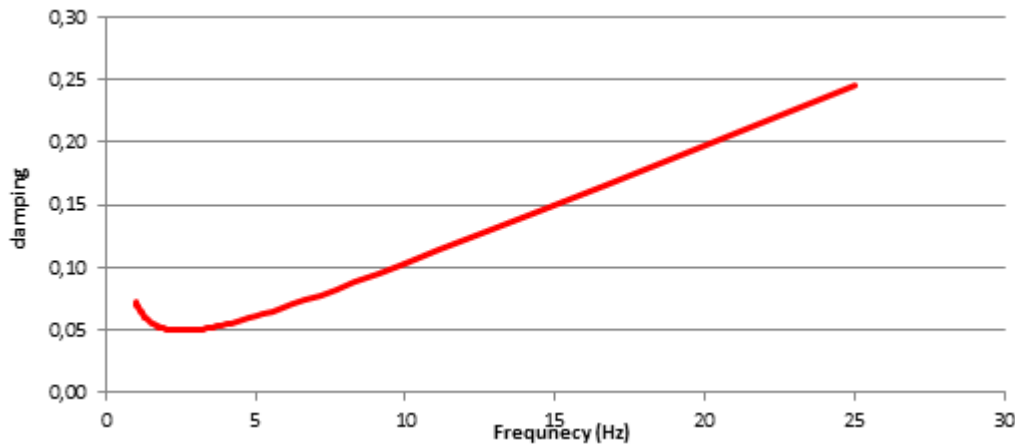


Figure 7.3 - Rayleigh damping model.

Also the mechanical properties and the connections between the elements respect the considerations made for the non-linear static analysis.

The reference mechanical properties used are repeated for the sake of clarity in Table 7.1.

Property	stone masonry	brick masonry	connection	concrete
Density (kg/m^3)	2000	1800	2000	2400
Compressive strength f_c (MPa)	4	4	2	-
Young's modulus E (MPa)	$500 \times f_c$ (2000)	$500 \times f_c$ (2000)	$50 \times f_c$ (100)	30000
Tensile strength f_t (MPa)	$5\% f_c$ (0.2)	$5\% f_c$ (0.2)	$1\% f_c$ (0.02)	-
Poisson's ratio ν	0.2	0.2	0.2	0,2
Fracture energy G_{ft} (N/m)	50	50	5	

Table 7.1 - Mechanical properties – dynamic analysis.

The N2 method [Fajfar, 2000] is adopted to compare the performances derived from the pushover analysis with the results from dynamic analysis. First, the MDOF system is transformed into a SDOF system. Then the capacity curve is bilinearized following the energy balance principle, i.e. by equating the areas between the bilinear and the capacity curve. Finally, the seismic required is determined and it corresponds to the abscissa of the intersection point between the curve of bilinear capacity and the inelastic response spectrum.

In order chose the most appropriate response spectrum to compare the performances derived from the pushover analysis with the results of the dynamic analysis different response spectra are considered.

In the following figure, the obtained spectra for the main horizontal directions Y (NS) and X (EW), which are carried out using the accelerogram that was measured at the station AQU, have been compared with different elastic response spectra according to the Italian seismic code [DM 14/01/2008].

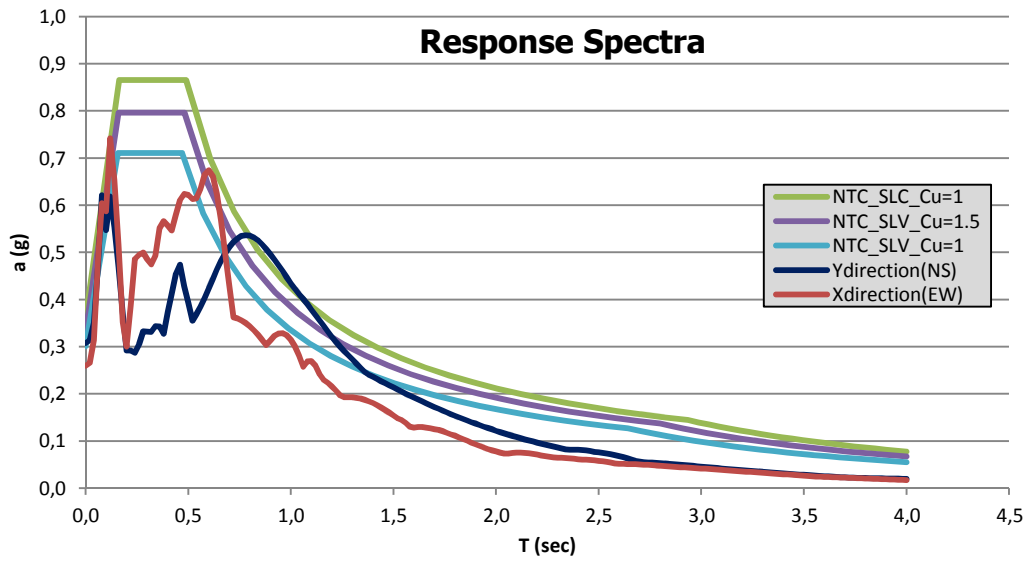


Figure 7.4 – comparison between response spectra.

Consequently, the response spectrum chosen for the comparison between the pushover analysis and the dynamic analysis is calculated using life safety as target performance level and class equal to II.

The seismic action has been calculated using the program "Spettri NTC 2008" and values obtained are as follows:

Peak ground acceleration	a_g	0.261g
Maximum spectral amplification factor	F_0	2.364
Period corresponding to the beginning of the section with constant speed of the horizontal acceleration spectrum	T_c^*	0.347 s
Nominal lifetime of the building	V_N	50
Importance factor	C_u	1,00
Probability of exceedance	P_{VR}	10%
Structure factor	q	2.25
Type soil	B	
Amplification stratigraphic coefficient	S_S	1.154
	C_C	1.360
Amplification topographic coefficient	S_T	1.000
Period corresponding to the beginning of the spectrum section with constant acceleration	T_B	0.157 s
Period corresponding to the beginning of the spectrum section with constant speed	T_C	0.471 s
Period corresponding to the beginning of the spectrum section with constant displacement	T_D	2.643 s

Table 7.2 – Seismic action (pushover analysis).

7.3 EARTHQUAKE X DIRECTION

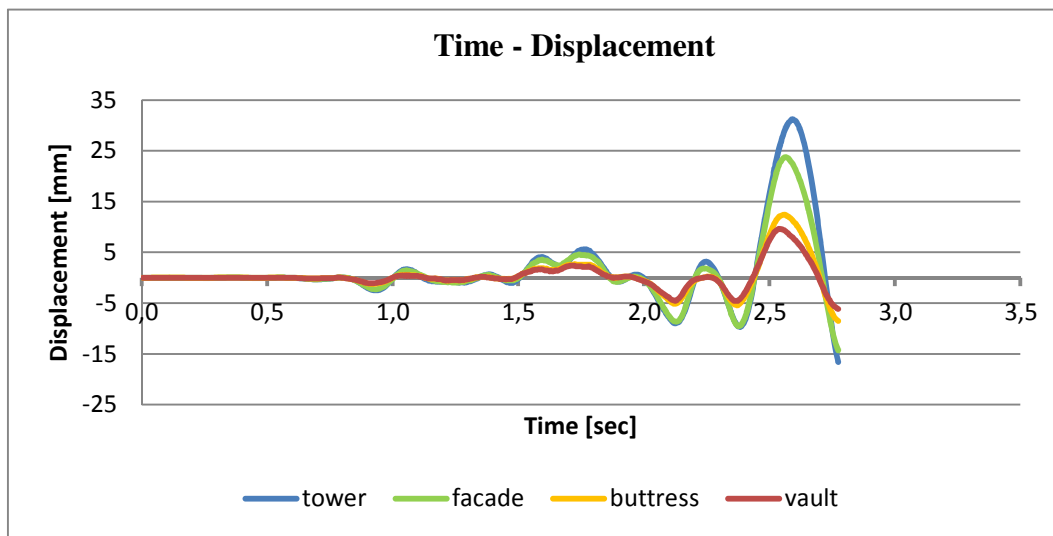


Figure 7.5 – Time-Displacement curve at the top of the tower, top of the nave wall, top of buttress and on the vaults.

In the X direction, the collapse mechanisms are the loss of balance of the chapel's vaults and the overturning of the façade, like in the static analysis.

The analysis stops at time t equal to 2.78 seconds and so before the entire 12 seconds of the accelerogram applied. The maximum displacement of the structure occurs, in all control points considered, at a time included between 2.53 and 2.59 seconds.

The dynamic analysis compared with the static analysis presents smaller strain that are less concentrated in the connection areas between the walls and more diffused both in the vaults that in the top wall of the left façade.

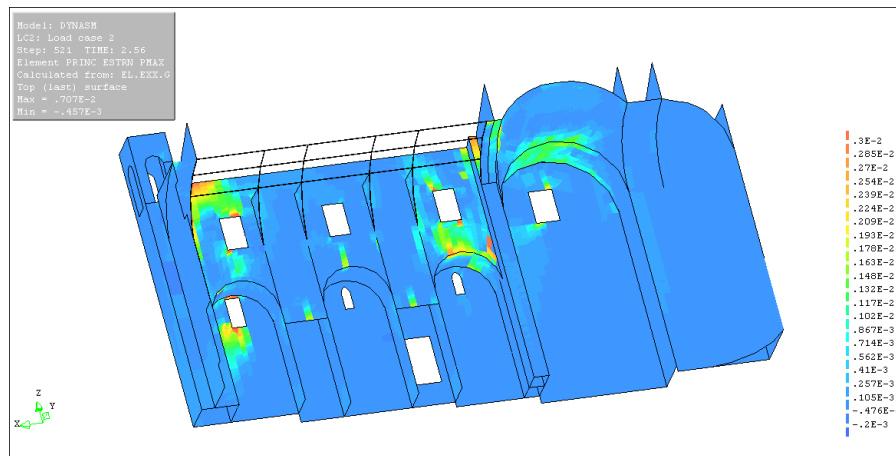


Figure 7.6 - Principal tensile strain to the period $T=2.56$ sec, X direction (vaults view).

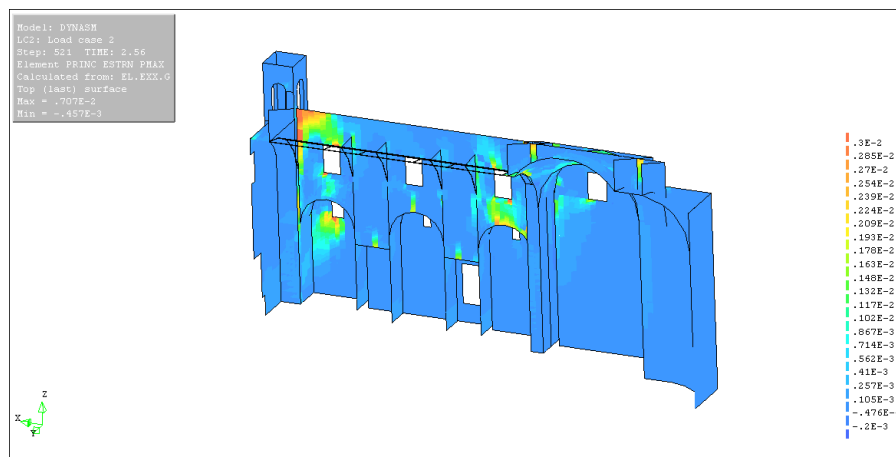


Figure 7.7 - Principal tensile strain to the period $T=2.56$ sec, X direction (internal view).

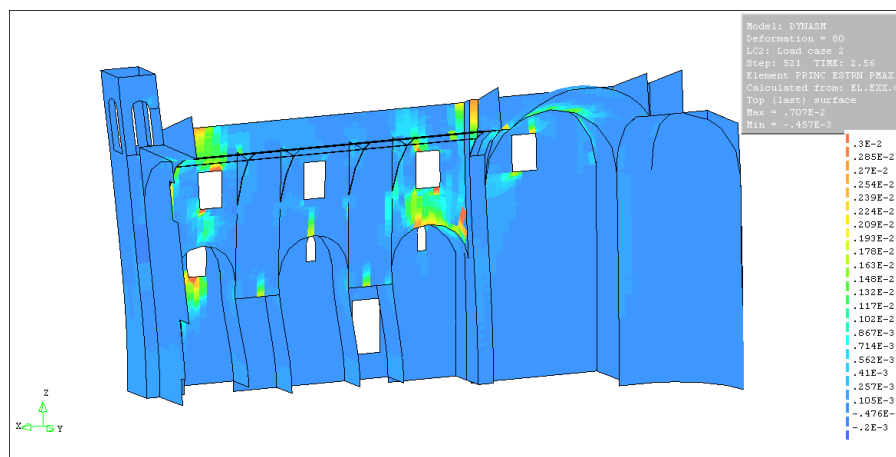


Figure 7.8 - Deformation to the period $T=2.56$ sec, X direction (internal view).

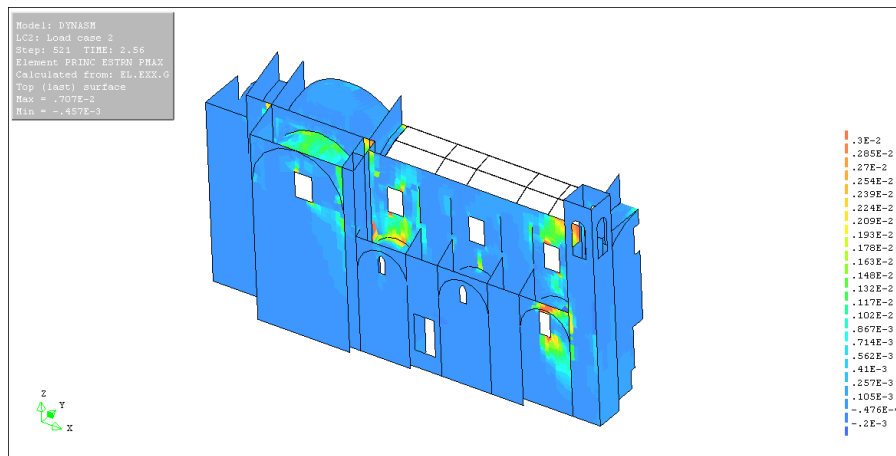


Figure 7.9 - Principal tensile strain to the period $T=2.56$ sec, X direction (external view).

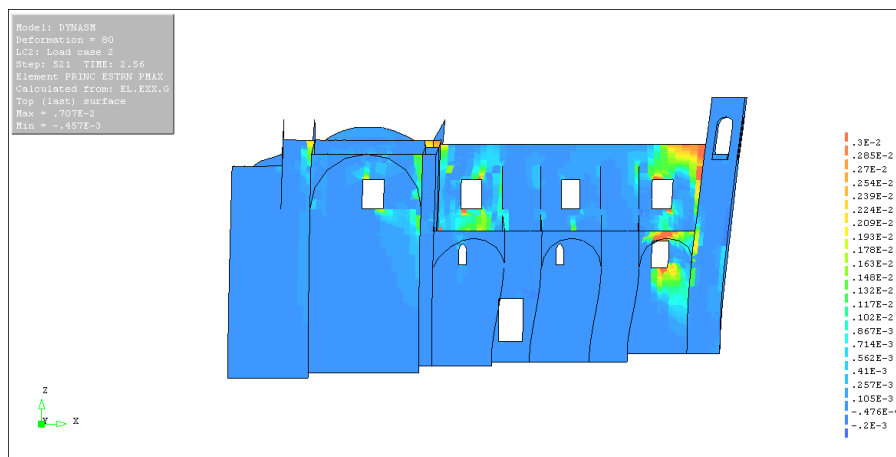


Figure 7.10 - Deformation to the period $T=2.56$ sec, X direction (external view).

In addition, a comparison of seismic requests in terms of maximum displacements, at various points of the church, can be done. In the X direction, the maximum displacement from the pushover analysis results to be similar to that of dynamic analysis, at each considered point.

Along the building height, the displacements obtained from the pushover analysis are greater than those of the dynamic analysis, while they are smaller at the top. In fact the maximum displacement of dynamic analysis at the top of the buttress is equal to 12.4 mm, the required displacement found with the static analysis is 14.6 mm.

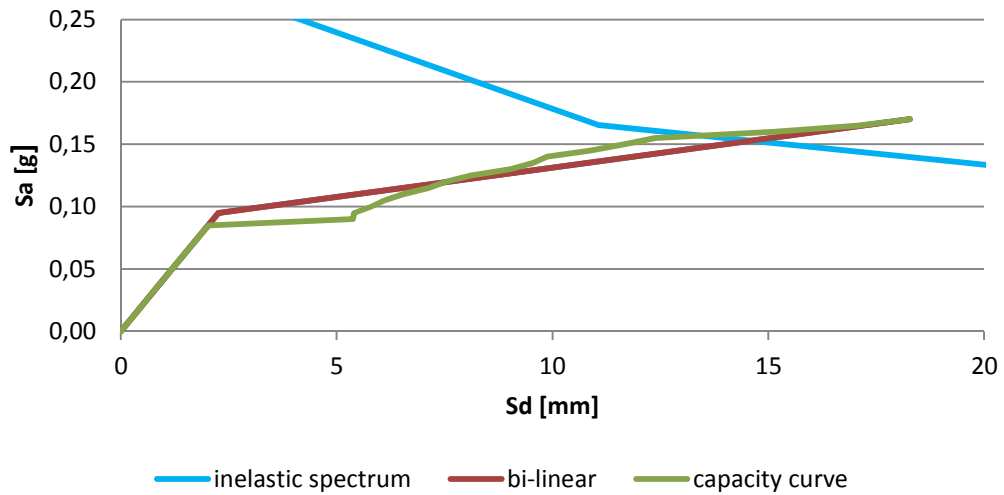


Figure 7.12 – Displacement request at the top of the buttress obtained from the N2 method (X direction).

The maximum displacement of dynamic analysis at the top of the main facade is equal to 23.3 mm, the required displacement found with the static analysis is 21.3 mm.

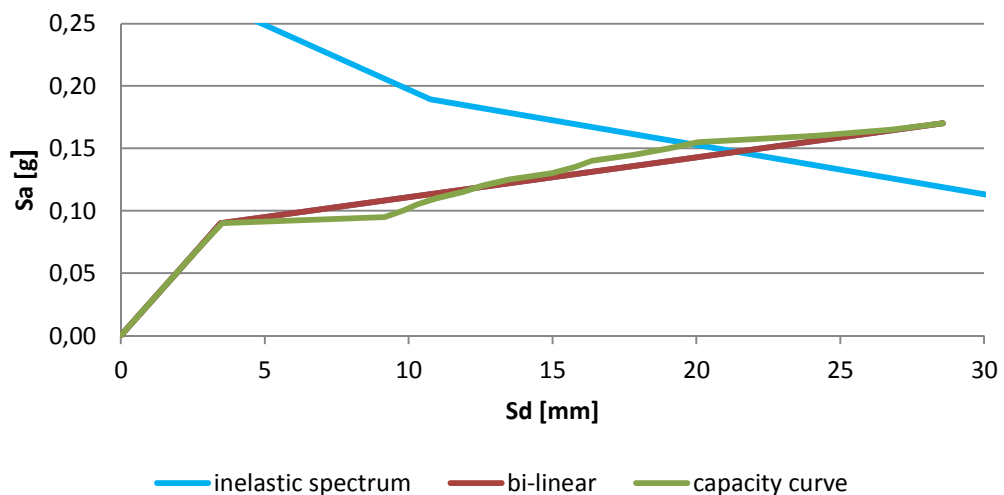


Figure 7.11 – Displacement request at the top of the main facade obtained from the N2 method (X direction).

7.4 EARTHQUAKE Y DIRECTION

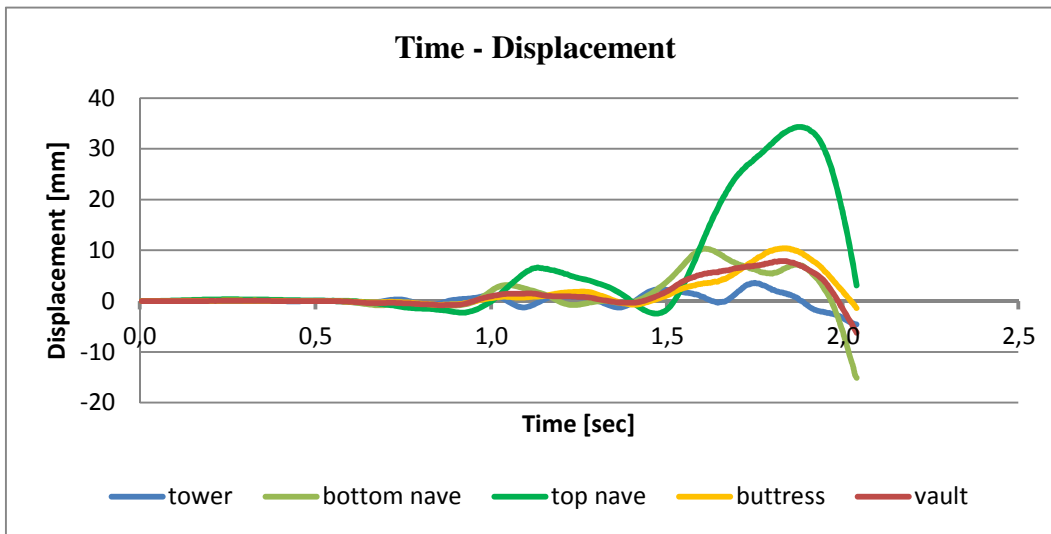


Figure 7.13 – Time-Displacement curve at the top of the tower, top of the bottom wall on the left facade, top of the top wall on the left facade, top of buttress and on the vaults.

In the Y direction, the collapse mechanism is the overturning of the top wall of lateral facade, like in the static analysis. The analysis stops at time t equal to 2.04 seconds and so before the entire 12 seconds of the accelerogram applied. The maximum displacement of the structure occurs at a different time for each control point considered. The top wall of the left facade is the part of the church that has the maximum displacement. This occurs at a time equal to 1.86 seconds. The dynamic analysis compared with the static analysis presents smaller strain but they are distributed in the same way on the structure.

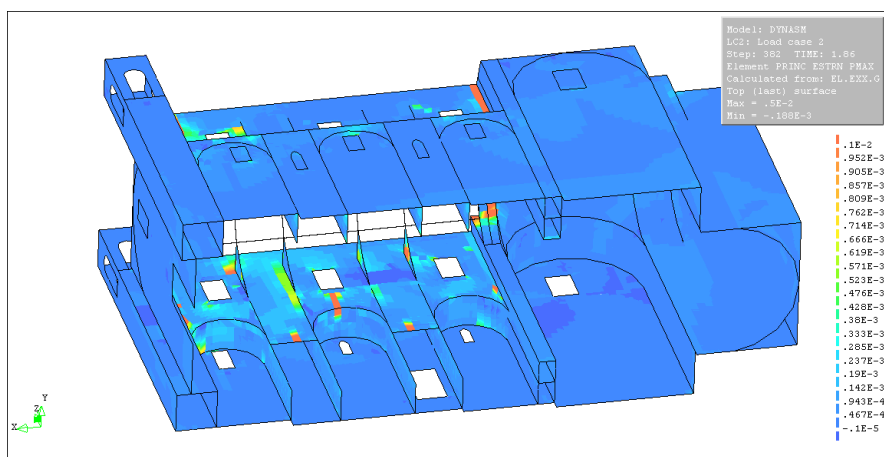


Figure 7.14 - Principal tensile strain to the period $T = 1.86$ sec, Y direction (internal view).

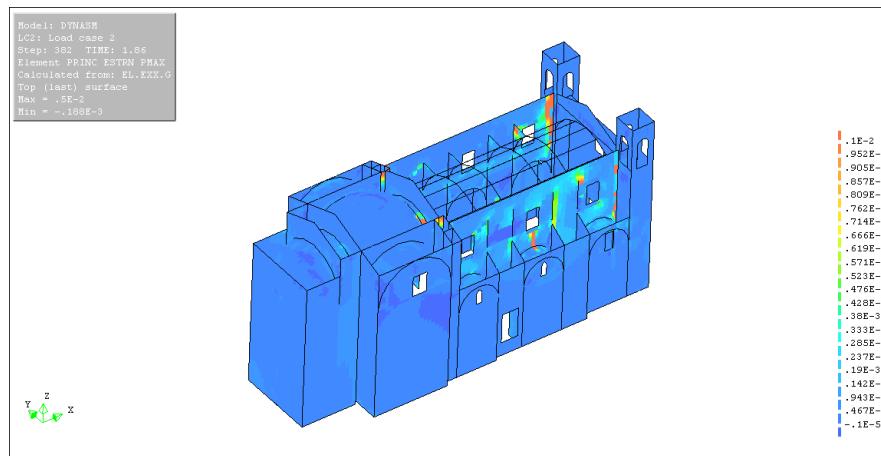


Figure 7.15 - Principal tensile strain to the period $T = 1.86$ sec, Y direction (external view).

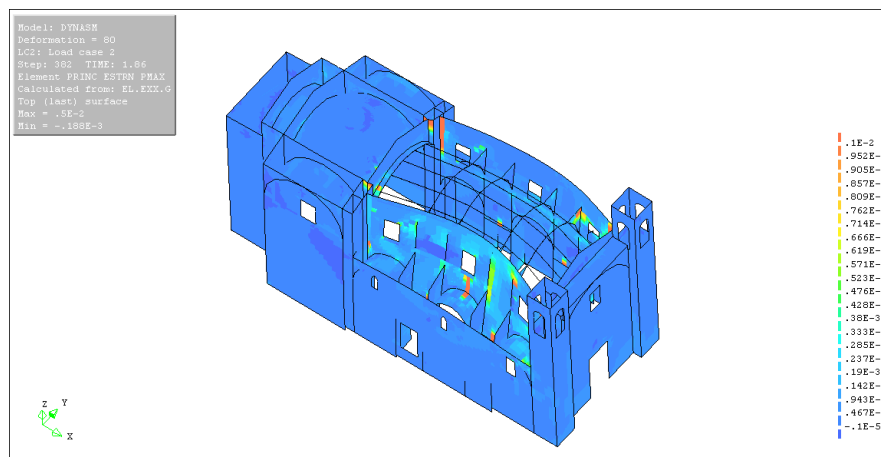


Figure 7.16 – Deformation to the period $T = 1.86$ sec, Y direction (external view).

In addition, a comparison of seismic requests in terms of maximum displacements, at various points of the church, can be done. In the Y direction, the maximum displacement from the pushover analysis results to be greater than that of dynamic analysis, at each considered point. The displacement difference grows with increasing height of the chosen control point and when the walls are positioned orthogonally to the seismic force. In the dynamic analysis the maximum displacements are lower than 10 mm while in the pushover analysis the buttresses arrive at a displacement of 33.1 mm.

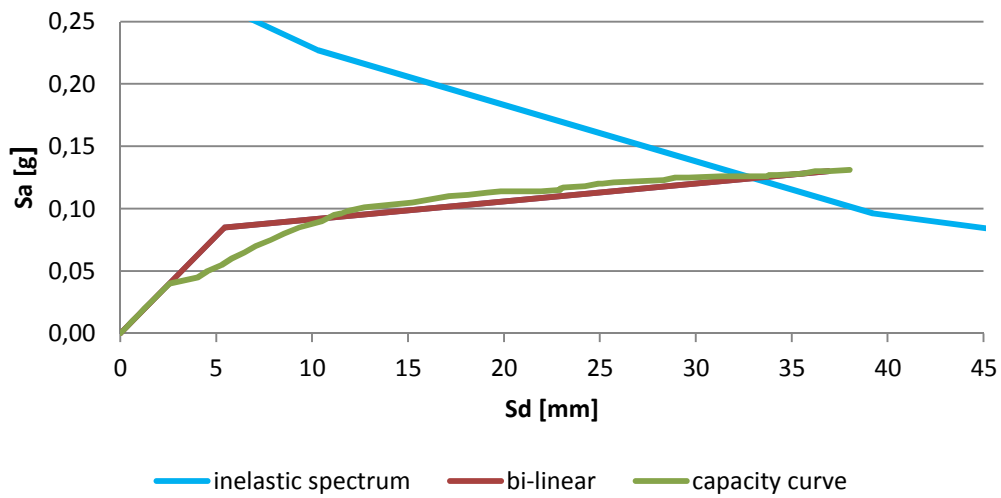


Figure 7.17 - Displacement request at the top of the buttress obtained from the N2 method (Y direction).

The maximum displacement of dynamic analysis at the top of the top wall of the nave is equal to 34.3 mm, the required displacement found with the static analysis is 88.7 mm.

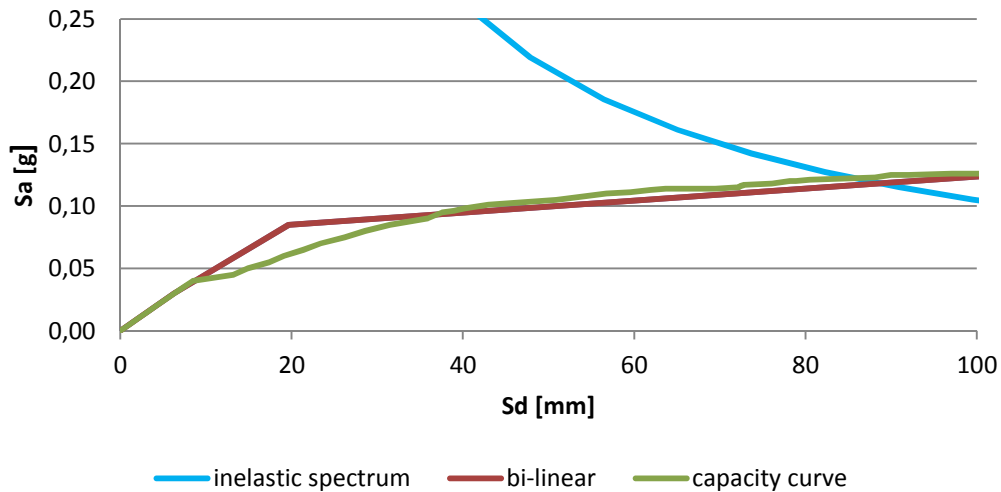


Figure 7.18 - Displacement request at the top of the top wall of the nave obtained from the N2 method (Y direction).

7.5 SUMMARY

In both principal directions the mechanisms of collapse are the same, both in the dynamic and pushover analyses.

In the dynamic analysis the principal tensile strain are smaller in both directions and in the X direction they are also distributed in a different way on the surfaces. In the dynamic analysis the strain is less concentrated in the connection points between the walls and it is more distributed in the areas of the lateral façade where, in the real case, the collapse has occurred. In fact this collapse can be seen under the roof in the right part of the lateral facade, near the connection between tower and facade and in the left part of the lateral facade just above the vault. However, the values of pushover analysis are much larger than that from dynamic analysis.

Both in the longitudinal and transversal directions the maximum displacements obtained from dynamic analysis, at each control point chosen, are smaller than those obtained from pushover analysis.

Generally the displacements in the dynamic analysis are lower than in the pushover analysis, possibly because the latter only considers the movements referred to the first vibration mode so that all displacements have the same direction.

In the X direction, all displacements from the pushover analysis are similar to those from the dynamic analysis and the structure movement probably refers to the first vibration mode.

In the Y direction, on the contrary the dynamic displacements derived from the analysis are smaller than those obtained from the pushover analysis.

This may be due to the complex dynamic response of the church along that direction. Furthermore, in accordance with the N2 method, this procedure for the displacements calculation, leads to an overestimation of the displacement demand in the Y direction (therefore enhancing safety). In contrast to that, in the X direction, the procedure gives displacements similar to real ones, allowing however a lower safety factor.

This may be due to a difficulty to represent such a complex dynamic behavior through an incremental static analysis.

8. FINAL CONCLUSIONS

8.1 GENERAL CONCLUSIONS

Three different methods of analysis, namely kinematic limit analysis, pushover analysis and time domain nonlinear dynamic analysis have been successfully used to characterize the dynamic response of a historical masonry church (Sant Marco church in L'Aquila) and to gain a better understanding of the collapsing mechanism actually activated during the Abruzzo earthquake of 2009.

The comparison among the three methods has given satisfactory and informative and has provided, in most cases, similar results with regards to the seismic capacity and damage. The predicted collapse mechanisms have been the same, in both directions, in all methods used.

According to the analyses carried out, and in agreement with the real observations, the main collapse mechanism of the structure is due to the out of plane movement of the buttresses supporting the chapel vaults. This mechanism evolves causing a loss of balance of the overstanding vaults. The collapse of this vaults leads to the destruction of the overstanding lateral facade wall. The subsequent activated mechanism is the overturning of the main facade and its detachment from the nave walls. The fact that the buttresses of the structure are not adequately connected to the exterior perimeter wall has significant influence on the resulting collapse mechanisms and the corresponding capacity.

8.2 COMPARISON BETWEEN THE METHODS

In the longitudinal direction, the first mechanism that might occur in the church is the out of plane movement of the buttresses supporting the chapel vaults. This mechanism evolves up to a value of about 0.098g for both kinematic and structural analysis, causing a loss of balance in the overlying vaults. The collapse of this vaults leads to the fall of the overstanding wall. The following step is the overturning of the main facade, that is well connected to the lower wall of the lateral facade, with an acceleration value of about 0.17g.

In comparison with the static analysis, the dynamic analysis presents smaller amount of damage that is less concentrated in the connection areas between the walls and more diffused in the vaults and in the top wall of the left facade. In contrast, the maximum displacement from the pushover analysis results to be similar to that of dynamic analysis, at each considered control point. Along the building height, the displacements obtained from the pushover analysis are greater than those of the dynamic analysis, while they are smaller at the top. In fact, the maximum displacement of dynamic analysis at the top of the buttress is equal to 12.4 mm, the required displacement found with the static analysis is 14.6 mm. The maximum displacement of dynamic analysis at the top of the main facade is equal to 23.3 mm, the required displacement found with the static analysis is 21.3 mm.

In the transversal direction, the overturning of the lateral facade's top wall occurs. The activation coefficient of the mechanism resulting from the kinematic analysis is equal to 0.099g, while that obtained through the structural analysis is 0.131g.

Compared with the static analysis, the dynamic analysis presents smaller amount of damage, but it is uniformly distributed on the structure. Also the maximum displacement from the pushover analysis results to be greater than that of dynamic analysis, at each considered control point. The displacement difference grows with increasing height of the chosen control point and when the walls are positioned orthogonally to the seismic force. In the dynamic analysis the maximum displacements are lower than 10 mm, while in the pushover analysis the buttresses arrive at a displacement of 33.1 mm.

The maximum displacement of dynamic analysis at the top of the top wall of the nave is equal to 34.3 mm, the required displacement found with the static analysis is 88.7 mm.

8.3 COMPARISON WITH REAL COLLAPSES AND LIMITATIONS OF METHODS

The difference among the various methods is particularly evident in the mechanism of loss of balance of the arches.

The FE model inevitably considers the different interdependent elements. Consequently, the seismic action in the direction perpendicular to the buttresses is partially absorbed by the main facade that is well connected to the walls of the nave. The main facade is more resistant than the buttresses so that its collapse occurs at a higher seismic coefficient. In support of this hypothesis, the analysis was carried out applying inferior mechanical properties to the buttresses. This analysis shows that the decrease of the tensile strength of the buttresses has a great influence on the global structure behavior. The seismic factor drastically decreases even if the collapse mechanism is still the loss of balance of the main facade. This conclusion confirms the interdependence of the various elements, but this circumstance rarely occurs in existing buildings.

The development of mechanisms of collapse was especially frequent in churches, in spite of the good characteristics of the masonry and it was caused by the loss of equilibrium of the rigid blocks. Consequently, damages take place at local level and the structure can be divided into macroelements characterized by a mostly independent structural behaviour from the rest of the building.

The kinematic method is an approach suitable to describe the real behavior of the church. However, it is difficult to predict the collapse mechanism before an earthquake. This is due to the fact that a careful study of all possible mechanisms that may occur is required. In addition, it's necessary to know the disconnections between wall panels involved in the loss of balance and the real locations of hinges or cracks are difficult to predict. However, in order to consider the results obtained through each method as valid, a deep knowledge of the structure is indispensable.

8.4 SEISMIC CAPACITY

The safety factor provides information about the comparison between the seismic action demand and the capacity of the structure under particular load pattern and so it allows to check if the occurred displacements caused the collapse. The safety factor is obtained through the ratio between the ultimate displacement (d_u) and the demand displacement (Δ_d). Generally, new buildings' safety level is acceptable if greater than 2. On the other hand, no minimum safety level was defined by Italian

code for existing buildings, but they must reach an established safety level only in “seismic upgrading”, which is the case of heavy and wide interventions [DM 14/01/2008; §8.4 and Circolare 617 02/02/2009; §C8.4].

The displacements are derived from the nonlinear static analysis except for the buttress. The buttress displacements are obtained by means of the kinematic analysis, since the pushover analysis stops when the first local collapse in the whole construction occurs. As already mentioned in the previous chapters, the FE model inevitably considers the different interdependent elements and the collapse, in the longitudinal direction, is not the overturning of the buttresses but that of the main façade. For this reason, the pushover analysis does not provide the ultimate displacement of the buttresses, which is therefore derived from the kinematic analysis but using the same response spectrum that was used for the comparison between the pushover analysis and the dynamic analysis.

The safety factors against the overturning of the façade, of the buttresses and of the top wall of the lateral façade are 1.20, 0.84 and 1.32.

These safety levels give satisfactory values. In fact, the material of the lateral façade doesn't crash but it presents partial collapses. The tower begins to detach from the nave walls and the buttresses displacement is high enough to cause a loss of balance of the overstanding vaults.

These considerations underline the importance in the existing buildings of the chosen control point. In the historical building, where the different elements are not well connected, every macroelement has a different structural behaviour and so the larger displacement, or the displacement that leads the collapse of a building part, cannot be the displacement on the top of the church. The careful study of the control point chosen is needed.

8.5 INTERVENTION NEEDS AND POSSIBLE ACTIONS

On the basis of the damage and failure mechanisms activated during the earthquake and identified by this study, it is possible to propose a set of strengthening interventions for the seismic retrofit of the Church.

In the designed interventions a particular attention has to be paid to the principles of conservation of the values of cultural and artistic heritage. The selected interventions are based on the principles of compatibility and durability, that is to say the original construction techniques, reversibility or removability and minimizing costs and intervention while ensuring their effectiveness.

The proposed interventions primarily aimed at:

- making effective connections between vertical elements and between vertical elements and roof or curved elements,
- introducing new resistant elements to reduce thrusts given by vaults or the roof,
- improving the quality of the masonry by means of consolidation or replacement.

The proposed interventions to improve the seismic response are listed in the following items:

- Reconstruction of the masonry destroyed by the earthquake (lateral facade, vaults, buttresses) applying the technique of the “scuci-cuci” with the insertion of bracing stones placed at regular intervals in order to obtain a monolithic transverse and accurate connection.
- Realization of connections between the lateral facade and the buttresses and among the lateral facade, the transept and the main facade using the technique of “scuci-cuci”.
- Restoration of the facade, the portals and other elements made of stone.
- Removing addition or alterations to the original structure that increased the building vulnerability, such as the box in RC above the presbytery and the prefabricated beams of the roof, or at least reducing their destabilizing effects in case of earthquake. In the case of masonry portions with deep lesions or particularly damaged but in limited areas, like the lateral façade’s portion, the technique of the “scuci-cuci” can be coupled to local injections of hydraulic lime mortar. The interventions of consolidation must be applied, as much as possible, in a regular and uniform way. The excessive execution of interventions on limited portions of the building may significantly change the distribution of stiffness.
- Insertion of ties in the longitudinal direction of the church, located near the top wall of the lateral facade and under the windows at the bottom of the

barrel vault. Ties will also be introduced in the transverse direction of the church at the roof level. The ties must be anchored to the masonry through anchorages plates. They enhance the box behavior of the building and improve the in-plane behavior. Local consolidation of the masonry in the anchorage area would be necessary.

- Insertion of steel ties that allows lightness and limits invasiveness. The steel ties properly work as a connection among the wooden elements of the roof and enhance the distribution of the loads coming from the roof beams. If necessary, the existing roof may be replaced by a lighter wooden one with truss and X-shape bracing of wooden planks and screwed steel bands. Keeping the wooden roof, the masses in the highest part of the building are decreased and hence the inertial seismic forces in case of earthquake. The consolidation in the local point of contact between wall and roof would be necessary.
- Getting back the stiffening of “frenelli”, which are present in the extrados of the nave arches. If necessary, FRP composite strips may be applied on the arches extrados. Subsequent reconstruction of the barrel vault of “cannucciato” (reed).

8.6 FUTURE RESEARCH

The present study has shown that the pushover, nonlinear dynamic and kinematic analyses can provide reliable results when applied to existing masonry structures, like the church analyzed. The FE analysis combined with the kinematic analysis is always the most suitable technique to perform. In doing so, it is possible to come to more founded and certain conclusions. However, it would be necessary to extend the comparison among different methods to a variety of structures, in order to gain more experience and confidence in the use of one specific method instead of another one. In addition, the investigation and the development of non-destructive inspection techniques that preserve the monument and the materials are desirable. Thus, the study of the possible collapse mechanisms is easier, more precise and less uncertain. Non-destructive tests (NDT) and moderate-destructive tests (MDT) should be preferred to destructive test. In practice, nowadays, a very

limited number of pits that allow direct observation and laboratory testing are normally acceptable. For this reason, only limited and partial information can be collected and additional assumptions on morphology and material properties may be needed in order to elaborate a model. The addition of these qualitative considerations often implies a high level of uncertainty which adds to that already involved in the calculation method. Furthermore, some additional studies on reinforcing techniques using new composite materials and on their adhesion systems are advised. This permits the development of innovative interventions designed to increase strength and reduce the deformability of the vaults. The contribution of strengthening materials and reparation techniques is required to reestablish their performance and to prevent the brittle collapse of the masonry in possible future dangerous conditions. Finally a study concerning the finite element model is recommended in order to obtain a modeling that may lessen the dependence between the various elements. After the whole analysis is performed, the results, besides being valid for new buildings with a box behavior, may better reflect the behavior of existing buildings.

REFERENCES

Brencich A, Gambarotta L, Lagomarsino S, “A macroelement approach to the three-dimensional seismic analysis of masonry buildings”. In: Proc of the XI European conf on earthquake engineering, Paris, France, 1998

Circolare 617 02/02/2009. “Istruzioni per l’Applicazione delle Norme Tecniche per le Costruzioni di cui al DM 14/01/2008”. Infrastructure Ministry, Official Gazette of the Italian Republic, 26 February 2009. (Italian)

Cundall PA, Hart P, “A computer model for simulating progressive large scale movements in blocky rock systems”. In: Proc of the symposium of the int society of rock mechanics. Nancy, France, vol 1, 1971

Cuzzilla R, “Application of Capacity Spectrum Method to Gothic constructions”. Master’s Thesis, Advanced Masters in Structural Analysis of Monuments and Historical Constructions, Barcelona, Spain, 2008

Del Monte E, “L’analisi statica non lineare secondo il D.M. 14/01/2008”. Firenze, Italy, 2010. Source: www.dicea.unifi.it/~emadelmo/lezione26042010.htm.

Di Tommaso A, Focacci F, Saetta A, “Meccanismi di collasso delle costruzioni storiche per azione sismica ed interventi compatibili di miglioramento mediante materiali compositi”. Venezia, Italy, 2007

DM 14/01/2008. "Norme Tecniche per le Costruzioni". Infrastructure Ministry, Official Gazette of the Italian Republic, 4 February 2008. (Italian)

EERI Special Earthquake Report (2009). “The Mw 6.3 Abruzzo, Italy, Earthquake of April 6, 2009”. Source: <http://www.eeri.org>

Giuffrè A, “Lecture sulla meccanica delle murature storiche”. Kappa, Rome, Italy, 1990

Giuffrè A, “Vulnerability of historical cities in seismic areas and conservation criteria”. In: Congress “Terremoti e civiltà abitative”, Annali di Geofisica, Bologna, Italy, 1995

Karantoni FV, Fardis MN, “Effectiveness of seismic strengthening techniques for masonry buildings”. J Struct Eng ASCE, 1992

Fajfar P, “A nonlinear analysis method for performance-based seismic design”.
Earthquake Spectra, 16(3): 573-592, 2000

Fajfar P, “Capacity spectrum method based on inelastic demand spectra”. Earthq
Eng Struct Dyn 28:979–993, 1999

Galli P. et al., RPT02 – 09.04.2009 “Report on the effects of the Aquilano
earthquake of 6th April 2009”, 2009. Source:
http://www.mi.ingv.it/eq/090406/quest_eng.html

ICOMOS-ISCARSAH recommendations. “Recommendations for the analysis,
conservation and structural restoration of architectural heritage”. International
Scientific Committee for Analysis and Restoration of Structures of Architectural
Heritage, 2005.

Lagomarsino S, “On the vulnerability assessment of monumental buildings”. Bull
Earthq Eng 4:445–463. European Commission, Brussels, 2006

Lagomarsino S, Giovinazzi S, Podestà S, Resemini S, “An advanced approach to
earthquake risk scenarios with application to different European Towns”. RISK-
UE-EVK4-CT-2000-00014, WP5: Vulnerability assessment of historical and
monumental buildings, 2003

Linee Guida. “Linee Guida per la Valutazione e Riduzione del Rischio Sismico
del Patrimonio Culturale del Ministero per i Beni e le Attività Culturali”.
Consiglio Superiore dei Lavori Pubblici, Official Gazette of the Italian Republic,
29 January 2008. (Italian)

Lourenço PB, “Structural Masonry Analysis: Recent Developments And
Prospects”, Portugal, 2007

Magi J, “Seismic vulnerability of historical structures - Case study: San Marco
church in the sequence of 2009 Abruzzo earthquake”. Master’s Thesis, Advanced
Masters in Structural Analysis of Monuments and Historical Constructions,
Padova, Italy, 2009

Milano L, Mannella A, Morisi C, Martinelli A, “Schede illustrative dei principali
meccanismi di collasso locali negli edifici esistenti in muratura e dei relativi
modelli cinematici di analisi”. ReLUIS, 2009. Source: www.reluis.it

Modello A-DC – “Scheda per il rilievo del danno ai beni culturali – Chiese. Abaco dei meccanismi di collasso delle chiese”, 2006. Source: www.protezionecivile.it.

Modena C, et al, 2009. “Damage assessment report of July 2009 on the San Marco Church, L’Aquila (Italy)”. Source: <http://terremotoabruzzo09.itc.cnr.it/>.

Modena C, Valluzzi MR, Da Porto F, Casarin F, Munari M, Mazzon N, Panizza M, “Assessment and improvement of the seismic safety of historic constructions”. Padova, Italy, 2008

Munari M, “Metodi di analisi semplificata di edifici esistenti in muratura”. Corso di Problemi strutturali dei Monumenti e dell’Edilizia Storica, Padova, Italy, 2010

Munari M, “Sviluppo di procedure per valutazioni sistematiche di vulnerabilità sismica di edifici esistenti in muratura”. Ph.D. Thesis, Padova, Italy, 2009

NIKER Project – Universitat Politècnica de Catalunya, “New integrated knowledge based approaches to the protection of cultural heritage from earthquake-induced risk - Deliverable 8.4: Reliably quantification of building performance and response parameters for use in seismic assessment and design”, Barcelona, Spain, 2012

NIKER Project – Universitat Politècnica de Catalunya, “New integrated knowledge based approaches to the protection of cultural heritage from earthquake-induced risk - Deliverable 8.3: Parametric study of buildings according to geometry, intervention techniques, stiffness of horizontal elements, connections”, Barcelona, Spain, 2012

Pelà L, “Continuum Damage Model for Nonlinear Analysis of Masonry Structures”. International Ph.D. Thesis, Barcelona, Spain, 2009

Politecnico di Milano, Università degli Studi di Padova, Soprintendenza ai Beni Architettonici e Paesaggistici dell’Abruzzo, Arcidiocesi di L’Aquila, “Chiesa Di San Marco – L’Aquila”, Italy, 2009

Programma “C-Sisma” ver.3.1-PRO, Italy, 2010

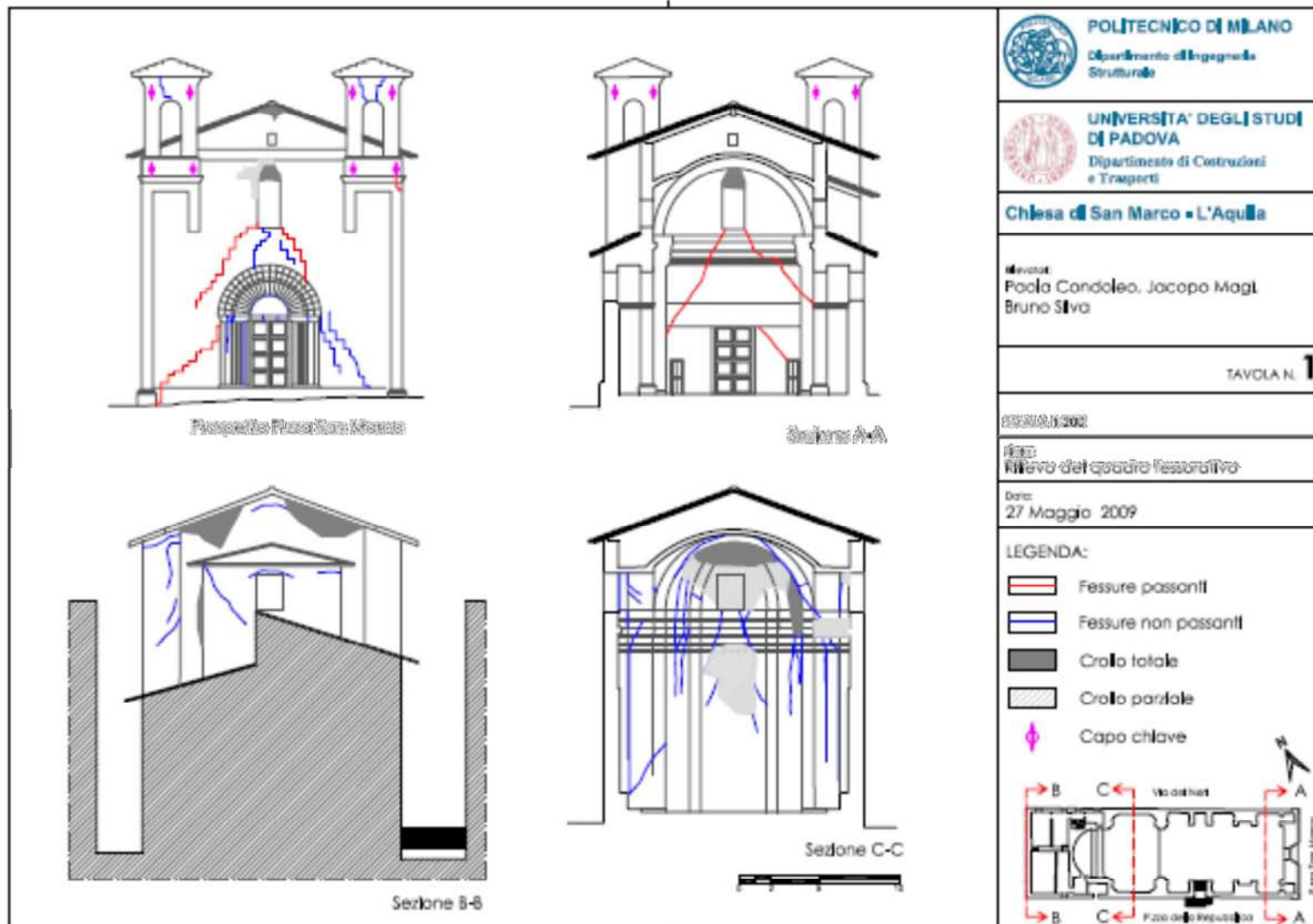
Programma “Spettri NTC 2008” ver.1.0.3, Italy, 2008. Source: <http://www.cslp.it>

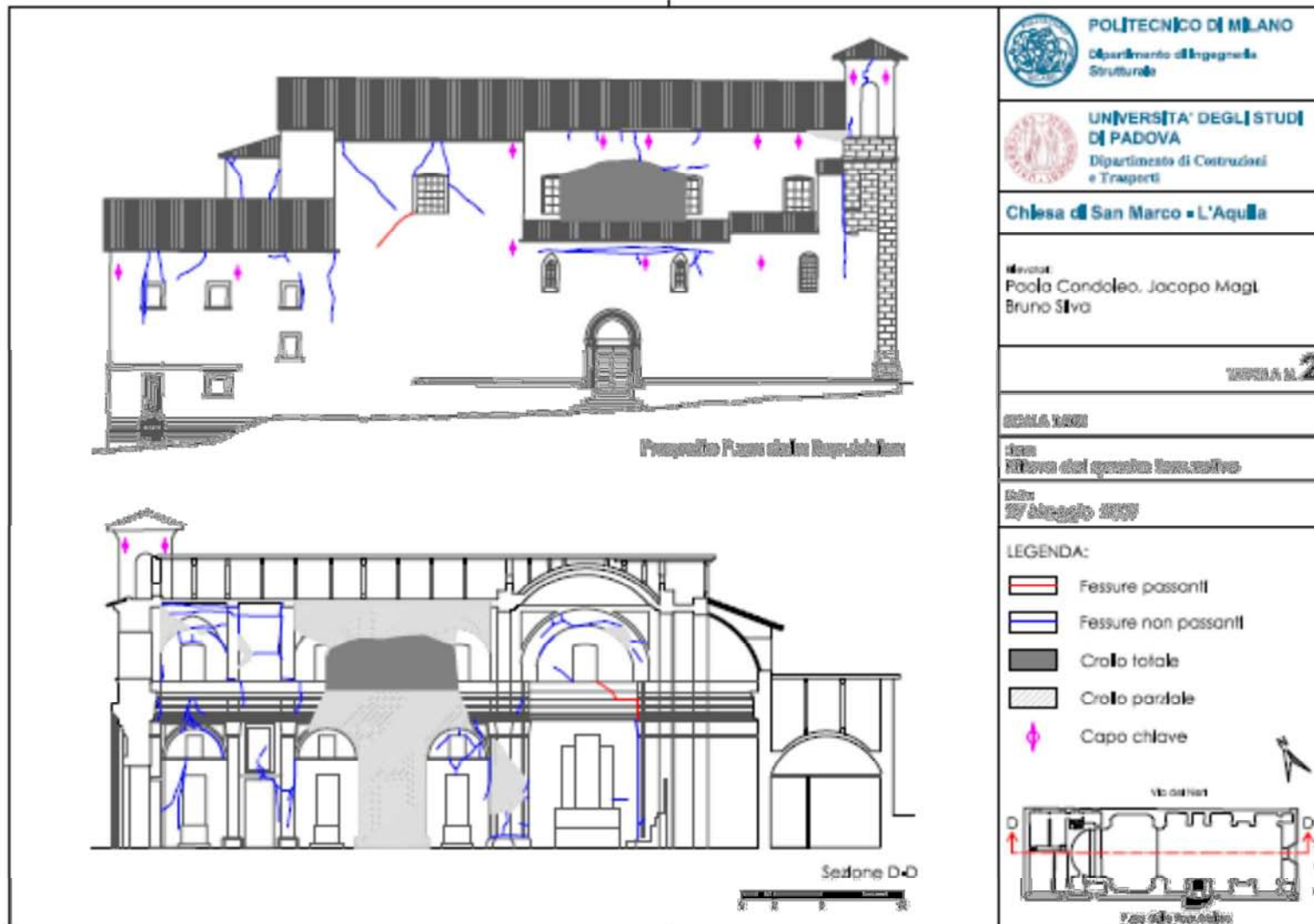
Roca P, Cervera M, Gariup G, Pelà L, “Structural Analysis of Masonry Historical Constructions. Classical and Advanced Approaches” CIMNE, Barcelona, Spain, 2010

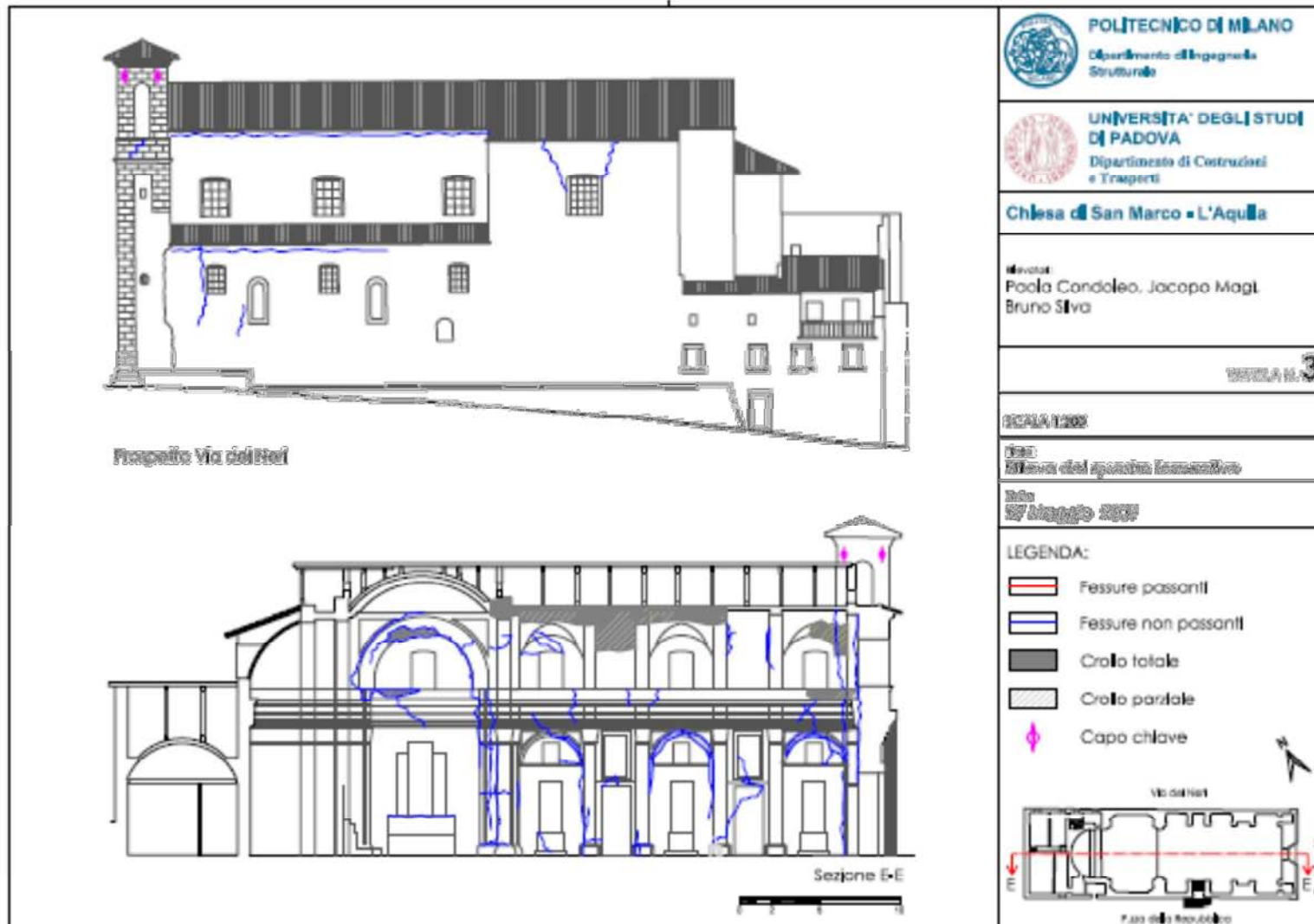
Zografou AI, “Structural Modeling of masonry structures severely damaged by earthquake – Case study of St.Marco’s church in L’Aquila”. Master’s Thesis, Advanced Masters in Structural Analysis of Monuments and Historical Constructions, Padova, Italy, 2010

APPENDIX A1: PHOTOGRAPHIC REPORT

A1.1 DAMAGE ANALYSIS







A1.2 INTERVENTIONS

Interventions in 1970

- Replacement of the cover

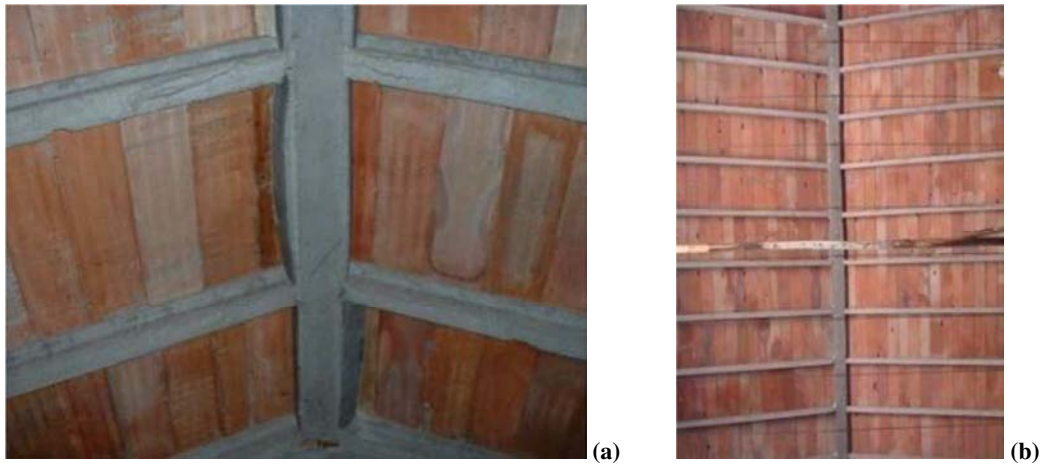


Figure A21 - Covering made by prefabricated beams

- Realization of a RC box over the presbytery

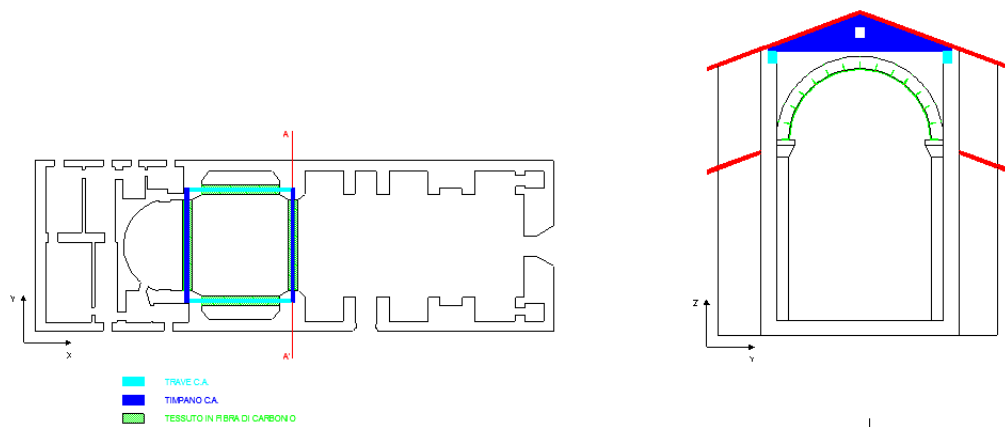


Figure A1.2 – Location of the RC elements

Interventions in 2005

- Replacing the old eaves

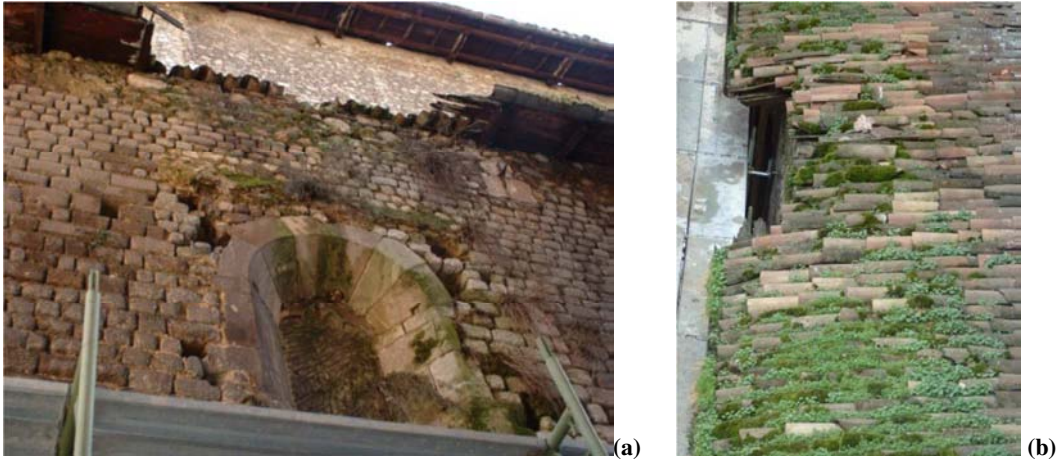


Figure A1.3 - Eaves before the intervention

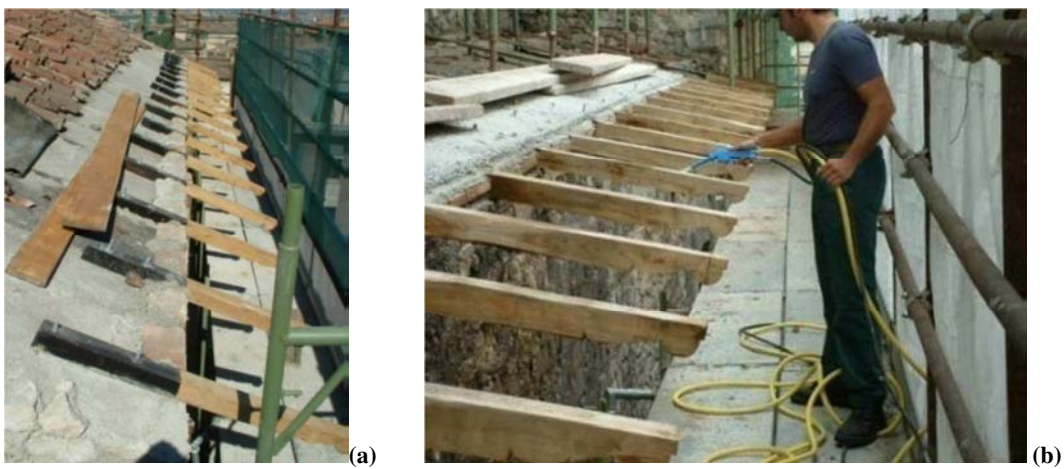


Figure A1.4 - New eaves

- **Renovation of the bell towers roof**



Figure A1.5 - old bell towers roof



Figure A1.6 - new bell towers roof

- Renovation of the church roof



(a)



(b)



(c)



(d)

Figure A1.7 - building phases

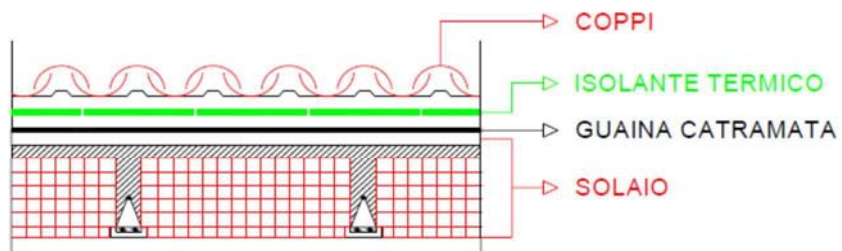


Figure A1.8 - Roof section.

- **Maintenance of the lateral facades and main façade**



Figure A1.9 - maintenance work on the church façades

- **Application of Carbon Fibre on the intrados of the arches of the dome in the transept**



(b)



(c)



(d)



(e)



(f)



(g)

Figure A1.10 - phases of FRP installation

A1.3 PRESENT STATE

- APSE COLLAPSE



(a)



(b)



(c)



(d)

Figure A1.11 - apse collapse

- DOME COLLAPSE



Figure A1.12 - dome collapse

- BARREL VAULT COLLAPSE



Figure A1.13 - barrel vault collapse

- RC ELEMENTS COLLAPSE



(a)



(b)



(c)

Figure A1.14 - RC tympanum collapse

- LATERAL FAÇADE PARTIAL COLLAPSE



Figure A1.15 – left façade collapse

- OUT-OF PLANE MOVEMENT OF THE MAIN FAÇADE

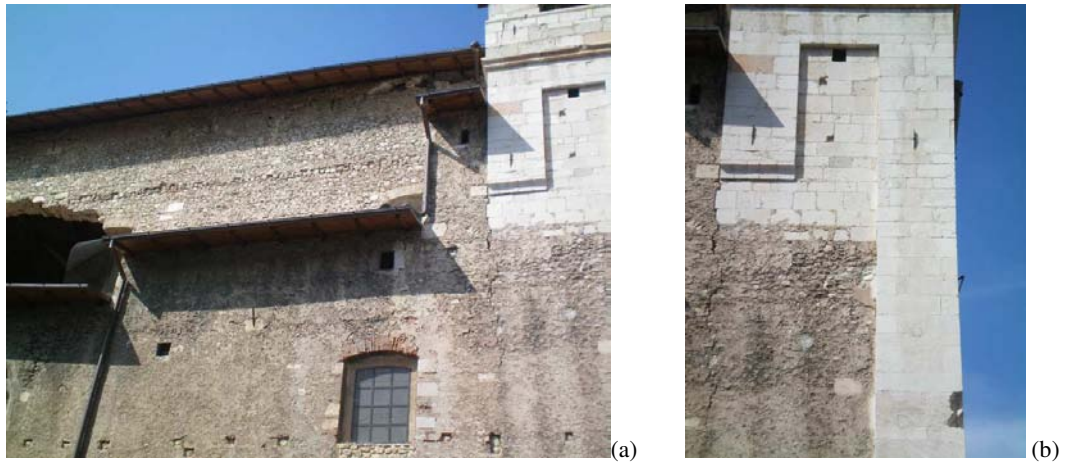


Figure A1.16 - Out-of-plane movement of the main façade.

- IN- PLANE MOVEMENT OF THE MAIN FAÇADE



(a)



(b)



(c)



(d)



(e)



(f)

Figure A1.17 - In-plane movement of the main façade.

- OUT-OF-PLANE MOVEMENT OF THE BUTTRESSES



(a)



(b)



(c)



(d)



(e)



(f)

Figure A1.18 – Out-of-plane movement of the chapel walls.

- SEPARATION OF RIGHT FACADE



(a)



(b)

Figure A1.19 - right façade

- GOOD RESPONSE OF A BELL TOWERS



(a)



(b)

Figure A1.20 - bell towers

- CHAPELS VAULTS COLLAPSE



(a)



(b)



(c)



(d)



(e)



(f)



(g)



(h)



(i)



(l)



(m)

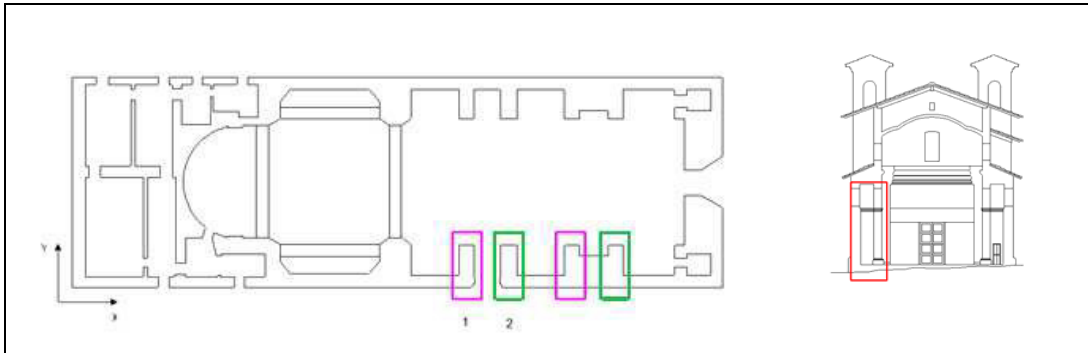


(n)

Figure A1.21 – Chapels vaults collapse.

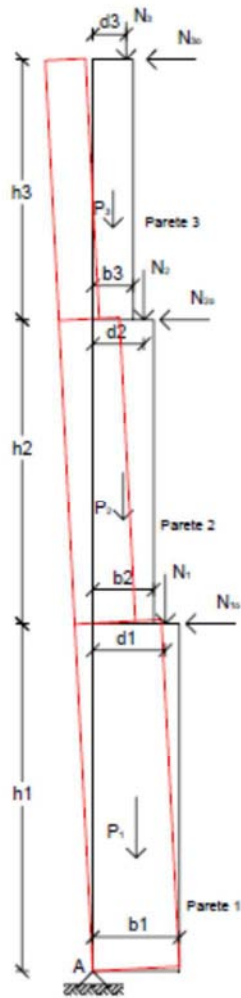
APPENDIX A2: CALCULATION RESULTS

A.2.1 EARTHQUAKE X DIRECTION



Out of plane movement of a monolithic wall simply supported

Buttress 1:



Geometrical properties

H1	3.5	m
B1	0.85	m
H2	2.5	m
B2	0.85	m
H3	2	m
B3	0.85	m
H _{tot}	8	m

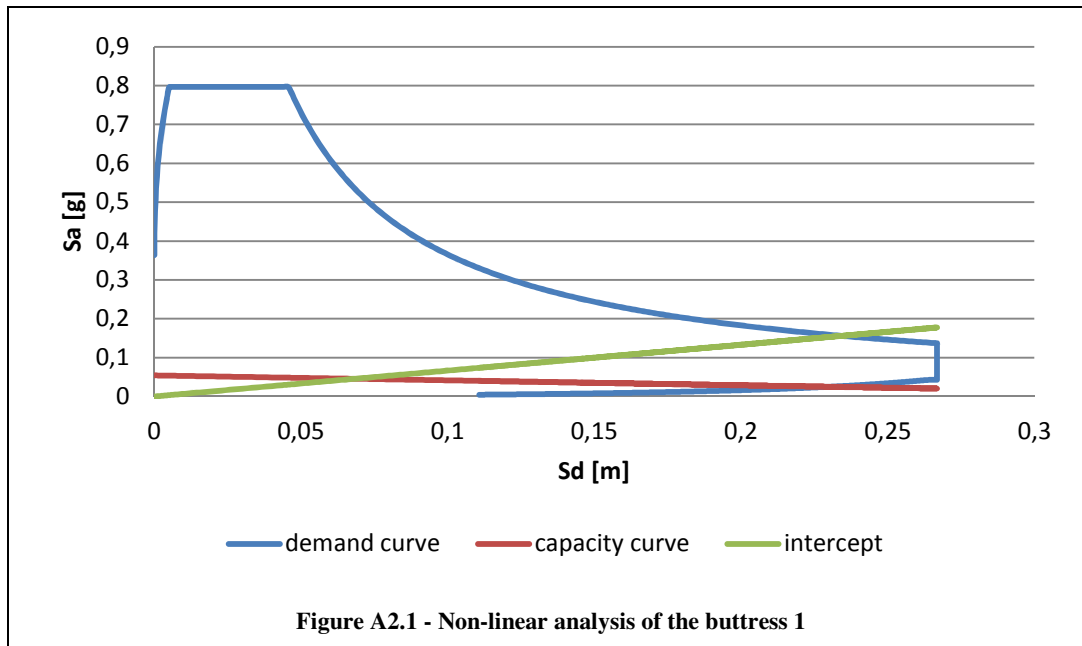
Loads

P1	59.5	KN
N1	12.8	KN
N1o	-3.9	KN
D1	0.14	m
P2	42.5	KN
N2	15.9	KN
N2o	5.8	KN
D2	0.70	m
P3	34	KN
N3	275.35	KN
D3	0.45	m

Material properties

f _c	4	MPa
f _t (5% f _c)	0.2	MPa
γ	20	KN/m ³

$$c = \frac{a}{g} = 0.060$$



Mass involved	M*	99.34	Kg	
Fraction of mass involved	e*	0.92		
Spectral acceleration which activates the mechanism	a ₀ *	0.053g		
Final spectral displacement	d _u *	0.171	m	
SLU WITH LINEAR ANALYSIS	a*	0.167g		NOT CHECKED
SLU WITH NON LINEAR ANALYSIS	Δd	0.235	m	NOT CHECKED

By performing the non-linear analysis, the value obtained was $d_u^* = 0.171$ m, while the value required by the Italian code was $\Delta d = 0.235$ m. The calculated value is far from the required one.

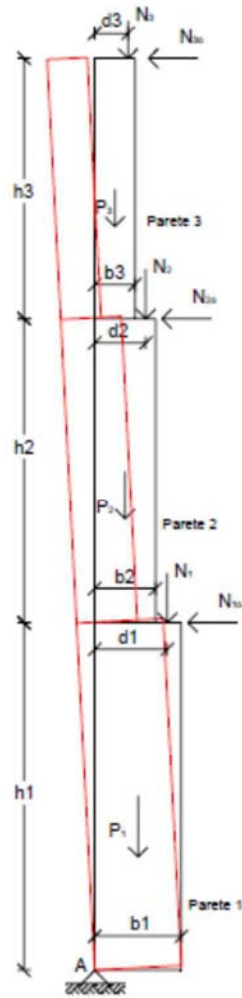
The buttress has been divided into three part and to the upper end of each part were applied loads due to:

- the geometry and the self-weight of the smallest vault, the dead load of the wall resting on the smaller vault,
- the geometry and the self-weight of the biggest vault,
- the dead load of the upper wall of the lateral façade and of the roof.

The horizontal force of the vault, that is associated to its geometry, contributes to the calculation of stabilizing-overturning moment. However, this force isn't linked to a mass and therefore mustn't be counted in the calculation of the inertia force and in the calculation of the mass involved in the mechanism.

Out of plane movement of a monolithic wall simply supported

Buttress 2:



Geometrical properties

H1	3.5	m
B1	0.85	m
H2	2.5	m
B2	0.85	m
H3	2	m
B3	0.85	m
H _{tot}	8	m

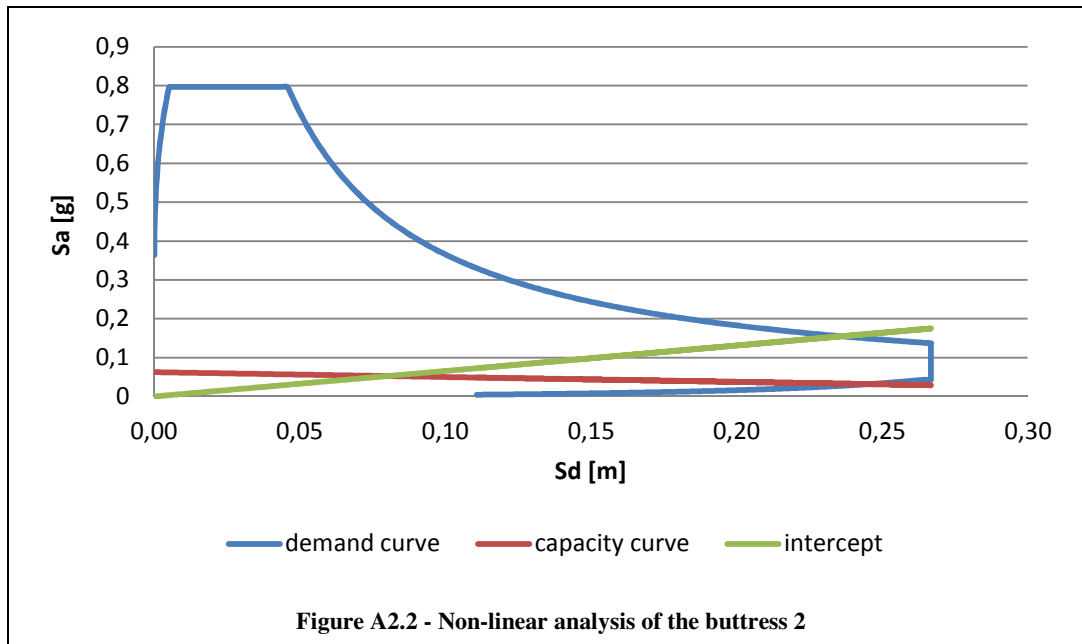
Loads

P1	59.5	KN
N1	12.8	KN
N1o	3.9	KN
D1	0.70	m
P2	42.5	KN
N2	15.9	KN
N2o	-5.8	KN
D2	0.14	m
P3	34	KN
N3	275.35	KN
D3	0.40	m

Material properties

f _c	4	MPa
f _t (5% f _c)	0.2	MPa
γ	20	KN/m ³

$$c = \frac{a}{g} = 0.069$$



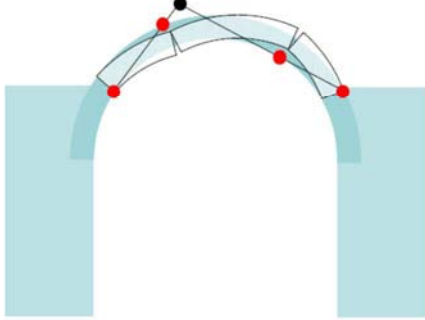
Mass involved	M^*	99.34	Kg	
Fraction of mass involved	e^*	0.92		
Spectral acceleration which activates the mechanism	a_0^*	0.061g		
Final spectral displacement	d_u^*	0.200	m	
SLU WITH LINEAR ANALYSIS	a^*	0.167g		NOT CHECKED
SLU WITH NON LINEAR ANALYSIS	Δd	0.235	m	NOT CHECKED

By performing the non-linear analysis, the value obtained was $d_u^* = 0.200$ m, while the value required by the Italian code was $\Delta d = 0.235$ m. The calculated value is far from the required one.

The buttress has been divided into three part and to the upper end of each part were applied loads due to:

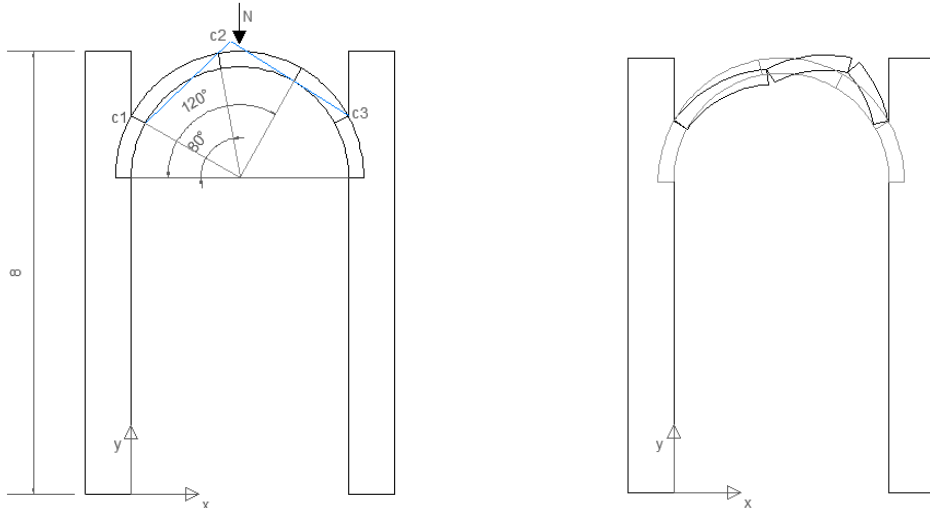
- the geometry and the self-weight of the smallest vault, the dead load of the wall resting on the smaller vault,
- the geometry and the self-weight of the biggest vault,
- the dead load of the upper wall of the lateral façade and of the roof.

The horizontal force of the vault, that is associated to its geometry, contributes to the calculation of stabilizing-overturning moment. However, this force isn't linked to a mass and therefore mustn't be counted in the calculation of the inertia force and in the calculation of the mass involved in the mechanism.

Loss of balance of a single arch			
Arch:			
 <p style="text-align: center;">Mechanism type 1</p>	Geometrical properties		
	Re	2.28	m
	Ri	2	m
	s	0.85	m
	L	4	m
	θ1	29	°
	θ2	80	°
	θ3	120	°
	θ4	153	°
	Loads		
	PV	28.80	KN
	N	636.96	KN
	D	2.00	m
Material properties			
fc	4	MPa	
ft (5% fc)	0.2	MPa	
γ	20	KN/m ³	
$c = \frac{a}{g} = 0.911$			

The value of the collapse coefficient is very high as a consequence it is difficult that this is the mechanism that has led to the collapse.

The vertical loads considered in this analysis are: the vault self-weight and the dead load of the wall and of the roof resting on the vault.



Loss balance of the arch and of both buttresses

Arch:

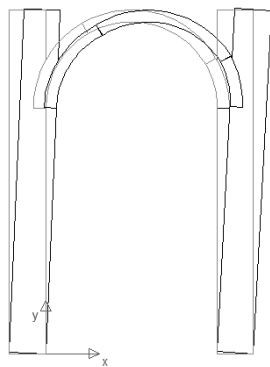
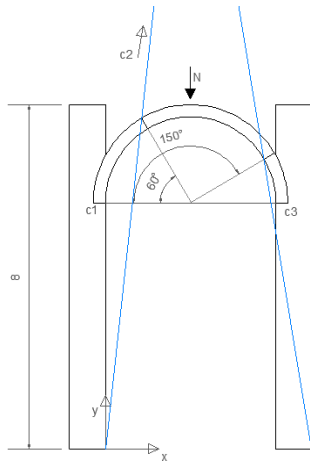
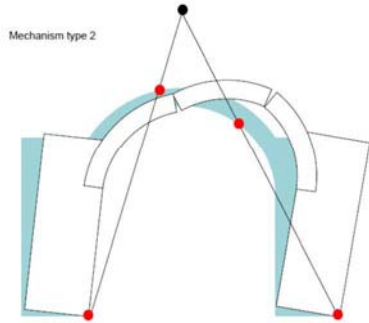


Figure A2.4 –collapse mechanism of arch and of both buttresses.

Geometrical properties

B	0.85	m
H	8	m
Re	2.28	m
Ri	2	m
s	2.4	m
L	0.85	m
θ1	- 91	°
θ2	60	°
θ3	150	°
θ4	244	°

Loads

PP	326.4	KN
N1	115.6	KN
D1	- 0.425	m
PV	28.8	KN
N2	636.96	KN
D2	2.00	m
PP	115.6	KN
N3	342.37	KN
D3	4.425	m

Material properties

fc	4	MPa
ft (5% fc)	0.2	MPa
γ	20	KN/m ³

$$c = \frac{a}{g} = 0.031$$

Figure A2.3 – collapse mechanism of a single arch.

The value of the collapse coefficient is too low but it does not seem to be what caused the collapse.

This is probably due to the fact that, considering a unitary depth, the buttresses are slender in comparison to the vault.

The vertical loads considered in this analysis are:

- the vault self-weight and the dead load of the wall and of the roof resting on the vault.
- the buttresses self-weight and the dead load of the wall and of the roof resting on the buttresses.

Loss balance of the arch and of one buttress

Arch:

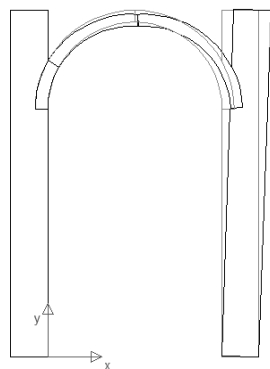
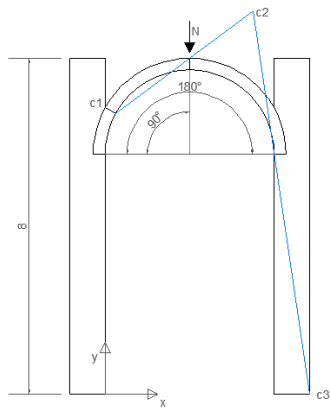
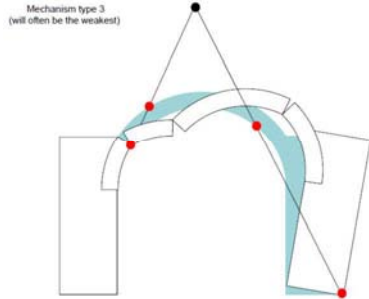


Figure A2.5 –collapse mechanism of arch and of one buttress.

Geometrical properties

B	0.85	m
H	8	m
Re	2.28	m
Ri	2	m
s	0.85	m
L	4	m
θ1	29	°
θ2	90	°
θ3	180	°
θ4	244	°

Loads

PV	28.80	KN
N1	636.96	KN
D1	2.00	m
PP	115.6	KN
N2	342.37	KN
D2	4.425	m

Material properties

fc	4	MPa
ft (5% fc)	0.2	MPa
γ	20	KN/m ³

$$c = \frac{a}{g} = 0.912$$

The value of the collapse coefficient is very high as a consequence it is difficult that this is the mechanism that has led to the collapse.

The vertical loads considered in this analysis are:

- the vault self-weight and the dead load of the wall and of the roof resting on the vault.
- the right buttress self-weight and the dead load of the wall and of the roof resting on the buttress.

Loss balance of two consecutive arches

Arches:

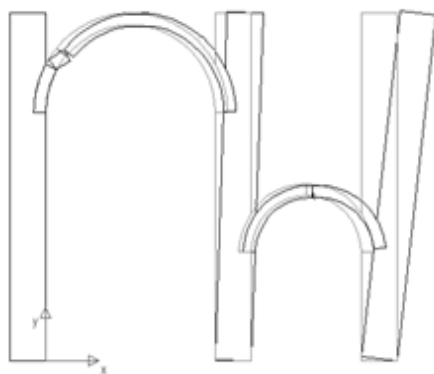
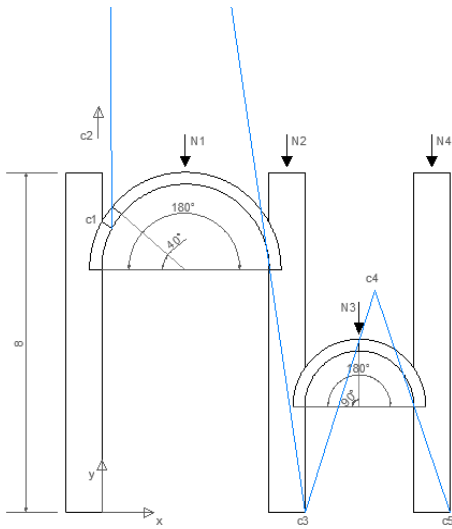
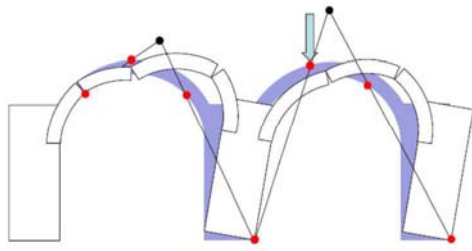


Figure A2.6 – collapse mechanism of two consecutive arches case a.

Geometrical properties

B	0.85	m
H	8	m
s	0.85	m
Re1	2.28	m
Ri1	2	m
L1	4	m
θ1	29	°
θ2	40	°
θ3	180	°
θ4	244	°
Re2	1.58	m
Ri2	1.3	m
L2	2.6	m
β1	90	°
β2	180	°
β3	230	°

Loads

PVg	28.8	KN
N1	636.96	KN
D1	2.00	m
PP	115.6	KN
N2	342.37	KN
D2	4.425	m
PVp	19.38	KN
N3	4.16	KN
D3	6.15	m
PP	115.6	KN
N4	342.37	KN
D4	7.875	m

Material properties

fc	4	MPa
ft (5% fc)	0.2	MPa
γ	20	KN/m ³

$$c = \frac{a}{g} = 0.095$$

The value of the collapse coefficient has a value credible but the position of the hinges does not seem to be that which is verified in the real case.

The vertical loads considered in this analysis are:

- the vaults self-weight and the dead load of the wall and of the roof resting on the vaults,
- the buttresses self-weight and the dead load of the wall and of the roof resting on the buttresses.

Loss balance of two consecutive arches

Arches:

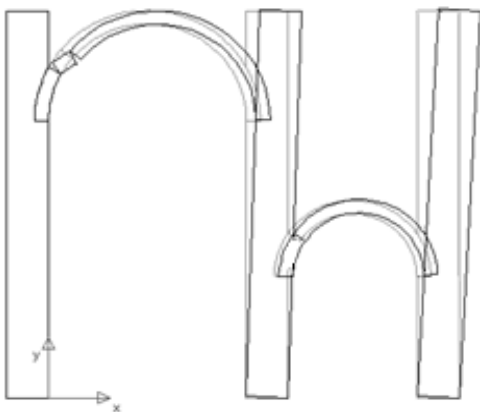
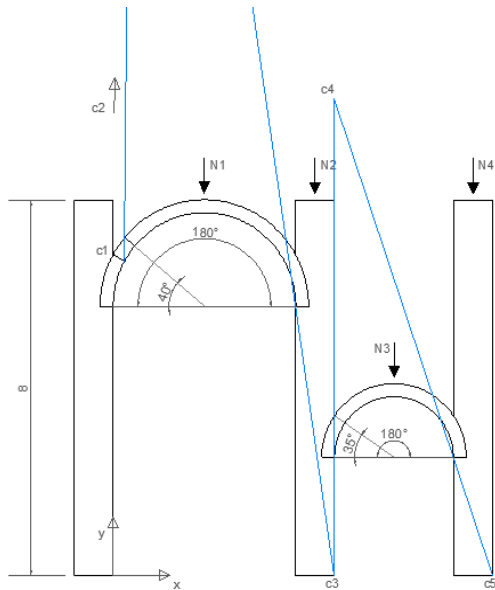
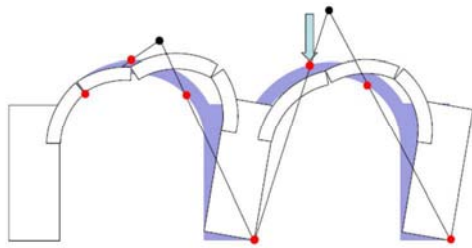


Figure A.2.7 – collapse mechanism of two consecutive arches case b.

Geometrical properties

B	0.85	m
H	8	m
s	0.85	m
Re1	2.28	m
Ri1	2	m
L1	4	m
θ_1	29	°
θ_2	40	°
θ_3	180	°
θ_4	244	°
Re2	1.58	m
Ri2	1.3	m
L2	2.6	m
β_1	35	°
β_2	180	°
β_3	230	°

Loads

PV _g	28.80	KN
N1	636.96	KN
D1	2.00	m
PP	115.6	KN
N2	342.37	KN
D2	4.425	m
PV _p	19.38	KN
N3	4.16	KN
D3	6.15	m
PP	115.6	KN
N4	342.37	KN
D4	7.875	m

Material properties

f_c	4	MPa
f_t (5% f_c)	0.2	MPa
γ	20	KN/m ³

$$c = \frac{a}{g} = 0.150$$

In this case the position of the hinges has been changed so as to locate them in a position closer to reality. Despite the value of the collapse coefficient is plausible it is greater than in the previous case.

The vertical loads considered in this analysis are:

- the vaults self-weight and the dead load of the wall and of the roof resting on the vaults,
- the buttresses self-weight and the dead load of the wall and of the roof resting on the buttresses.

Loss balance of two consecutive arches at the same height

Arches:

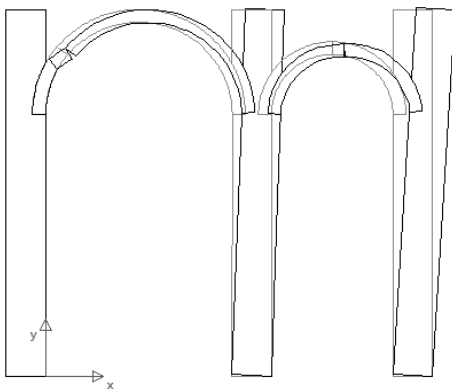
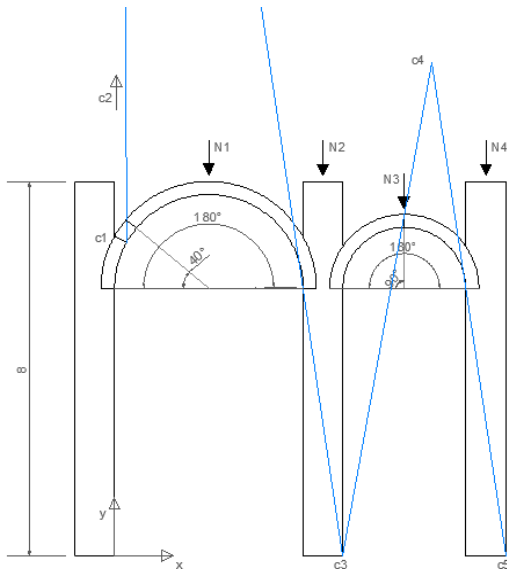
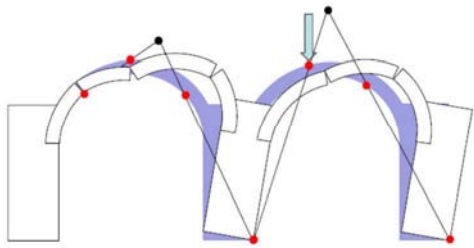


Figure A2.8 – collapse mechanism of two consecutive arches at the same height.

Geometrical properties

B	0.85	m
H	8	m
s	0.85	m
Re1	2.28	m
Ri1	2	m
L1	4	m
θ_1	29	°
θ_2	40	°
θ_3	180	°
θ_4	244	°
Re2	1.58	m
Ri2	1.3	m
L2	2.6	m
β_1	90	°
β_2	180	°
β_3	250	°

Loads

PVg	28.8	KN
N1	636.96	KN
D1	2.00	m
PP	115.6	KN
N2	342.37	KN
D2	4.425	m
PVp	19.38	KN
N3	4.16	KN
D3	6.15	m
PP	115.6	KN
N4	342.37	KN
D4	7.875	m

Material properties

f_c	4	MPa
f_t (5% f_c)	0.2	MPa
γ	20	KN/m ³

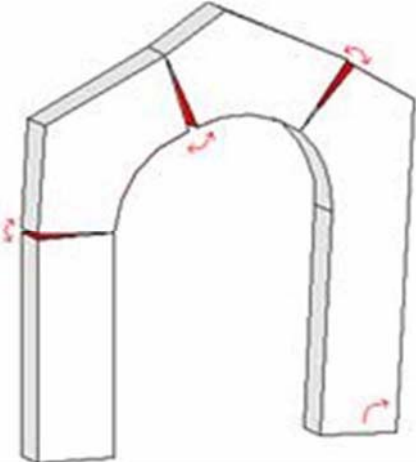
$$c = \frac{a}{g} = 0.134$$

In this case it has been assumed that inside the wall, overlying the smallest vault, occurs the formation of an resistant arch. For this reason, the mechanism has been verified assuming two vaults of the same height. Despite the value of the collapse coefficient is plausible it is greater than in the previous case. The vertical loads considered in this analysis are:

- the vaults self-weight and the dead load of the wall and of the roof resting on the vaults,
- the buttresses self-weight and the dead load of the wall and of the roof resting on the buttresses.

Loss balance of two consecutive arches with resisting spandrels

Arches:

	Geometrical properties		
	B	0.85	m
H	8	m	
s	0.85	m	
Re1	2.28	m	
Ri1	2	m	
L1	4	m	
θ1	29	°	
θ2	70	°	
θ3	120	°	
θ4	244	°	
Re2	1.58	m	
Ri2	1.3	m	
L2	2.6	m	
β1	90	°	
β2	180	°	
β3	230	°	
Loads			
PVg	28.80	KN	
N1	636.96	KN	
D1	2.00	m	
PP	115.6	KN	
N2	342.37	KN	
D2	4.425	m	
PVp	19.38	KN	
N3	342.37	KN	
D3	7.875	m	
PP	115.6	KN	
Material properties			
fc	4	MPa	
ft (5% fc)	0.2	MPa	
γ	20	KN/m ³	
$c = \frac{a}{g} = 1.184$			

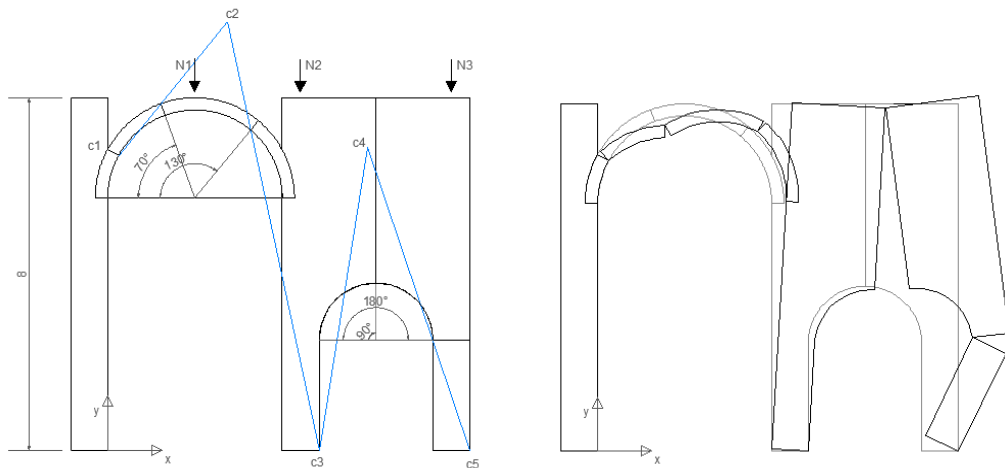


Figure A2.9 – collapse mechanism of two consecutive arches with resisting spandrels case a.

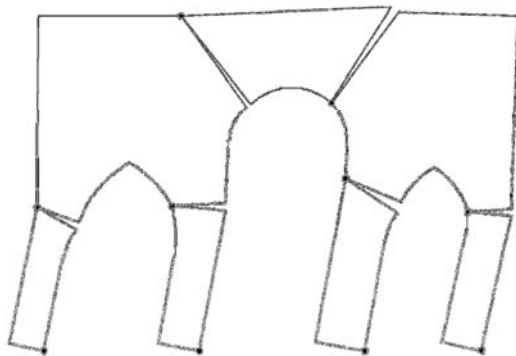
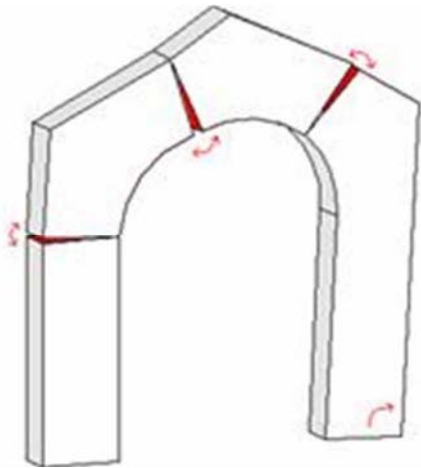
Assuming the arches with resisting spandrels, the collapse coefficient grows a lot. This mechanism does not occur in the reality because the wall over the smaller vault is thin, it has low quality and it isn't connected with the buttresses .

The vertical loads considered in this analysis are:

- the vaults self-weight and the dead load of the wall and of the roof resting on the vaults,
- the buttresses self-weight and the dead load of the wall and of the roof resting on the buttresses.

Loss balance of two consecutive arches with resisting spandrels

Arches:



Geometrical properties

B	0.85	m
H	8	m
s	0.85	m
Re1	2.28	m
Ri1	2	m
L1	4	m
θ1	29	°
θ2	50	°
θ3	110	°
θ4	244	°
Re2	1.58	m
Ri2	1.3	m
L2	2.6	m
β1	35	°
β2	180	°
β3	230	°

Loads

PVg	28.8	KN
N1	636.96	KN
D1	2.00	m
PP	115.6	KN
N2	342.37	KN
D2	4.425	m
PVp	19.38	KN
N3	342.37	KN
D3	7.875	m
PP	115.6	KN

Material properties

fc	4	MPa
ft (5% fc)	0.2	MPa
γ	20	KN/m ³

$$c = \frac{a}{g} = 0.099$$

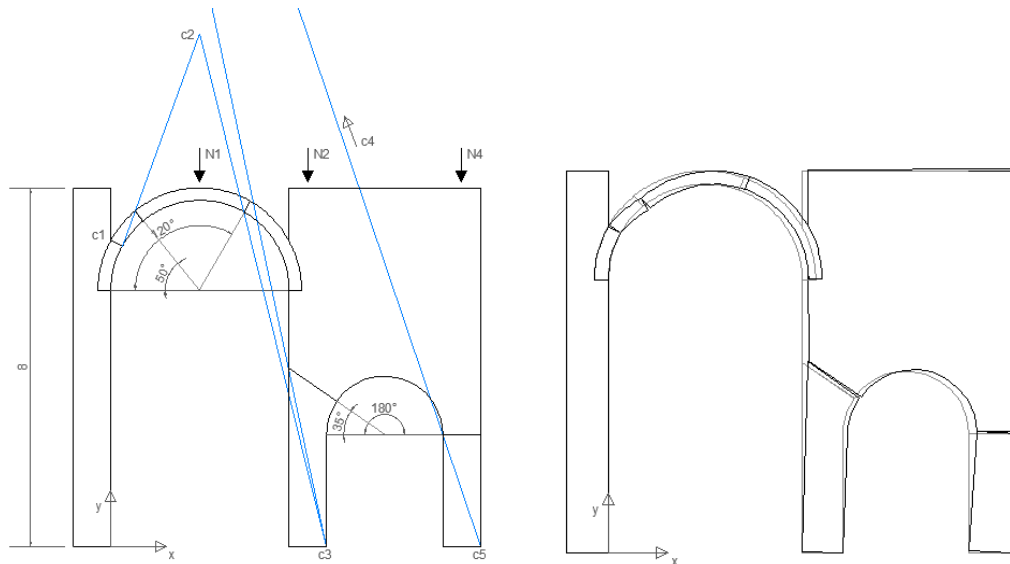
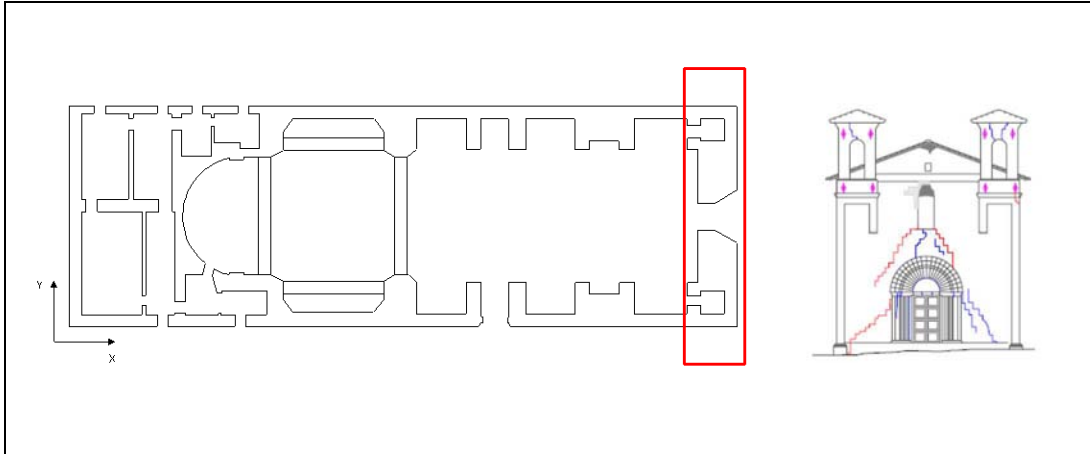


Figure A2.10 – collapse mechanism of two consecutive arches with resisting spandrels case b.

In this case the arches were supposed with resisting spandrels but assuming the break in the foothills. The collapse coefficient assumes a plausible value and also the position of the hinges is very similar to the real case. Therefore, it can be the mechanism that was triggered during the earthquake.

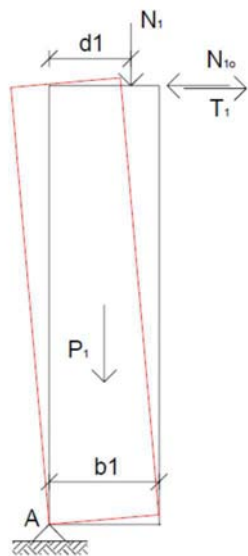
The vertical loads considered in this analysis are:

- the vaults self-weight and the dead load of the wall and of the roof resting on the vaults,
- the buttresses self-weight and the dead load of the wall and of the roof resting on the buttresses.



Out of plane movement of a monolithic wall simply supported

Main facade:



Geometrical properties		
H1	15	m
B1	2.50	m
Loads		
P1	750	KN
N1	55.00	KN
N1o	-	KN
D1	0.74	m
Material properties		
fc	4	MPa
ft (5% fc)	0.2	MPa
γ	20	KN/m ³

$$c = \frac{a}{g} = 0.152$$

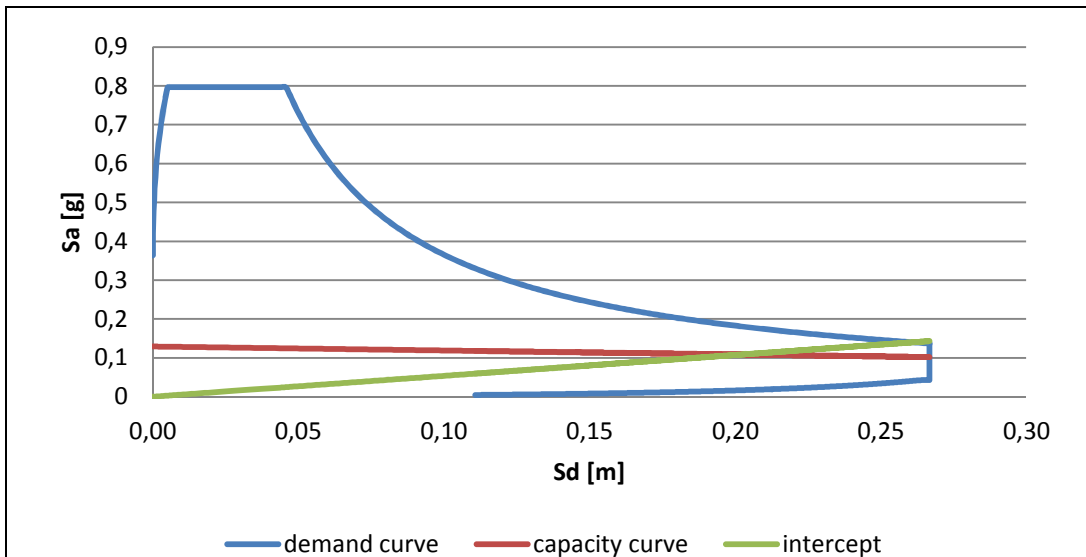
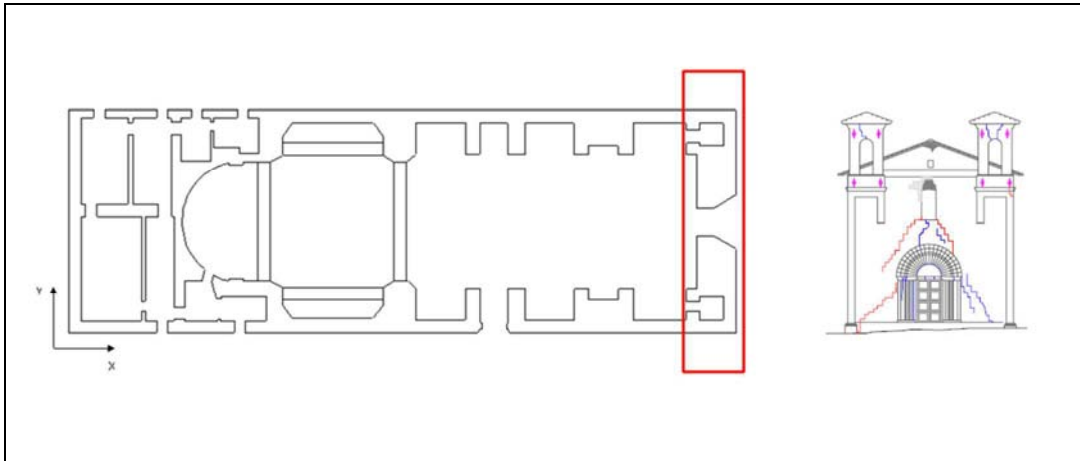


Figure A2.11 - Non-linear analysis of the main façade (simply supported)

Mass involved	M^*	1243.59	Kg	
Fraction of mass involved	e^*	0.95		
Spectral acceleration which activates the mechanism	a_0^*	0.129g		
Final spectral displacement	d^*u	0.506	m	
SLU WITH LINEAR ANALYSIS	a^*	0.167g		NOT CHECKED
SLU WITH NON LINEAR ANALYSIS	Δd	0.260	m	CHECKED

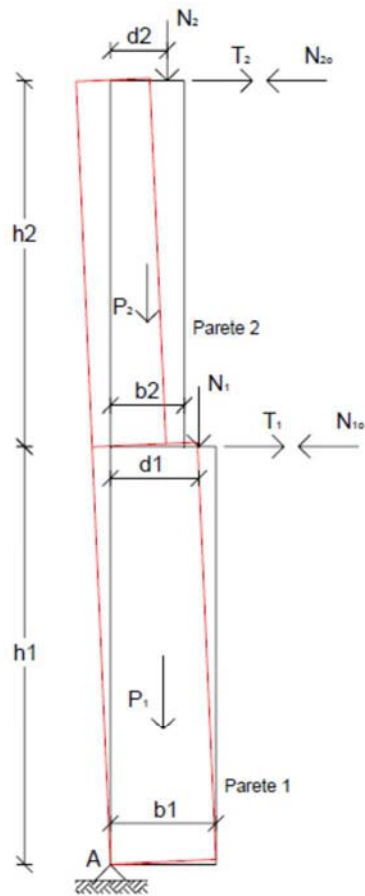
By performing the non-linear analysis, the value obtained was $d_u^* = 0.506$ m, while the value required by the Italian code was $\Delta d = 0.260$ m. The calculated value is much higher than the required one.

The barrel vault of the nave doesn't transmit practically any orthogonal force on to the analysed façade, as so the only external forces applied in this structural element are the vertical loads coming from the bell towers. The load applied over the frontal wall, is equal to half weight of the tower. This consideration is related with the fact that only half part of the bell tower is directly acting over the façade. The lateral façade wall was supposed not connected to the main facade, at least up to the highest part of the lower wall on the left facade.



Out of plane movement of a monolithic wall simply supported and partially connected with the orthogonal walls

Main facade:



Geometrical properties

H1	4	m
B1	2.50	m
H2	11	m
B2	2.50	m

Loads

P1	200	KN
N1o	- 19	KN
P2	550	KN
N2	55.00	KN
D2	0.74	m

Material properties

fc	4	MPa
ft (0.5% fc)	0.02	MPa
γ	20	KN/m ³

* $N1o = (ft * 8 * 0.95 * 10^3) / 8$

$c = \frac{a}{g} = 0.163$

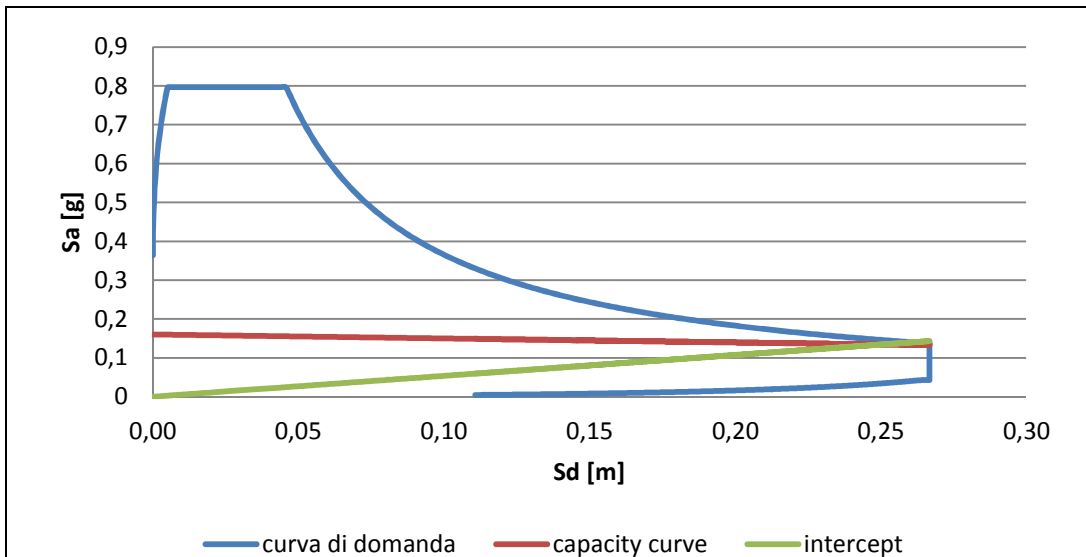


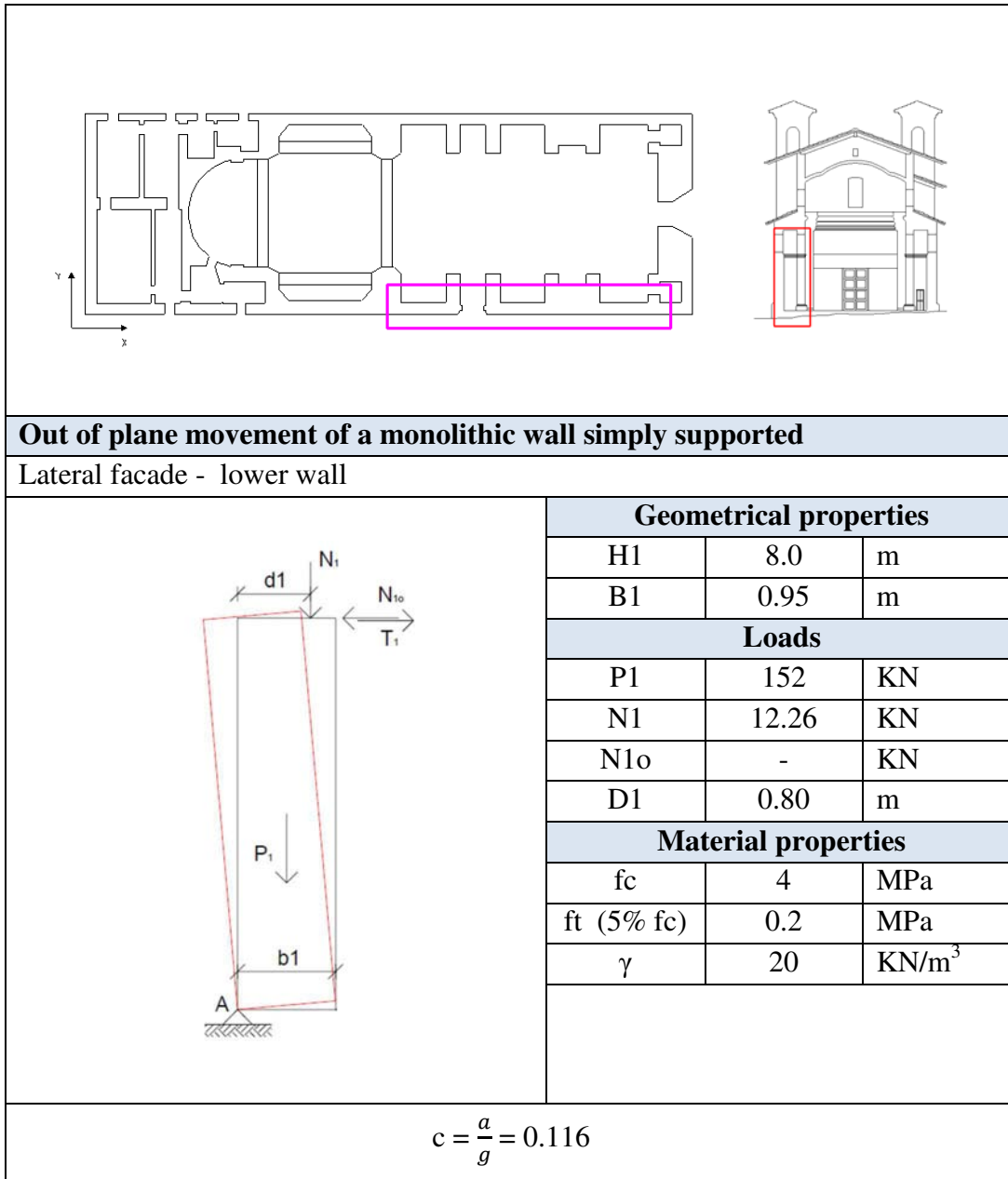
Figure A.2.12 - Non-linear analysis of the main façade (partially connected).

Mass involved	M^*	1243.59	Kg	
Fraction of mass involved	e^*	0.95		
Spectral acceleration which activates the mechanism	a_0^*	0.139g		
Final spectral displacement	d_u^*	0.628	m	
SLU WITH LINEAR ANALYSIS	a^*	0.167g		NOT CHECKED
SLU WITH NON LINEAR ANALYSIS	Δd	0.260	m	CHECKED

By performing the non-linear analysis, the value obtained was $d_u^* = 0.628$ m, while the value required by the Italian code was $\Delta d = 0.260$ m. The calculated value is much higher than the required one.

The barrel vault of the nave doesn't transmit practically any orthogonal force on to the analysed façade, as so the only external forces applied in this structural element are the vertical loads coming from the bell towers. The load applied over the frontal wall, is equal to half weight of the tower. This consideration is related with the fact that only half part of the bell tower is directly acting over the façade. The lateral façade wall was supposed connected to the main facade, at least up to the highest part of the lower wall on the left facade. For this reason, in order to calculate the activation of the out of plane movement on the main facade, the wall has been divided into two parts and a horizontal force of retention was taken into consideration.

A.2.2 EARTHQUAKE Y DIRECTION



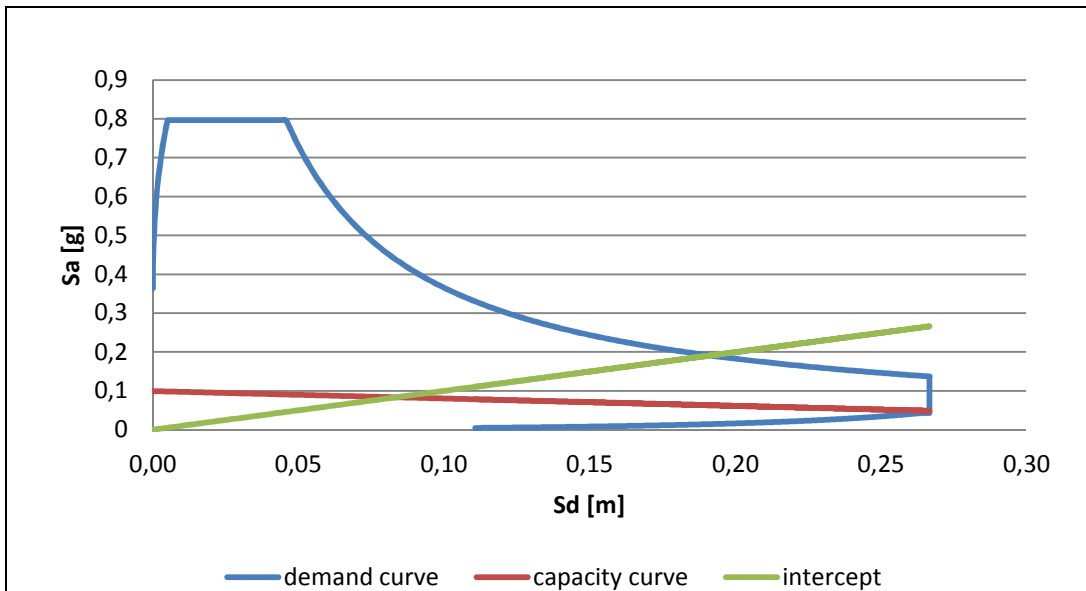


Figure A2.13 - Non-linear analysis of the lower wall of the lateral façade (simply supported)

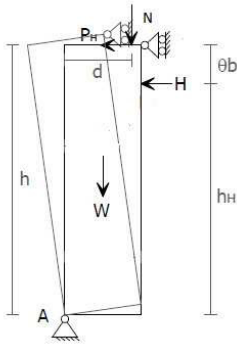
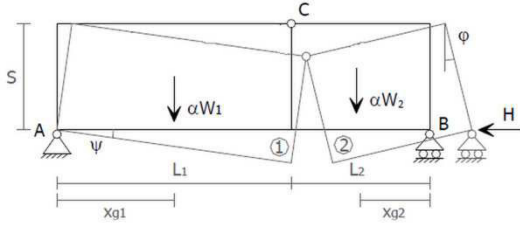
Mass involved	M^*	325.46	Kg	
Fraction of mass involved	e^*	0.94		
Spectral acceleration which activates the mechanism	a_0^*	0.099g		
Final spectral displacement	d_u^*	0.209	m	
SLU WITH LINEAR ANALYSIS	a^*	0.167g		NOT CHECKED
SLU WITH NON LINEAR ANALYSIS	Δd	0.191	m	CHECKED

By performing the non-linear analysis, the value obtained was $d_u^* = 0.209$ m, while the value required by the Italian code was $\Delta d = 0.191$ m. The calculated value is quite close to that required but it is sufficient to check the analysis.

The vertical loads considered in this analysis are the wall self-weight and the dead load of the chaples' roof resting on the lower wall of the lateral façade.

Horizontal deflection

Lateral facade - lower wall



$$H = \frac{1}{Hh} \left(P \frac{S}{2} + Nd \right)$$

Geometrical properties

s	0.95	m
L	20.60	m
b	8.00	m

Loads

H	2108.4	KN
N	252.56	KN
P	3131.2	KN

Geometrical properties (orthogonal wall)

s	2.50	m
h	15.00	m
b	8.00	m
θ	0.5	

Loads (orthogonal wall)

P	6000	KN
N	440	KN
d	0.74	m
Htraz	-152	KN
ht	4.00	m

Material properties

fc	4	MPa
ft (0.5% fc)	0.02	MPa
γ	20	KN/m ³

$$c = \frac{a}{g} = \frac{8Hs}{(P+N)L} = 0.230$$

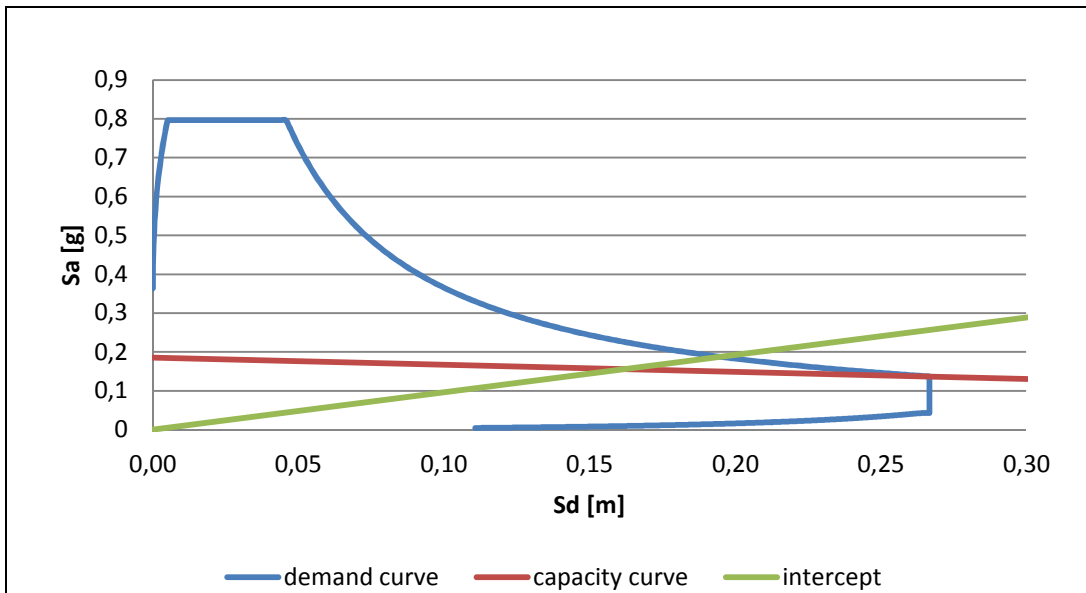


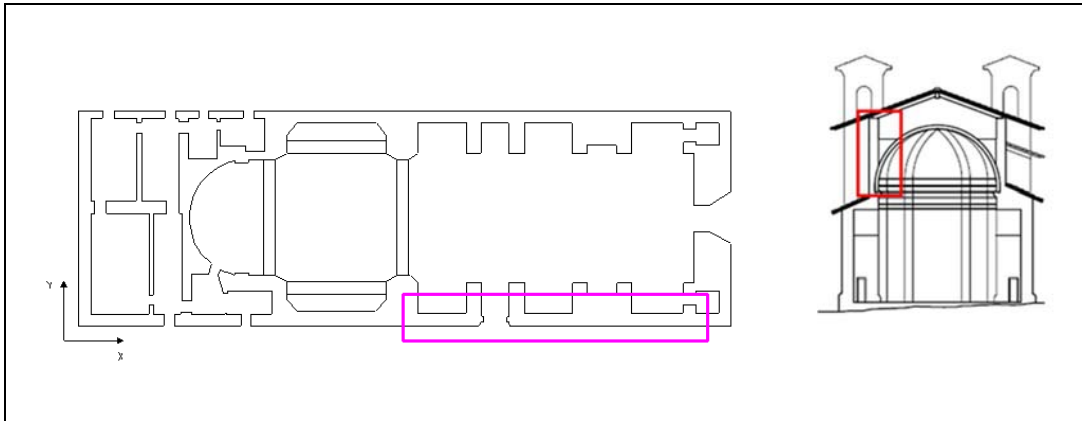
Figure A2.14 - Non-linear analysis of the lower wall of the lateral façade (horizontal deflection)

Mass involved	M^*	344.93	Kg	
Fraction of mass involved	e^*	1		
Spectral acceleration which activates the mechanism	a_0^*	0.185g		
Final spectral displacement	d_u^*	0.405	m	
SLU WITH LINEAR ANALYSIS	a^*	0.167g		NOT CHECKED
SLU WITH NON LINEAR ANALYSIS	Δd	0.200	m	CHECKED

By performing the non-linear analysis, the value obtained was $d_u^* = 0.185$ m, while the value required by the Italian code was $\Delta d = 0.200$ m. So the horizontal deflection of the bottom wall not effectively confined is checked for the non-linear analysis. This means that the wall is confined in respect of movements in the plane.

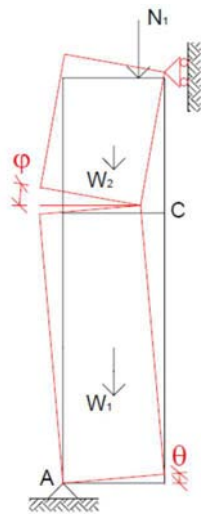
The term H is the resistance offered by the orthogonal walls that oppose themselves to the in-plane movement of the analyzed wall. The limit force H is calculated considering the limit equilibrium conditions for the overturning of the main façade that is partially connected.

The vertical loads considered in this analysis are the wall self-weight and the dead load of the chapels' roof which rests on the lower wall of the lateral façade.



Vertical deflection

Lateral facade - top wall



Geometrical properties

H1	7.5	m
B1	0.80	m

Loads

P1	120.00	KN
N1	39.24	KN

Material properties

fc	4	MPa
ft (5% fc)	0.2	MPa
γ	20	KN/m ³

$$c = \frac{a}{g} = 0.517$$

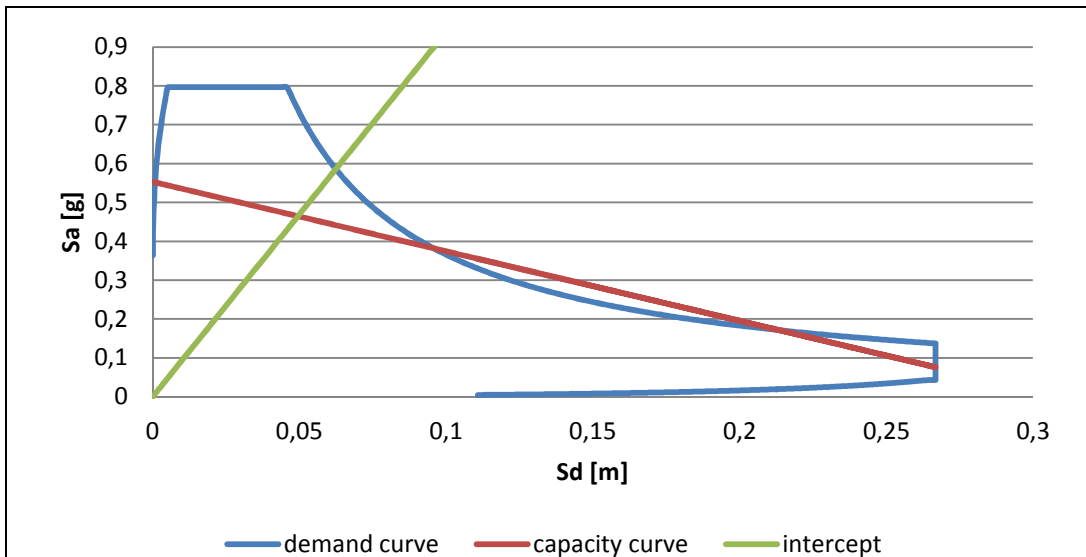


Figure A2.15 - Non-linear analysis of the top wall of the lateral façade (vertical deflection).

Mass involved	M^*	251.98	Kg	
Fraction of mass involved	e^*	0.75		
Spectral acceleration which activates the mechanism	a_0^*	0.556g		
Final spectral displacement	d_u^*	0.124	m	
SLU WITH LINEAR ANALYSIS	a^*	0.216g		CHECKED
SLU WITH NON LINEAR ANALYSIS	Δd	0.062	m	CHECKED

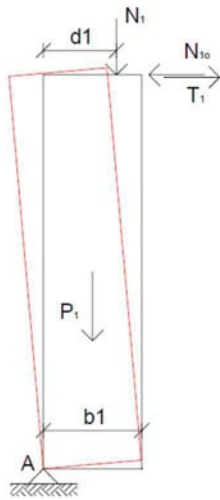
This mechanism has been studied considering just the upper part of the lateral wall, in order to verify the presence of a relation between it and the partial collapse of the lateral façade occurred during the earthquake.

However, applying the kinematic method to the mechanism of vertical deflection of the top wall even linear analysis is checked.

The vertical loads considered in this analysis are related with the roof self-weight. The horizontal forces coming from the roof are balanced by the presence of steel ties.

Out of plane movement of a monolithic wall simply supported

Lateral facade - top wall



Geometrical properties

H1	7.5	m
B1	0.80	m

Loads

P1	120.00	KN
N1	39.24	KN
N1o	-	KN
D1	0.65	m

Material properties

fc	4	MPa
ft (5% fc)	0.2	MPa
γ	20	KN/m ³

$$c = \frac{a}{g} = 0.099$$

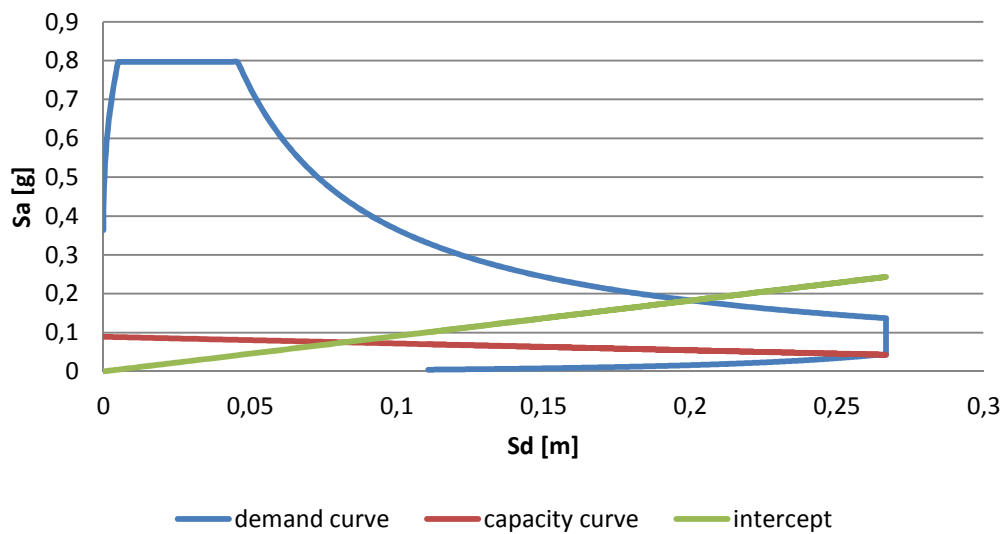


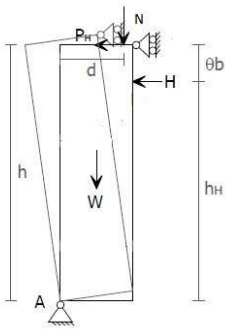
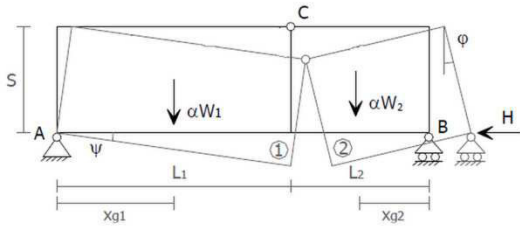
Figure A2.16 - Non-linear analysis of the top wall of the lateral facade (overturning).

Mass involved	M*	298.68	Kg	
Fraction of mass involved	e*	0.89		
Spectral acceleration which activates the mechanism	a ₀ *	0.089g		
Final spectral displacement	d _u *	0.205	m	
SLU WITH LINEAR ANALYSIS	a*	0.216g		NOT CHECKED
SLU WITH NON LINEAR ANALYSIS	Δd	0.200	m	CHECKED

This mechanism has been studied considering just the upper part of the lateral wall, in order to verify if the roof, in measure, opposed this collapse mechanism. By performing the non-linear analysis, the value obtained was $d_u^* = 0.205$ m, while the value required by the Italian code was $\Delta d = 0.200$ m. The calculated value is quite close to that required but it is sufficient to check the analysis. The load applied is the same as in the previous case: the self-weight roof.

Horizontal deflection

Lateral facade - top wall



$$H = \frac{1}{Hh} \left(P \frac{S}{2} + Nd \right)$$

Geometrical properties

s	0.80	m
L	20.60	m
b	7.50	m

Loads

H	749.65	KN
N	808.34	KN
P	4272.0	KN

Geometrical properties (orthogonal wall)

s	2.50	m
h	15.00	m
b	8.00	m
theta	0.5	

Loads (orthogonal wall)

P	6000	KN
N	440	KN
d	0.74	m
Htraz	-152	KN
ht	4.00	m

Material properties

fc	4	MPa
ft (0.5% fc)	0.02	MPa
gamma	20	KN/m ³

$$c = \frac{a}{g} = \frac{8Hs}{(P+N)L} = 0.071$$

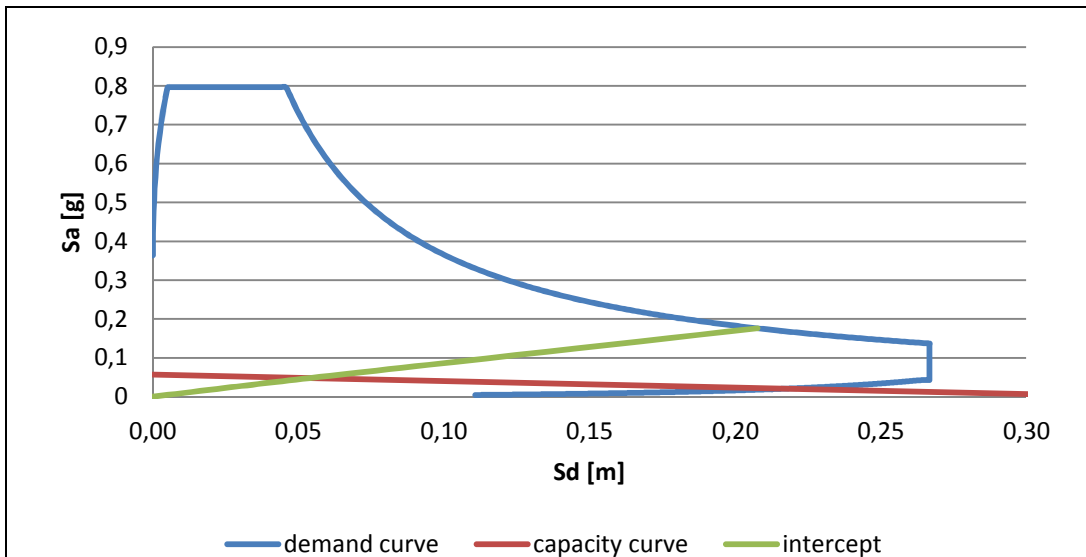


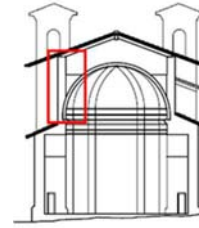
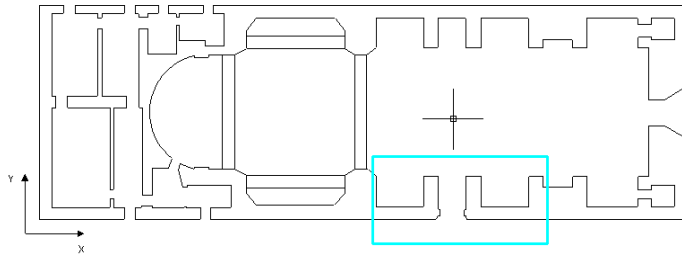
Figure A2.17 - Non-linear analysis of the top wall of the lateral façade (horizontal deflection)

Mass involved	M^*	334.39	Kg	
Fraction of mass involved	e^*	1		
Spectral acceleration which activates the mechanism	a_0^*	0.057g		
Final spectral displacement	d_u^*	0.136	m	
SLU WITH LINEAR ANALYSIS	a^*	0.216g		NOT CHECKED
SLU WITH NON LINEAR ANALYSIS	Δd	0.208	m	NOT CHECKED

By performing the non-linear analysis, the value obtained was $d_u^* = 0.136$ m, while the value required by the Italian code was $\Delta d = 0.208$ m. So the horizontal deflection of the bottom wall not effectively confined is checked for the non-linear analysis. This means that the wall isn't confined in respect of movements in the plane. The collapse coefficient is very low, probably, because at the top of the main façade the displacement is large. So the top wall of the lateral façade can easily move in his plan. The displacement is large because the main façade is very high and it isn't completely connected to the orthogonal walls.

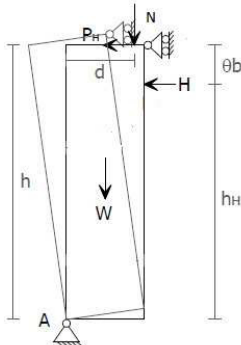
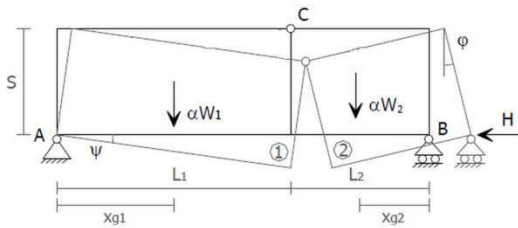
The term H is the resistance offered by the orthogonal walls that oppose themselves to the in-plane movement of the analyzed wall. The limit force H is calculated considering the limit equilibrium conditions for the overturning of the main façade that is partially connected.

The vertical loads considered in this analysis are the wall self-weight and the dead load of the nave roof.



Horizontal deflection

Lateral facade - masonry strip between the two covers



$$H = \frac{1}{Hh} (P \frac{S}{2} + Nd)$$

Geometrical properties

s	0.80	m
L	12.30	m
b	0.50	m

Loads

H	56.27	KN
N	1958.65	KN
P	98.4	KN

Geometrical properties (orthogonal wall)

s	0.85	m
h	8.00	m
b	0.5	m
theta	0.5	

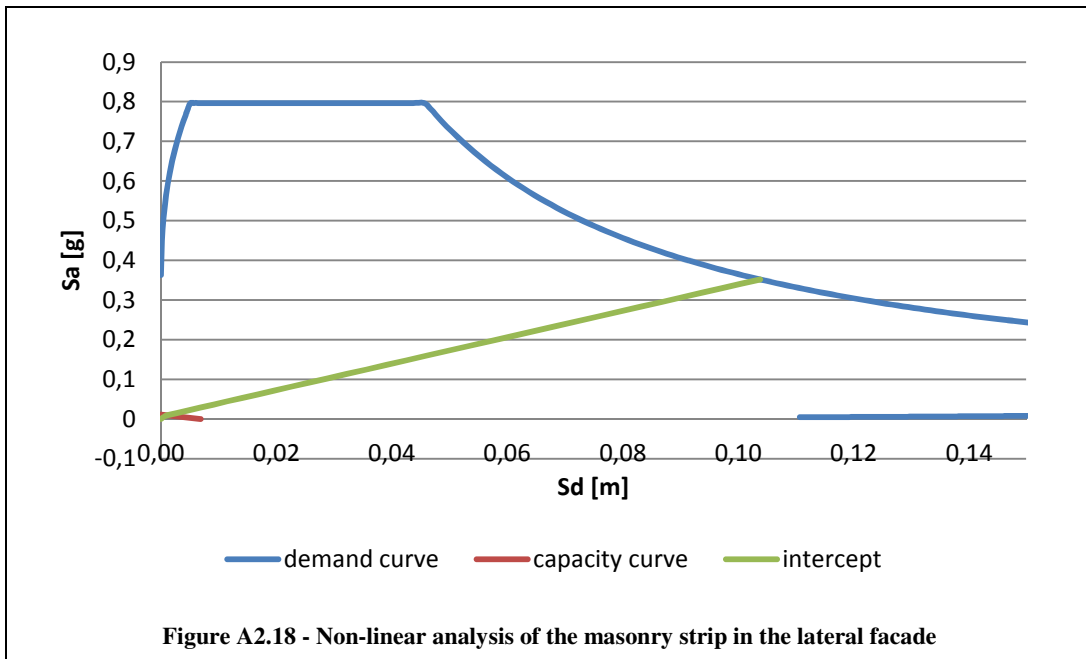
Loads (orthogonal wall)

P	326.4	KN
N	660.85	KN
d	0.45	m

Material properties

fc	4	MPa
ft (0.5% fc)	0.02	MPa
gamma	20	KN/m ³

$$c = \frac{a}{g} = \frac{8Hs}{(P+N)L} = 0.014$$



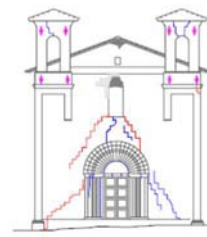
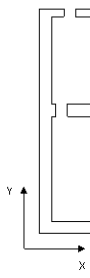
Mass involved	M*	209.69	Kg	
Fraction of mass involved	e*	1		
Spectral acceleration which activates the mechanism	a ₀ *	0.011g		
Final spectral displacement	d _u *	0.003	m	
SLU WITH LINEAR ANALYSIS	a*	0.216g		NOT CHECKED
SLU WITH NON LINEAR ANALYSIS	Δd	0.103	m	NOT CHECKED

By performing the non-linear analysis, the value obtained was $d_u^* = 0.003$ m, while the value required by the Italian code was $\Delta d = 0.103$ m. So the horizontal deflection of the bottom wall not effectively confined is checked for the non-linear analysis. This means that, probably, the out of plane movement of the buttresses supporting the chapel vaults causes a horizontal deflection of the strip of masonry between the two covers, different in height, on the left side facade. The collapse of this strip of wall leads to the destruction of the overstanding wall. The roof of the chapels, as we have already mentioned, presents constant height and thickness on both lateral sides, except for the portion of the front left facade which has a lower height. This portion is lean and presents a greater free mass in comparison with that of the opposite facade, making it more vulnerable to out-of-the-plane forces.

The term H is the resistance offered by the orthogonal walls that oppose themselves to the in-plane movement of the analyzed wall. The limit force H is calculated considering the limit equilibrium conditions for the overturning of the buttress.

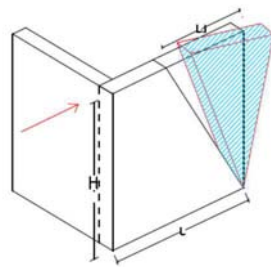
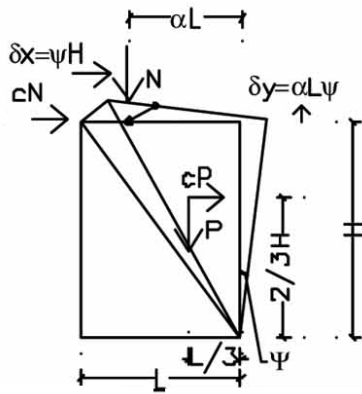
The vertical loads considered in this analysis are:

- the strip of wall self-weight and self-weight of the overstanding wall,
- the dead load of the nave roof.



Plane movement of a limited portion of the wall

Main facade:



Geometrical properties

H	15	m
B	2.5	m
L	16.0	m
L1	8.00	m

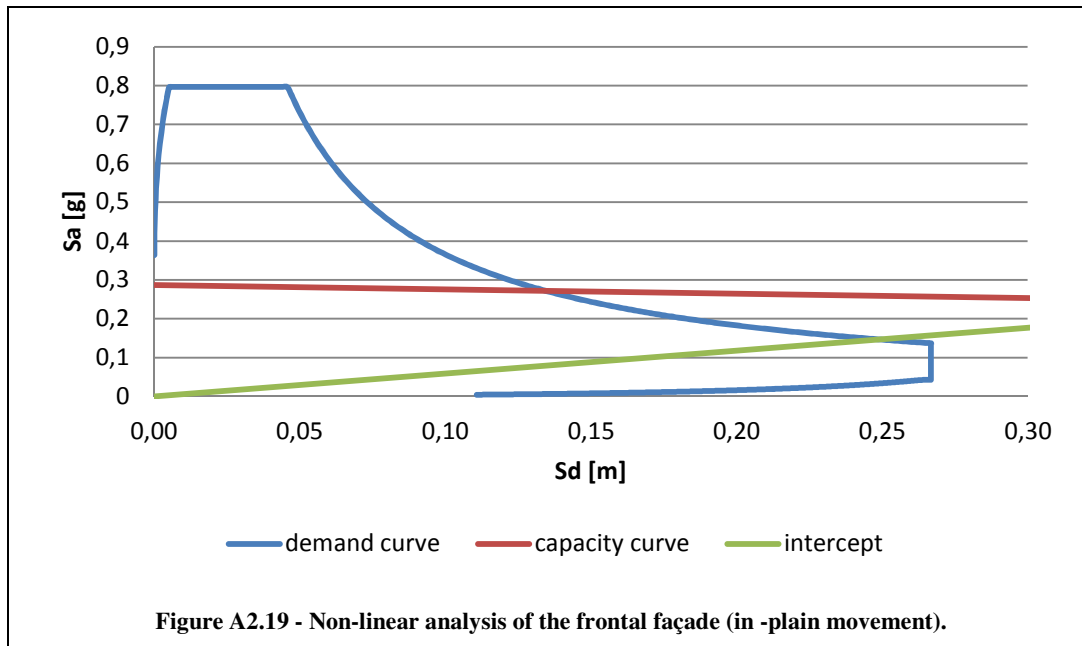
Loads

P	3000	KN
N	440	KN
$\alpha L1$	1.75	

Material properties

f_c	4	MPa
f_t (5% f_c)	0.2	MPa
γ	20	KN/m ³

$$c = \frac{a}{g} = \frac{\frac{P L_1}{3} + N \alpha L_1}{\frac{P^2}{3} H + N H} = 0.349$$



Mass involved	M^*	342.46	Kg	
Fraction of mass involved	e^*	0.98		
Spectral acceleration which activates the mechanism	a_0^*	0.287g		
Final spectral displacement	d_u^*	1.027	m	
SLU WITH LINEAR ANALYSIS	a^*	0.167g		CHECKED
SLU WITH NON LINEAR ANALYSIS	Δd	0.256	m	CHECKED

By performing the non-linear analysis, the value obtained was $d_u^* = 1,027$ m, while the value required by the Italian code was $\Delta d = 0.256$ m. The calculated value is much greater than the required one.

This collapse mechanism has a seismic coefficient very high because it is in plane movement.

So before reaching the collapse, the wall must crack and the rotation mechanism must be activated. The facade, to rotate in its plane, must lift the self-weight and it must raise the tower weight which opposes the rotation.

The vertical loads considered in this analysis are related with the bell tower self-weight. This dead load is applied to half width of the tower.

